

ABSTRACT

Title of Document: ELEVATED TEMPERATURE EFFECTS ON
CAROTENOID BIOSYNTHESIS IN THE
DIPLOID STRAWBERRY, FRAGARIA
VESCA

Melantha E. Jackson, Doctor of Philosophy,
2015

Directed By: Professor Herman Sintim
Department of Chemistry and Biochemistry

Carotenoids, a subfamily of the isoprenoids, are one of the most diverse classes of secondary metabolites distributed throughout nature. They are lipophilic in nature, and include over 600 tetraterpenoid compounds synthesized by plants, bacteria, and fungi. Carotenoids, as the major pigment responsible for the red, yellow, and orange colors of fruits and vegetable, help promote human health and wellness by serving as antioxidants and precursors to vitamin A. Climate changes that threaten plant reproduction, negatively impact crop production worldwide. Little is understood about the chemistry of carotenoids in plant reproductive structures. Insight into the metabolic roles and functions of carotenoids in plant reproduction and, the effects of abiotic stresses on carotenoid biosynthesis in these structures would globally impact agriculture production by reducing yield loss. The potential for these metabolites to protect the reproductive structures under elevated temperature

stress was assessed using biochemical analysis, genomics, and genetic studies. Fourteen candidate genes involved in carotenoid biosynthesis were identified, revealing three small gene families. Quantitative real-time polymerase chain reaction (qPCR) expression analysis of these genes and targeted metabolic profiling using liquid chromatography-high resolution mass spectrometry (LC-HRMS) throughout plant development under control and moderately elevated temperature stress showed that gene expression and metabolite accumulation are tissue specific and differentially responsive to elevated temperature stress. Three phytoene synthase genes were identified and characterized. Genomic analyses revealed that the *PSY* gene family exhibits functional diversity in plant tissues, both with respect to location and stage of development, as well as in response to abiotic stress.

ELEVATED TEMPERATURE EFFECTS ON CAROTENOID BIOSYNTHESIS IN
THE DIPLOID STRAWBERRY, FRAGARIA VESCA

By

Melantha E. Jackson

Dissertation submitted to the Faculty of the Graduate School of the
University of Maryland, College Park, in partial fulfillment
of the requirements for the degree of
Doctor of Philosophy
2015

Advisory Committee:
Professor Herman Sintim, Chair
Dr. Janet P. Slovin
Professor Frederick Khachik
Professor Douglas Julin

Professor Nicole LaRonde LeBlanc
Professor Liangli Yu

© Copyright by
Melantha E. Jackson
2015

Dedication

This document is dedicated to my family for their continuous support and unconditional love.

Acknowledgements

This journey in obtaining my doctorate has not been easy. It has been long, stressful, and full of sacrifices. However, through it all I have persevered and this experience will forever serve as a reminder of the endless possibilities when you refuse to give up. I would be remiss if I did not recognize the people that have helped me reach this point. This section, which has been a joy to write, is a tribute to all the individuals that have contributed in one way or another to the completion of this dissertation and my academic success.

First and foremost I must thank God. Without your grace and many blessings none of this would be possible.

“Many, Lord my God, are the wonders you have done, the things you planned for us. None can compare with you; were I to speak and tell of your deeds, they would be too many to declare.”

Psalms 40:5

I would like to thank Janet P. Slovin, my advisor at the U.S. Department of Agriculture in Beltsville, MD for the opportunity to continue on with my Ph.D. by accepting me into her group and creating a project for me to work on. Thank you for believing in me and for all the hours, days, and years invested in making me a better scientist. Your enthusiasm and immense knowledge has been a constant source of encouragement and guidance throughout this journey. I will forever appreciate the working environment that you provided and the countless times you fought to ensure that I had the resources needed to complete my project. Thank you for your interest

in my personal life and treating me like family. Your home was always filled with stimulating conversation and love.

My next biggest thanks must go to Dr. Frederick Khachik for agreeing to serve as my co-advisor at the University of Maryland. Thank you for all of your support. I would also like to thank the members of my committee, Dr. Herman Sintim, Dr. Nicole LaRonde LeBlanc, Dr. Douglas Julin, and Dr. Liangli Yu for their time spent reading this dissertation and taking part in the defense.

Many thanks to Dr. Jerry Cohen and his research group at the University of Minnesota for granting me access to the research facilities necessary to complete this research. Huge thanks to Dr. Dan Abate Pella and Dr. Dana Freund for their technical assistance with the LC-MS analyses. Much appreciation to Dr. Pei Chen, Dr. Edith Blackwell, and the entire Food Composition and Methods Development Laboratory in Beltsville, MD for allowing me to use their software to finish the MS analyses.

To Dr. José Die, a U.S. Department of Agriculture Visiting Scientist from Spain, thank you for your many pearls of wisdom that extends far beyond your technical competencies. I have been blessed to have you as a friend as well as a scientific resource.

I would like to thank my undergraduate research advisor, Dr. Michelle Boucher for being such a wonderful mentor and encouraging me to apply to graduate school.

I would like to express my appreciation to all my friends who have supported me throughout my journey in graduate school, including, Curissa Taylor, Yondel Benjamin-Gilfurt, Dr. Williamson Oloo, and Dr. Chris Sims. Special thanks to Dr.

Cassandra Taylor for connecting me with Janet Slovin, and Dr. Rennisha Wickham and Dr. Dominique Downing for their encouragement during the really difficult times.

Last but certainly not least, I would like to acknowledge my family for their unwavering love and support. In particular, I wish to thank my parents, Margaret and Joseph Jackson, for providing me with the foundation to succeed in life. The importance of spirituality, education, and hard work instilled in me from an early age enabled me to achieve this milestone. To my brothers and sisters, Kenny, Jodeya, Orlan, Margaret, and Richie, thank you for serving as a sounding board, and providing support and the much needed distractions while writing this dissertation. I am also very blessed to have an amazing support system that extends beyond my immediate family. Thank you to my Aunt Zedar, Uncle Harold and Uncle Dan for their honest opinions and discussions about life.

Table of Contents

Dedication	ii
Acknowledgements	iii
Table of Contents	vi
List of Tables	ix
List of Figures	x
Abbreviations	xiv
Chapter 1: Introduction	1
Overview	1
1.1 Plant Responses to Abiotic Stress	2
1.2 Secondary Metabolites	3
1.3 Carotenoids	4
1.3.1 Chemical Structure and Properties of Carotenoids	5
1.3.2 Functional Roles of Carotenoids in Plants	7
1.3.3 Health Benefits of Carotenoids	10
1.3.4 Carotenoid Biosynthesis in Plants	11
1.4 Effects of Heat Stress on Plant Reproductive Development	18
1.5 Some Important Crops of the Rosaceae Family	20
1.6 The Model Strawberry Plant, <i>Fragaria vesca</i>	20
1.8 Objectives	22
Chapter 2: Selection and Validation of Diploid Strawberry, <i>Fragaria vesca</i> Reference Genes for Gene Expression Studies using Real-Time PCR	23
Abstract	23
2.1 Introduction	24
2.2 Materials and Methods	27
2.2.1 Plant Material	27
2.2.2 Plant Growth at Elevated Temperatures	28
2.2.3 Tissue Sampling	28
2.2.4 RNA Isolation	28
2.2.5 Reverse Transcription and Quality Assessment	29
2.2.6 Candidate Reference Genes and Primer Design	30
2.2.7 Measurement of mRNA levels by qPCR	30
2.2.8 Data Analysis	33
2.2.9 Validation with FveSTI	34
2.3 Results	34
2.3.1 Candidate Reference Genes	34

2.3.2 Expression Profiles of Reference Genes	36
2.3.3 Gene Expression Stability Analysis	37
2.3.4 Reference Gene Validation.....	40
2.4 Discussion.....	42
2.5 Acknowledgements	46
2.6 Supplemental Information.....	46
Chapter 3: Metabolic and Gene Expression Analysis of Strawberry Carotenogenesis in Response to Elevated Temperature.....	50
Abstract	50
3.1 Introduction	51
3.2 Materials and Methods	56
3.2.1 Plant Material and Stress Treatment.....	56
3.2.2 Modified Alexander’s Staining Analysis for Pollen Viability	56
3.2.3 RNA Extraction and cDNA synthesis	57
3.2.4 Real-Time Quantitative PCR (qPCR) Analysis	59
3.2.5 Carotenoid Extraction.....	59
3.2.6 Analysis of Carotenoids by LC-MS	60
3.2.7 Carotenoid Biosynthesis Genes Identification and Sequence Analysis ..	61
3.3 Results	62
3.3.1 Pollen Viability.....	62
3.3.2 Expression of Carotenoid Biosynthesis Gene During Anther Development.....	69
3.3.3 Carotenoid Analysis	70
3.3.4 Effects of Elevated Temperature on Expression of Carotenoid Biosynthesis Genes.....	74
3.4 Discussion.....	76
3.5 Acknowledgements	79
3.6 Supplemental Information.....	79
Chapter 4: Identification and Characterization of Three Phytoene Synthase Genes from the Diploid Strawberry, <i>Fragaria vesca</i>	84
Abstract	84
4.1 Introduction	85
4.2 Materials and Methods	88
4.2.1 Plant Material and Stress Treatment.....	88
4.2.2 RNA Extraction and cDNA synthesis	88
4.2.3 Quantitative Gene Expression Analysis	89
4.2.4 Analysis of Alternative Splicing	90
4.2.5 Functional Analysis in <i>Escherichia coli</i>	90
4.2.6 Bioinformatic Analysis.....	93
4.3 Results	93
4.3.1 Sequence and Phylogenetic Analysis	93
4.3.2 Promoter Analysis	98
4.3.3 Expression Profiles of PSY Family Members.....	100
4.3.4 Alternative Splicing Analysis.....	103

4.3.5 PSY Functional Complementation Analysis in <i>Escherichia coli</i>	104
4.4 Discussion.....	105
4.5 Acknowledgements	108
4.6 Supplemental Information.....	108
Chapter 5: General Conclusions and Future Perspectives	111
References.....	115

List of Tables

Table 2.1: General description, <i>F. vesca</i> gene number, and biological functions for reference genes evaluated.....	32
Table 2.2: Candidate reference gene, primer sequences, amplicon size and T _m , and reaction characteristics.....	36
Table 2.3: Consensus ranking of the reference genes determined using geNorm and NormFinder within RefFinder, and geNorm+qBase and NormFinder as stand alone programs.....	40
Table 3.1: Primer sequences for genes involved in carotenoid biosynthesis in strawberry.....	58
Table 3.2: Percentage of viable pollen in control plants and plants growing at elevated temperature.....	62
Table 3.3: <i>F.vesca</i> , Hawaii-4 genes encoding enzymes involved in carotenoid biosynthesis	65
Table 3.4: Expression of carotenoid biosynthesis genes in developing anthers of <i>F. vesca</i> 5AF7.....	70
Table 4.1: Primers used in this study.....	92

List of Figures

Figure 1.1: Chemical structure of some common carotenoids in the all- <i>trans</i> configuration.....	6
Figure 1.2: Some important apocrotenoids found in plants and animals	10
Figure 1.3: Schematic diagram of the carotenoid biosynthetic pathway in higher plant.....	14
Figure 1.4: Structures of phytoene (1), phytofluene (2), ζ -carotene (3), neurosporene (4) and lycopene (5), illustrating the conventional numbering system and Ψ -end group adopted for acyclic carotenoids.....	15
Figure 1.5: Structures of γ -carotene (6), δ -caroene (7), α -carotene (8) and β -carotene (9) with conventional numbering system and definition of β - and ϵ - end groups for cyclic carotenoids	16
Figure 1.6: Structures of monohydroxylated carotenoids, α -cryptoxanthin (10), zeinoxanthin (11) and β -cryptoxanthin (12).....	17
Figure 1.7: Structures of lutein (13), zeaxanthin (14) and violaxanthin (15).....	18
Figure 1.8: A: 5AF7 wild-type flower center with yellow anthers. B: Flower of the 5AF7 pale mutant with opaque white anthers.....	21
Figure 2.1: Dissociation curves of candidate reference genes showing single peaks.....	31
Figure 2.2: qPCR C_q values for the candidate reference genes in all samples.....	37
Figure 2.3: Average expression stability (M) of the candidate reference genes evaluated using geNorm. Horizontal numbers across the top represent CV values calculated using qBase.....	38
Figure 2.4: NormFinder stability values for candidate genes tested.....	39
Figure 2.5: A: Expression profile of <i>FveSTI</i> in receptacle and anther tissues under control and heat stressed conditions. B: Variation in <i>FveSTI</i> after normalization.....	42
Figure 3.1: The carotenoid biosynthetic pathway in higher plants. Names of compounds are bold and abbreviated names of enzymes are in red. PSY, phytoene	

synthase; PDS, phytoene desaturase; ZDS, ζ -carotene desaturase; 15-*cis*- ζ -carotene isomerase, ZISO; CRTISO, carotenoid isomerase; LCYB, lycopene- β -cyclase; LCYE, lycopene- ϵ -cyclase; BOHASE, β -carotene hydroxylase; EOHASE, ϵ -carotene hydroxylase.....53

Figure 3.2: Modified Alexander’s staining of *F. vesca* 5AF7 pollen from plants growing at **A:** 25°C day/20°C night. **B:** 32°C day/25°C night. Viable pollen stains magenta with a blue perimeter (black arrows) while aborted pollen appears light blue and transparent (green arrow).....54

Figure 3.3: Image adopted from Hollender et. al¹³⁴, showing the accumulation of a yellow pigment in anthers during development.....55

Figure 3.4: Conserved domains in the *F. vesca* carotenoid biosynthesis protein....68

Figure 3.5: LC-ESI-MS chromatograms of *F. vesca* leaves, petals, receptacles, anthers, and roots grown under control (25/20 °C) and heat stressed (32/25 °C) conditions.....73

Figure 3.6: Relative accumulation of carotenoids in leaves and floral organs of *F. vesca* grown under control (25/20°C) and moderate heat stress conditions (32/25°C)....74

Figure 3.7: Carotenoid biosynthesis gene expression in *F. vesca* in response to moderately elevated temperatures.....75

Figure 4.1: Intron-exon structures of *FvePSY* genes relative to *AtPSY*.....94

Figure 4.2: Multiple sequence alignment of PSYs from *F. vesca* and Arabidopsis.96

Figure 4.3: A neighbor-joining phylogram of PSY proteins divides the sequences into three clades.....97

Figure 4.4: Heat map of expression of *F. vesca PSY* genes in anthers from pre-meiosis (stages 7-8) to just before flower opening (stage 12) based on transcriptome data from Hollender et al. 2014¹⁴⁵101

Figure 4.5: Real-time PCR expression profiles of the *F. vesca PSY* gene family members in leaves, mature open flower (stage 13) organs, and roots from plants growing under control temperature conditions (25°C day/20°C night) and moderately elevated temperatures (32°C day/25°C night). Relative mRNA levels were

normalized to reference genes, *NMD* and *PP2A*. Error bars indicate SEM from two biological replicates.....102

Figure 4.6 **A:** RT-PCR analysis of *PSY* gene family showing intron retention in mRNA from leaves of *F. vesca* inbred lines **B:** Schematic representation of *FvePSY* transcripts that results in a protein with loss of catalytic domain.....104

Figure 4.7: Functional complementation assay of *F. vesca PSY* genes. Absorbance spectra of acetone extracts from *E. coli* transformed with pAC-85b, pAtPSY, pFvePSY1, pFvePSY2, and pFvePSY3 obtained from 400-800nm. β -Carotene absorption maximum is at 452nm.....105

List of Abbreviations

ABA	abscisic acid
ACT	actin
Acetyl-CoA	acetyl coenzyme A
AMD	age related macular degeneration
BLAST	basic local alignment search tool
BOHASE	β -carotene hydroxylase
bp	base pair(s)
cal	calorie
CAT	catalase
CCD	carotenoid cleavage dioxygenase
cDNA	complementary deoxyribonucleic acid
cm	centimeter(s)
C _q	quantification cycle
CRTISO	carotenoid isomerase
DMAPP	dimethylallyl pyrophosphate
DNA	deoxyribonucleic acid
dNTP	deoxyribonucleotide triphosphate
EF1 α	elongation factor 1 α
EFG	elongation factor G

EOHASE	ϵ -carotene hydroxylase
g	gram(s)
GAPDH	glyceraldehydes-6-phosphate dehydrogenase
GDR	Genome Database Rosceae
GGPP	geranylgeranyl pyrophosphate
IPP	isopentenyl pyrophosphate
LCYB	lycopene- β - cyclase
LCYE	lycopene- ϵ - cyclase
LHC	light-harvesting complex
LUT1	ϵ -carotene hydroxylase
LUT5	β -carotene hydroxylase
Mb	mega base pairs
MEP	2-C-methylerythritol 4-phosphate
mg	milligram(s)
min	minute(s)
ml	milliliter(s)
mm	millimeter
μ l	microliter(s)
μ M	micromolar
mRNA	messenger RNA
MVA	mevalonic acid
NAD	nicotinamide adenine dinucleotide
NADPH	nicotinamide adenine dinucleotide phosphate

NMD	NAD- dependent malic dehydrogenase
NCBI	National Center for Biotechnology Information
NCED	9- <i>cis</i> epoxycarotenoid dioxygenase
NPQ	non-photochemical quenching
NSY	neoxanthin synthase
Oligo dT	oligo deoxythymine
PCR	polymerase chain reaction
PDS	phytoene desaturase
PP2A	protein phosphatase 2A
PSY	phytoene synthase
PSI	photosystem I
PSII	photosystem II
qPCR	quantitative real-time PCR
RNA	ribonucleic acid
RQ	relative quantities
18s rRNA	18s ribosomal RNA
RPKM	reads per kilobase of transcript per million mapped reads
RPL36	ribosomal protein large subunit 36
ROS	reactive oxygen species
s	second(s)
SEM	standard error of mean
SGR	Strawberry Genome Resources
T _m	melting temperature

TUB	α -tubulin
UBQ	ubiquitin
VDE	violaxanthin de-epoxidase
ZDS	ζ -carotene desaturase
ZISO	15-cis- ζ -carotene isomerase
ZE	zeaxanthin epoxidase

Chapter 1: Introduction

Overview

Fruits and vegetables play an important role in human nutrition as sources of vitamins, minerals, and dietary fiber ¹. Epidemiological studies show that a high daily consumption of fruits and vegetables rich in phytochemicals, especially those having antioxidant activity, are strongly associated with a reduced risk for heart disease and certain forms of cancer ². Climatic change, that adversely affect fruit and vegetable crop production and quality, contribute to the billions of people that suffer from malnutrition worldwide ³. Current projections indicate that unless considerable efforts are made to secure our fragile food system, millions more could be at risk by 2050 ⁴.

The garden strawberry, a hybrid of two species, is a perennial herbaceous plant cultivated for its fruit ⁵. The berry, which is not the true fruit in the botanical sense, is a low calorie food (32 cal/100 g) rich in vitamins, minerals, and other health promoting phytonutrients, such as ellagic acid and anthocyanins ⁶. Strawberry production depends on the complete development of the reproductive structures and on fertilization, a process that is highly sensitive to climate change. Elevated temperatures, experienced during the summer months preclude high quality strawberry production in temperate zones by affecting fertilization ⁷. In many plants, the male gametophyte (anthers and pollen), as well as the female gametophyte (carpels) are yellow due to the presence of carotenoids, but the role(s) of these pigments have not been defined. Therefore, this work seeks to investigate the

protective roles of carotenoids during reproductive tissue development in the diploid strawberry, *Fragaria vesca*.

1.1: Plant Responses to Abiotic Stress

Adaptation is paramount for the survival of all organisms. Plants, as sessile organisms, must be able to quickly interpret and respond to abiotic (or climatic) stress factors that threaten their existence. Abiotic stresses such as extreme hot and cold temperatures, salt, drought, flooding and even pollution can cause extensive losses to crop production⁸. Such abiotic stresses, evoking a series of irreversible morphological, physiological, and biochemical changes, singularly or in combination with one another⁹, can be especially problematic for the growth and development of the reproductive organs, which are essential for the production of all non-leafy crops. In efforts to cope with these unfavorable growth conditions, plants have evolved intricate defense mechanisms that activate stress responses at multiple levels of organization. Some of the cellular and molecular responses conferring abiotic stress tolerance in plants include the production of osmoprotectants such as (sugars, proline, and betanine); chemical messengers (salicylic acid jasmonic acid and ethylene); detoxification enzymes (ascorbate peroxidase, glutathione reductase, superoxide dismutase, and catalase), and molecular chaperones^{10, 11}. To this list, one must also include a variety of regulatory proteins, such as transcription factors, protein phosphatases, and kinases that assist in regulating gene expression¹². Understanding the mechanisms by which plants perceive abiotic stressors and activate adaptive responses is of fundamental importance to developing stress tolerant crops¹³. Insight

into these mechanisms has primarily focused on the individual subcomponents such as proteins, metabolites and nucleic acids. This reductionist approach, while “effective in explaining the chemical basis of numerous living processes”¹⁴, is limited by its inability to properly analyze and account for the emergent properties that characterize complex systems¹⁵. Integrative approaches that include techniques, such as metabolomics, transcriptomics and genomics, offer a more holistic perspective to understanding how plants respond to stress.

1.2: Secondary Metabolites

Plants produce an enormous variety of organic compounds defined as secondary metabolites. Unlike primary metabolites, for example the carbohydrates, amino acids, and lipids, secondary metabolites do not appear to be required for basic metabolic processes, involved in growth and development. These natural products, once described as waste products of primary metabolism, can contribute to the overall survival of the plant by protecting against various environmental stresses^{16, 17}. Secondary metabolites, accounting for over 200,000 known chemical structures, also include compounds that defend against predators, or attract pollinators and seed dispersers, as well as being pharmaceuticals, agrochemicals, food additives, flavors, and cosmetic products¹⁸. Most secondary metabolites can be divided into three major groups: terpenoids, alkaloids, and phenolics according to their structure and biosynthetic origins.

Abscisic acid (ABA), derived from the terpenoid biosynthetic pathway, is a phytohormone involved in temperature, drought and osmotic stress¹⁹. Networks of

secondary metabolites including ascorbic acid, glutathione, tocopherols, anthocyanins and carotenoids that function as antioxidants defend against excessive levels of stress produced reactive oxygen species (ROS) to prevent oxidation of lipids, proteins and nucleic acids²⁰. These secondary metabolites can also have protective roles in response to thermal and light stress, making them ideal targets for plant breeding and engineering strategies.

1.3: Carotenoids

Carotenoids are a diverse group of isoprenoids produced by plants, bacteria, fungi and some blue-green algae^{21, 22}. However, they cannot be biosynthesized by animals and humans. Carotenoids are synthesized in nearly all types of plant plastids, including the chloroplasts (green photosynthetic plastids), chromoplasts (colored plastids), etioplasts (dark-grown precursors of the chloroplast), and amyloplasts (starch-storing plastids)²². In chloroplasts, carotenoids are associated with proteins embedded in the thylakoid membrane, while in the chromoplasts of flowers, fruits, and roots, they are stored as lipid bodies or crystalline structures²³. Carotenoids are also responsible for the red, yellow, and orange coloration in various animals, such as birds, fish, and crustaceans^{24, 25}. These lipophilic pigments in the feathers of house finches and flamingoes are used in courtship and as indicators of health^{24, 26}. Carotenoids may also enhance immune defenses in fishes^{24, 27}. Carotenoids have crucial roles in photosynthetic organisms, and perform important roles in ecology, and in their contributions to health and agriculture.

1.3.1: Chemical Structure and Properties of Carotenoids

Structurally, the carotenoids are comprised of eight isoprenoid units synthesized by a tail-to-tail linkage of two C₂₀ geranylgeranyl pyrophosphate molecules²⁸. All carotenoids are produced by modification of this C₄₀ carbon skeleton. The structural diversity of carotenoids achieved by differences in dehydrogenation, cyclization and hydroxylation levels has led to the characterization of over 700 compounds²⁹. Figure 1.1 illustrates the chemical structure of several common carotenoids. The polyene chain, which includes up to fifteen alternating double and single bonds is an essential spectroscopic feature of carotenoids (Figure 1.1)^{28, 30}. This highly conjugated system is responsible for carotenoids ability to absorb light in the visible region of the spectrum. At least seven alternating double and single bonds are needed for carotenoids to impart color^{28, 30}. This feature also provides the basis for carotenoids molecular shape and instability in the presence of light, oxygen and heat³⁰. Acidic and alkaline conditions can also be detrimental to the structural integrity of carotenoids. Therefore, work with carotenoids must be performed under subdued light in the absence of strong acids, bases, and molecular oxygen.

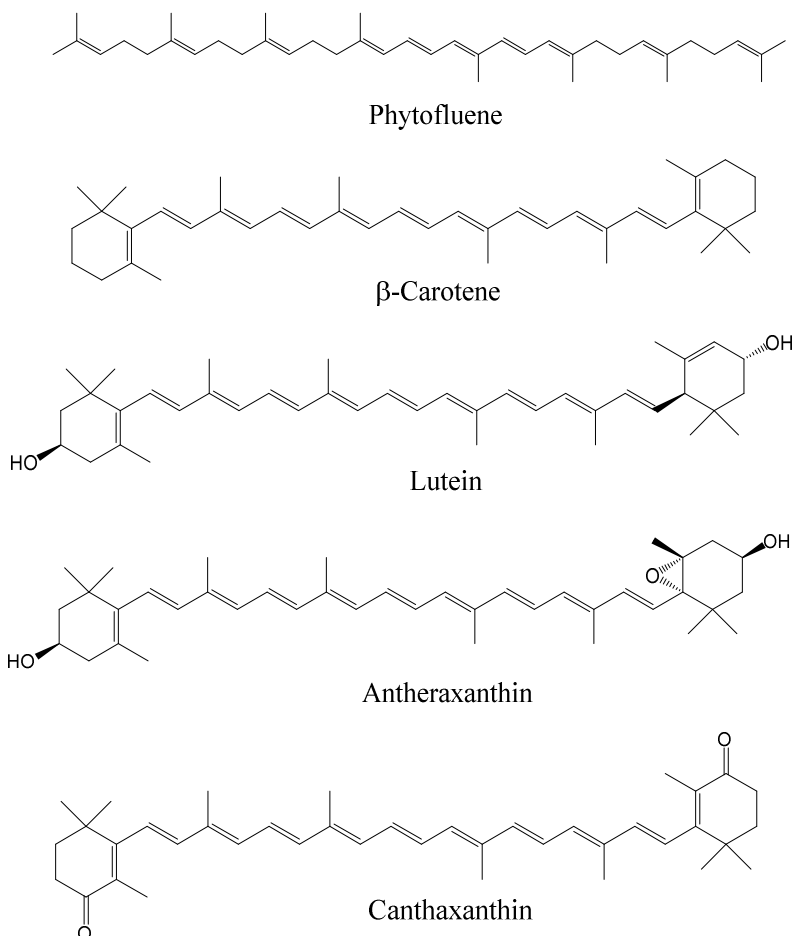


Figure 1.1. Chemical structure of some common carotenoids in the all-*trans*-configuration.

Carotenoids that contain only carbons and hydrogens are classified as carotenes, while oxygenated carotenoids containing hydroxyl, keto and epoxy groups are classified as xanthophylls^{28,30}. Carotenoids of both classes contain two of the seven possible C₉ end groups specified by Greek letter prefixes (ψ , β , ϵ , γ , κ , Φ , and χ)³¹. Carotenes devoid of any polar groups are fat-soluble and extremely hydrophobic. These carotenoids are often restricted to the inner membrane of lipids, except when complex with proteins as carotenoproteins³². Polar functional groups can alter the

solubility properties of carotenoids and influence their interaction with other molecules³⁰.

Each double bond of the polyene chain is capable of existing in either the *cis*- or *trans*- configuration, giving rise to several geometrical isomers²¹. It is common practice to use the *cis* and *trans* prefixes to describe the orientation of two substituent groups relative to the double bond. However, it is more correct to use the *E* and *Z* prefixes when designating the relative orientation of tri- and tetra-substituted alkenes. In nature, carotenoids are primarily found in the *all-E* (*trans*) configuration. It is well documented that the more thermodynamically stable *trans*-isomer is the major form present in fruits and vegetables, although small quantities of the *cis*- or *Z*-isomer can coexist³³. Thermal processing can also induce *trans-cis* isomerization in fruits and vegetable³³⁻³⁴. Due to their non-linear 'kink' structures, *cis*-isomers have greater solubility in mixed micelles and are less likely to aggregate or crystallize; as a result they are more readily absorbed and transported in comparison to their *all-trans* counterparts³⁵.

1.3.2: Functional Roles of Carotenoids in Plants

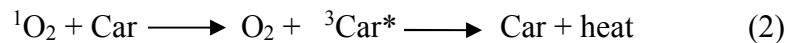
Carotenoids are essential components of the photosynthetic apparatus. Most carotenoids are non-covalently bound to either the core of photosystems I and II (PSI and PSII) or the antenna of light-harvesting complexes (LHCs)^{30,36}. The most abundant carotenoid found in PSI and PSII is β -carotene, while xanthophylls, such as lutein, appear to be the most abundant carotenoid in the antenna of LHCs^{30,36}. During photosynthesis carotenoids perform two principle functions. They serve as

accessory light-harvesting pigments and they are responsible for the photoprotection of the photosynthetic machinery³⁶. Their main role as accessory pigments is to absorb blue-green light energy (400-500nm) that is subsequently transferred to the excited singlet state of a neighboring chlorophyll molecule ($^1\text{Chl}^*$), where it can be transferred to the reaction center of PSII and used in photolysis (splitting of water molecules) (1)³⁶. Or $^1\text{Chl}^*$ can return to the ground state by emitting light (fluorescence) (2), or the $^1\text{Chl}^*$ can be dissipated harmlessly as heat through a non-photochemical quenching (NPQ) process (3)³⁶⁻³⁷. Members of the xanthophyll cycle, which include zeaxanthin, antherxanthin, and violaxanthin, are involved in the pH-dependent NPQ of excess light energy generated in the PSII³⁷⁻³⁸.



Photoprotection, a function of carotenoids that was first observed in bacteria³⁹, has been found to be particularly important for the survival of plants in aerobic environments. Irradiation of chlorophyll under high light conditions can generate triplet excited state chlorophyll molecules ($^3\text{Chl}^*$) that react with molecular oxygen to produce ROS, such as singlet oxygen ($^1\text{O}_2$), superoxide (O_2^-), and hydrogen peroxide (H_2O_2) and hydroxyl radicals ($\text{HO}\cdot$)^{36,40}. The constant production of $^1\text{O}_2$ formed predominately in the reaction center of PSII, is capable of oxidizing chlorophyll as well as proteins, lipids and nucleic acids, which can result in photoinhibition of the photosynthetic apparatus and photobleaching⁴⁰. To circumvent the effects of these

harmful reactions, carotenoids can provide protection in two ways: either by quenching $^3\text{Chl}^*$ (1) or by directly scavenging $^1\text{O}_2$ (2) ^{41,36}.



Carotenoids also fulfill ecological roles in plants by attracting pollinators and seed dispersers to brightly colored fruits and flowers. In addition, compounds derived from the oxidative cleavage of carotenoids, the apocarotenoids, serve as substrates in the production of plant volatiles, phytohormones, flavoring agents and vitamins ^{42, 43} (Figure 1.2). These degradation products, which have shortened carbon skeletons due to the cleavage of carbon-carbon double bonds, can be catalyzed by two different classes of cleavage enzymes. The first class of enzymes, the 9-*cis* epoxycarotenoid dioxygenases (NCEDs), are involved in the biosynthesis of ABA through the cleavage of neoxanthin and violaxanthin at the 11, 12 positions ⁴⁴. The second class of enzymes, the carotenoid cleavage dioxygenases (CCDs), requires Fe^{2+} as a cofactor for activity and are involved in the biosynthesis of strigolactone ^{45, 46}. CCD1 and CCD4 enzymes are associated with the production of several aldehyde and ketone compounds, such as α - and β -ionone, β -damascenone, β -cyclocitral, and geranylacetone ⁴³. These aroma compounds present in roses, petunias, blackberries, raspberries, cantaloupe, oranges, tomatoes, celery, peas, and carrots are also accredited with attracting pollinators and securing adequate seed dispersal ^{43, 47}.

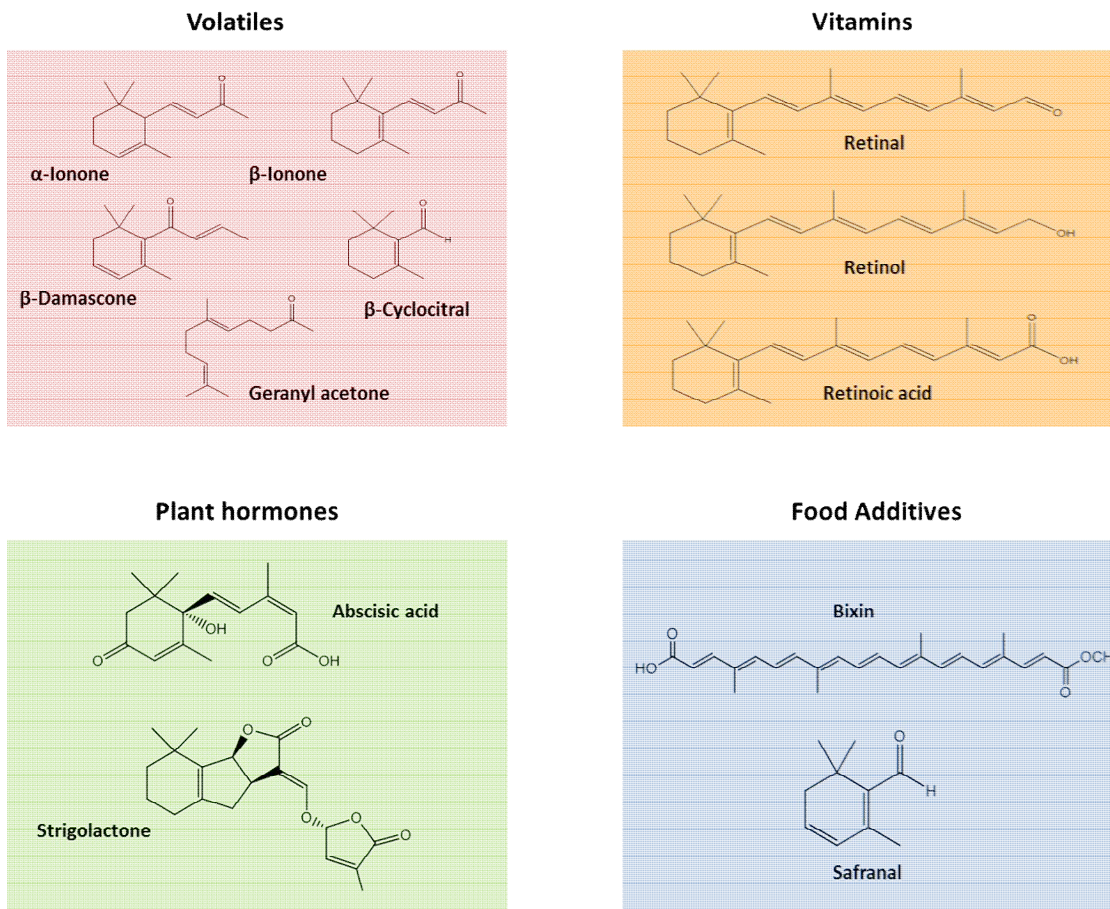


Figure 1.2. Some important apocarotenoids found in plants and animals.

1.3.3: Health Benefits of Carotenoids

Carotenoids cannot be synthesized by people and must be obtained through their diets. Carotenoid-rich foods, such as Brussels sprout, broccoli, carrots, sweet potatoes, pumpkin, tomatoes, watermelon, and apricots, have many health promoting properties. They serve as antioxidants, protecting cells and tissues from oxidative damage and some carotenoids are used as additives and natural colorants in the food and cosmetic industries^{24, 48}. Lutein and zeaxanthin are the two major carotenoids which gives the macular region of the retina its yellow color⁴⁹. These pigments, found in corn, and in leafy greens, such as kale and spinach, help promote visual

performance and maintain optimal eye health ⁵⁰. Berstein et.al show that lutein, zeaxanthin, and their geometric isomers are also present in a number of ocular tissues ⁵¹. In the iris, lutein and zeaxanthin are suspected to play a role in filtering out phototoxic short-wavelength light that can cause age-related macular degeneration of the eye (AMD) ⁵¹⁻⁵². Retinaldehyde, the chromophoric apocarotenoid that results from the oxidative cleavage of any carotenoid containing a β -ring (e.g. γ -carotene, β -carotene, α - carotene, and β - cryptoxanthin), is especially important for the prevention of vitamin A deficiency, nyctalopia (night blindness), xerophthalmia (dry eyes), and cataracts ⁵³. Retinol and retinoic acid, two additional forms of vitamin A, are required for normal skin, bone, and teeth growth and development ⁵³.

1.3.4: Carotenoid Biosynthesis in Plants

All isoprenoids are derived from isopentenyl pyrophosphate (IPP) and its allylic isomer, dimethylallyl pyrophosphate (DMAPP). For many years, it was assumed that these precursors were synthesized exclusively from acetyl-CoA through the mevalonic acid (MVA) pathway in all organisms. However, an alternative 2-C-methylerythritol 4-phosphate (MEP) pathway was discovered by Rohmer using isotope-labeling experiments in plants and bacteria ^{54,55}. Today, the MEP pathway, originally called the non-mevalonate pathway, is well established as an alternative route for supplying IPP to the carotenoid biosynthetic pathway, starting from glyceraldehyde phosphate and pyruvate in the plastids of higher plant systems⁵⁴⁻⁵⁵.

The first committed step begins with the production of phytoene (**1**) from two molecules of geranylgeranyl pyrophosphate, catalyzed by phytoene synthase (PSY)

(Figure 1.3)⁵⁶. Successive desaturation and isomerization reactions catalyzed by phytoene desaturase (PDS), ζ -carotene desaturase (ZDS), and two carotenoid isomerases (CRTISO) produce phytofluene (**2**), ζ -carotene (**3**), neurosporene (**4**), and lycopene (**5**), the red colored pigment associated with tomatoes, watermelon, guava and pink grapefruit (Figure 1.3). Studies show that tangerine tomato accumulates poly-Z- phytofluene, ζ -carotene, neurosporene, and lycopene instead of the all-E-isomer found in most tomatoes⁵⁷. The structures of compounds **1-5** are provided in Figure 1.4. Lycopene, as the branch carotenoid in the pathway can be cyclized at one or both ends of the molecule to yield γ -carotene (**6**), δ -carotene (**7**), α -carotene (**8**) and β -carotene (**9**) (Figure 1.3). The coordinated action of lycopene- β -cyclase (LCYB) and lycopene- ϵ -cyclase (LCYE) leads to the production of α -carotene, which contains two non-identical β - and ϵ - end groups, while two equivalences of LCYB results in the formation of β -carotene with two β -rings (Figure 1.3)⁵⁸. Although the presence of bicyclic carotenoids with two ϵ -rings has been evidenced in lettuce, the existence of these compounds in most plant species is uncommon⁵⁹. The structures of compounds **6-9** are provided in Figure 1.5. Enzyme mediated hydroxylation of α - and β -carotene produces α -cryptoxanthin (**10**), zeinoxanthin (**11**), β -cryptoxanthin (**12**), lutein (**13**), and zeaxanthin (**14**) (Scheme 1.3). α -Carotene is converted into lutein by two hydroxylation reactions catalyzed by β -carotene hydroxylase (LUT 5) and ϵ -carotene hydroxylase (LUT1). On the other side of the pathway, zeaxanthin is generated by addition of hydroxyl groups to the 3,3' position of both β -rings of β -carotene via β -carotene hydroxylases (BOHASE) that belong to the fatty acid hydroxylase family⁵⁹⁻⁶⁰. The structures of compounds **10-12** are illustrated in Figure

1.6. Epoxidation of zeaxanthin by zeaxanthin epoxidase (ZE) generates violaxanthin **(15)**. The reverse of this reaction catalyzed by violaxanthin de-epoxidase (VDE) gives rise to the xanthophyll cycle, which helps plants acclimate to high light conditions. The chemical structures of lutein **(13)**, zeaxanthin **(14)**, and violaxanthin **(15)** are depicted in Figure 1.7. The synthesis of neoxanthin, which represents the final step in carotenoid biosynthesis, is catalyzed by neoxanthin synthase (NSY). Neoxanthin, is also a precursor of the plant hormone, ABA⁵⁹⁻⁶⁰.

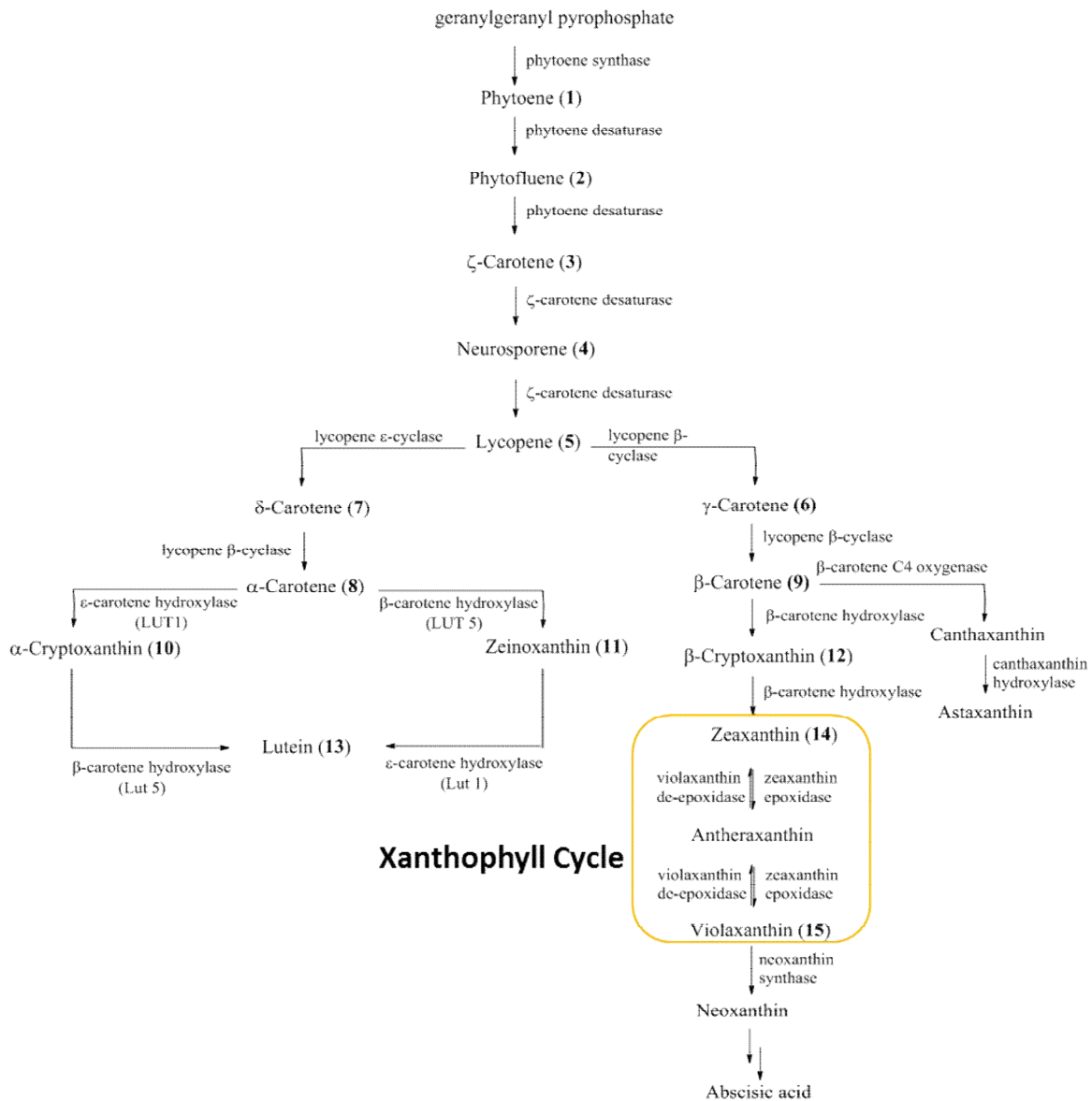
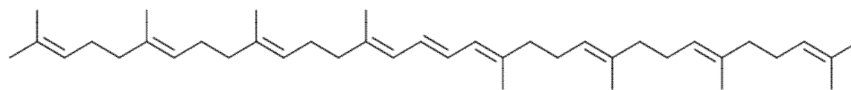
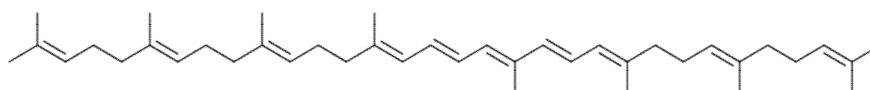


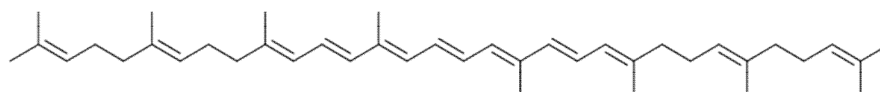
Figure 1.3. Schematic diagram of the carotenoid biosynthetic pathway in higher plants



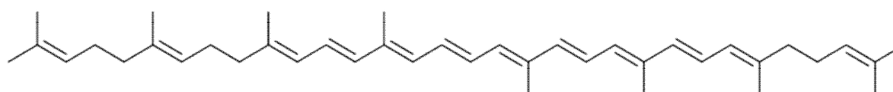
Phytoene [7, 8, 11, 12, 7', 8', 11', 12' -octahydro- ψ,ψ -Carotene] (1)



Phytofluene [7, 8, 11, 12, 7', 8' -hexahydro- ψ,ψ -Carotene] (2)



ζ -Carotene [7, 8, 7', 8' -hexahydro- ψ,ψ -Carotene] (3)



Neurosporene [7,8-dihydro- ψ,ψ -Carotene] (4)

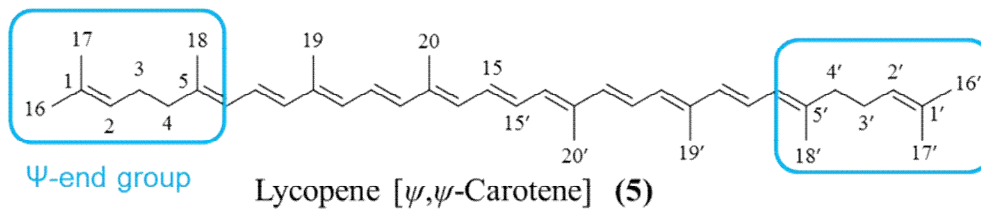


Figure 1.4. Structures of phytoene (1), phytofluene (2), ζ -carotene (3), neurosporene (4) and lycopene (5), illustrating the conventional numbering system and Ψ -end group adopted for acyclic carotenoids.

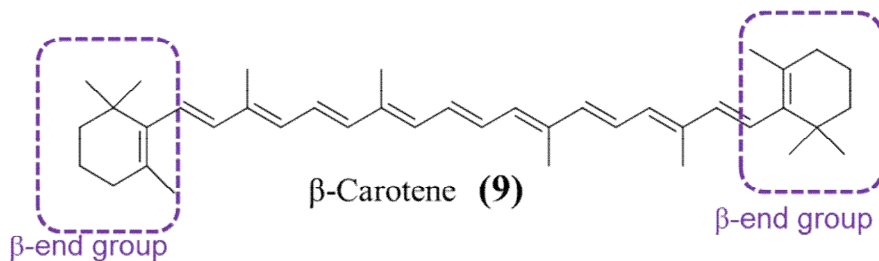
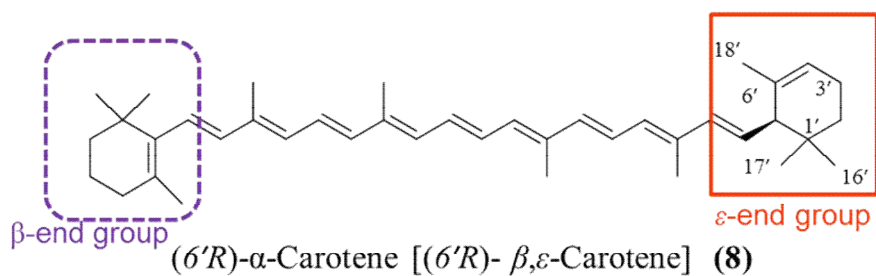
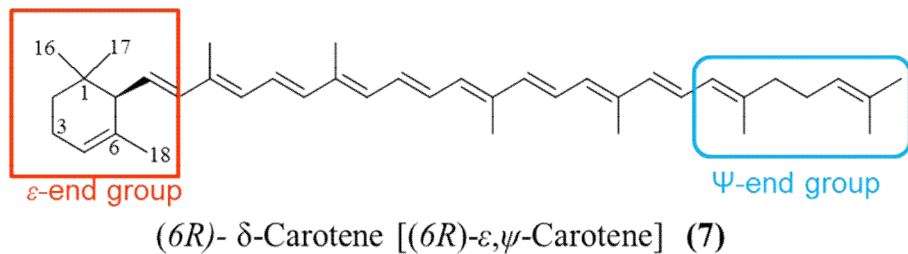
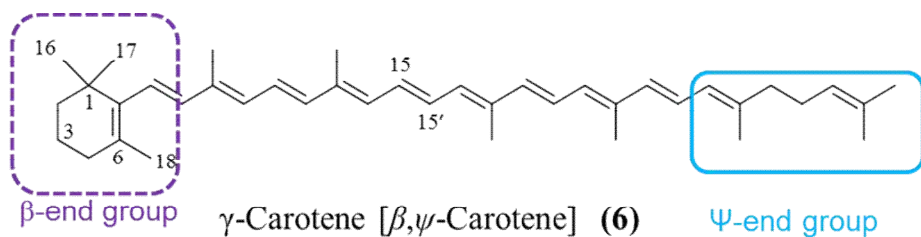
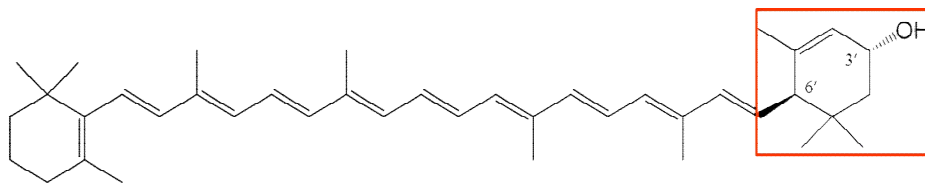
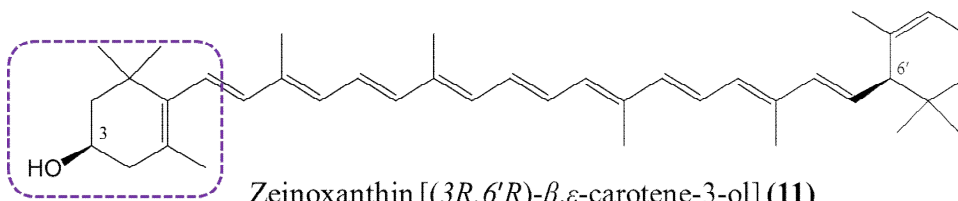


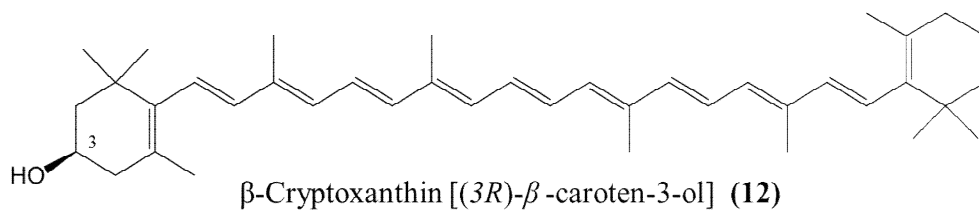
Figure 1.5. Structures of γ -carotene (6), δ -carotene (7), α -carotene (8) and β -carotene (9) with conventional numbering system and definition of β - and ϵ - end groups for cyclic carotenoids



α -Cryptoxanthin [(3'R, 6'R)- β,ϵ -caroten-3'-ol] (10)



Zeinoxanthin [(3R, 6'R)- β,ϵ -carotene-3-ol] (11)



β -Cryptoxanthin [(3R)- β -caroten-3-ol] (12)

Figure 1.6. Structures of monohydroxylated carotenoids, α -cryptoxanthin (10), zeinoxanthin (11) and β -cryptoxanthin (12).

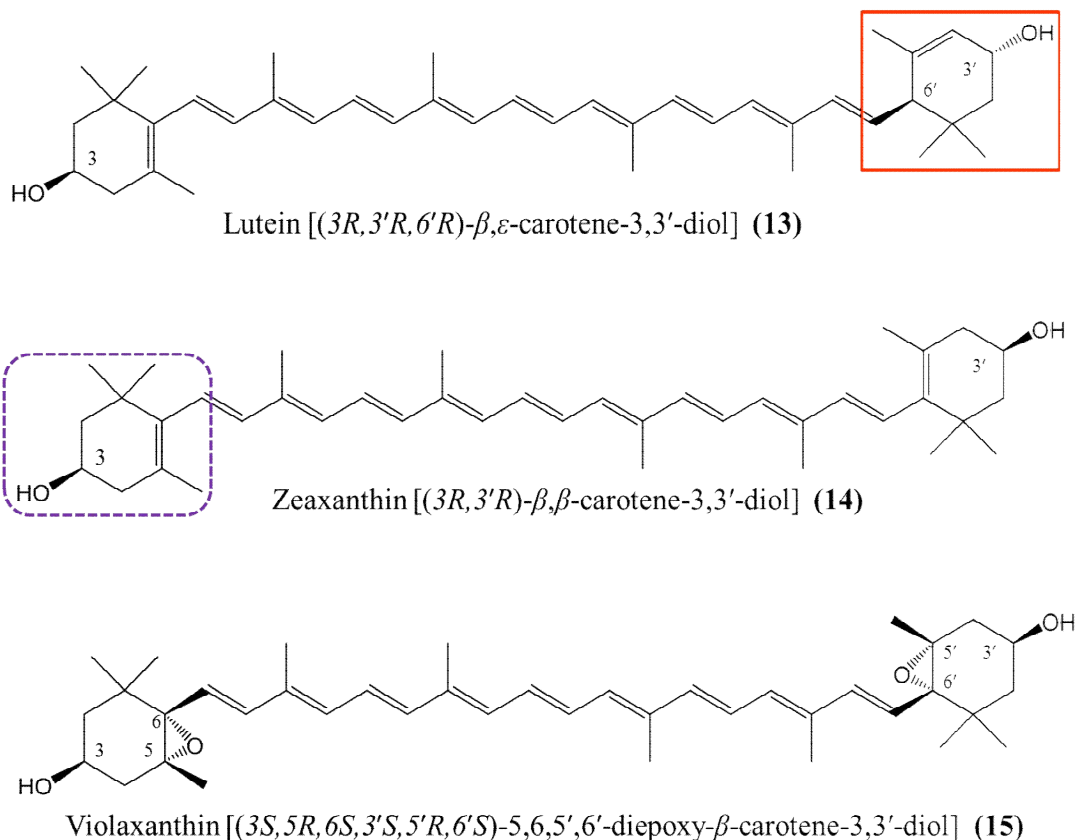


Figure 1.7. Structures of lutein (13), zeaxanthin (14) and violaxanthin (15).

1.4: Effects of Heat Stress on Plant Reproductive Development

In general, male gametophyte development in plants is highly susceptible to elevated temperature⁶¹. Developing and mature pollen present in anthers at peak hours in the day either fail to continue developing, or are damaged, preventing successful completion of the fertilization process. Fertilization results in embryo formation and in strawberry this initiates production of the plant hormone auxin, which is necessary for subsequent growth and development of the embryo, the seed (achene), and the accessory tissues underlying the receptacle that develop into the

strawberry fruit ⁶². In comparison to the male gametophyte, much less is known about how elevated temperatures affect female gametophyte and early embryo development in plants. Because this temperature effect on reproductive structures occurs widely throughout agriculturally important plants, even incremental improvements in tolerance to elevated temperatures in plants would have a global impact on strawberry production by decreasing yield loss and extending the productive season. Previous studies conducted on metabolomic responses to temperature stress in plants, in particular in the model species *Arabidopsis* ⁶³ did not address how carotenoid biosynthesis is affected by such stresses. There are no reports on carotenoid biosynthesis in plant reproductive tissues outside of flower petals and little is understood about the effects of temperature on expression of genes encoding carotenoid metabolic enzymes in these reproductive tissues. Cold temperatures were also found to reduce grain crop during reproductive organ development ⁶⁴, however, no attention was paid in this study to whether cold stress affects ROS scavenging due to an effect on carotenoid metabolism and function in such tissues.

It has been shown that heat stress affects seed production by primarily causing male sterility in *Arabidopsis* and barley ⁶⁵, although no attempt was made to determine if the carotenoid levels in anthers is affected by heat stress, thereby affecting the protection against ROS in these organs. The reproductive organs of strawberry, like those of many other plants and majority of the fruit crops in the Rosaceae family, are yellow to orange in color. Whether carotenoids are present in these tissues primarily to attract insect pollinators, or to protect reproductive structures from oxidative damage, or both, is unclear.

1.5: Some Important Crops of the Rosaceae Family

The Rosaceae or Rose family is the 19th largest flowering plant comprised of over 100 genera and 3,000 species of herbs, shrubs and trees ⁶⁶. This family of medium to large sized plants are widely distributed throughout the world, with many of the species existing in North America, Europe, and Asia. Several beloved, nutritionally valuable, and economically important fruit and nut crops including strawberry (*Fragaria x ananassa*), apple (*Malus domestica*), raspberry (*Rubus*), blackberry (*Rubus fruticosus*), cherry (*Prunus avium* and *Prunus cerasus*), pear (*Pyrus communis*), peach (*Prunus persica*), plum (*Prunus domestica*) and almond (*Prunus dulcis*), belong to the Rosaceae family ⁶⁶. The Rosaceae also contains a variety of ornamental and medicinal plants, such as rose, cherry blossom, pyracantha, and hawthorn.

1.6: The Model Strawberry Plant, *Fragaria vesca*

The cultivated strawberry, *F. × ananassa* ($2n = 8x = 56$), is one of the most genetically complex crop plants to study. Despite its ever growing consumption either fresh or in foods such as smoothies, cakes, pies, and preserves, *F. × ananassa* has an estimated genome size of 708-720Mb ^{67,68}, making genetic studies difficult to perform. An ancestor of the extant diploid woodland strawberry (*F. vesca*) is widely considered to be a progenitor of *F. × ananassa* and is an attractive system for genetic and functional genomic studies in strawberry. Compared to the commercial strawberry, *F. vesca*'s short seed to seed cycle (3-4 month) and smaller sequenced genome (~240Mb) ⁶⁹, permit forward and reverse genetic studies to be more easily

conducted. As a reference plant, strawberry presents other biological and developmental questions that existing plant models such as *Arabidopsis*, maize, and rice cannot address including whether axillary buds produce branch crowns or runners; dormant roots (as an herbaceous perennial); multiple individual pistils; and non-climacteric receptacle fruits. It is an attractive system for plant biologists in general. Transcriptome data from *F. vesca* anthers at several critical stages in development, before and during the stage when carotenoid biosynthesis has become visually evident are available from an ongoing NSF sponsored project that is a collaboration involving Dr. Zhongchi Liu of the University of Maryland, Dr. Janet Slovin of the USDA Agricultural Research Service, and Dr. Nadim Alkharouf, a bioinformaticist at Towson University. In addition, a mutant that has white instead of yellow anthers (Figure 1.8) was found in the M₂ generation of mutant plants resulting from ethyl methanesulfonate treatment of seeds of the inbred *F. vesca* line, 5AF7. Although this phenotype most probably results from a single recessive mutation, genetic analysis is currently underway to confirm this.



Figure 1.8 **A:** 5AF7 wild-type flower center with yellow anthers. **B:** Flower of the 5AF7 pale mutant with opaque white anthers

Work in the Slovin lab to develop the diploid woodland strawberry, *F. vesca*, as a model system for plants in the taxonomic family Rosaceae has documented the

deleterious effects of elevated temperature on flowering and fruit production in strawberry ⁷⁰. The diploid strawberry, with cultivars producing red or yellow berries, was useful for the identification of carotenoids in developing plant gametophytes, for studying how elevated temperatures affect their accumulation, and how this subsequently affects fertility in the commercial octoploid.

1.7: Objectives

The genomics aspects of this dissertation involves identification and annotation of genes in the published *F. vesca* genome that encode enzymes involved in carotenoid biosynthesis, and the analysis of expression of these genes in *F. vesca* reproductive organs. This novel project combines detailed analysis of carotenoids in strawberry plants with structural and functional genomics to build a foundation for understanding the roles of carotenoids in plant reproduction, and the effects of abiotic stresses such as elevated temperatures on carotenoid metabolism and function. Results should be applicable to other fruit producing plants of the Rosaceae family, given that these plants share a common ancestry and genomic similarities. The specific aims of this research were as followed:

1. Identification and characterization of genes in the published *F. vesca* genome sequence with potential to be involved in carotenoid metabolism
2. Comparison of carotenoid profiles in normal and heat stressed reproductive tissues during development.
3. Determination of expression patterns of genes involved in carotenoid biosynthesis during development in *F. vesca* using real-time quantitative PCR (qPCR).

Chapter 2: Selection and Validation of Diploid Strawberry, *Fragaria vesca* Reference Genes for Gene Expression Studies using Real-Time PCR

Abstract

Quantitative real-time PCR (qPCR) can be a highly sensitive and reliable tool for detecting and quantifying gene expression levels, assuming that unregulated and stably expressed reference genes are used for normalization. To date, there are no reports on a validated set of reference genes suitable for gene expression studies in the diploid strawberry, *Fragaria vesca*, or for plants growing under control and moderately elevated temperatures. Using two software applications, geNorm plus qBase, and NormFinder we evaluated the expression stability of ten candidate reference genes in different organs and tissues from plants growing at 32°C day/25°C night, temperatures routinely found during summer months in temperate climates, and from controls growing at 25°C day/20°C night. Statistical analyses revealed that protein phosphatase 2A Subunit A (Fve gene model #03773) and mitochondrial NAD-dependent malic dehydrogenase (Fve gene model #03093) were the most stably expressed reference genes overall in these tissues, and that the combination of these two genes provides the most robust normalization factor. Glyceraldehyde-3-phosphate dehydrogenase (Fve gene model #26415), a widely used reference gene, was identified as the least stably expressed reference gene.

Keywords: *Fragaria vesca*, heat stress, qPCR normalization, reference genes, strawberry

2.1: Introduction

Quantitative real-time polymerase chain reaction (qPCR) can be a useful tool for detecting and quantifying mRNA transcription levels due to its high sensitivity, reproducibility, and broad dynamic quantification capabilities⁷¹⁻⁷². In order to obtain accurate and reliable gene expression data, experimental variability such as variation in sample amount, RNA quality and quantity, as well as differences in enzymatic efficiency in reverse transcription^{71,73}, must be accounted for through normalization. Although there are many different normalization strategies available for quantitative studies^{74,75}, the most widely adopted approach is the use of one or more reference genes as an internal control, because both the reference gene and targeted gene are subjected to the same preparative measures⁷⁴.

Presently, it is customary to use genes such as glyceraldehyde-3-phosphate dehydrogenase (*GAPDH*), actin (*ACT*) or tubulin (*TUB*) for normalizing target gene expression levels because these genes are considered to be ubiquitously expressed in all cells and tissues^{76, 77, 78}. However, many studies have shown that the expression level of these commonly employed genes are regulated by different experimental conditions^{79, 80, 81}. An ideal reference gene should be expressed at a constant level across the samples to be analyzed, and should be unaffected by experimental treatment or conditions used. Several algorithms including geNorm⁸², NormFinder⁸³, qBase⁸⁴ and RefFinder⁸⁵ have been developed for identifying reference genes with the lowest expression variability under a given set of parameters. No studies to date have been able to demonstrate that a universal reference gene, with a constant level of expression across all tissues and experimental parameters, exists. For this reason, the

Minimal Information for Publication of Quantitative real-time PCR Experiments (MIQE) guidelines, designed to increase experimental reproducibility and promote continuity within the scientific community, require that all potential reference genes be validated across tissues and conditions of interest prior to use for normalization⁷³. Initial validation methods focused on securing reference genes for gene expression studies in humans, animals, fungi, and bacteria^{86,87,88}. In more recent years efforts have been extended to include various plant systems^{89, 90, 91}, given their importance as the major source of oxygen and food for all heterotrophs.

Plants, as sessile organisms are constantly surrounded by unfavorable environmental (abiotic) conditions that threaten their existence. Various abiotic stress conditions such as extreme temperatures, flooding, drought, high salinity and even air pollution can cause extensive losses in crop production, reducing yields for most major crops by more than 50%⁹⁻⁹². The ability to feed a growing population that is projected to reach 9 billion by the middle of this century will decline considerably as climates continue to erode already struggling food systems⁹³. To circumvent a global food crisis, research is underway to explore how to improve the adaptability of plants to their environment. Molecular strategies to breed more abiotic stress resistant crops, based on stress-responsive gene expression studies require the use of stably expressed reference genes⁹⁴.

To date, suitable reference genes for abiotic stress response studies have been reported for model and crop plants such as *Arabidopsis thaliana*⁹⁵, potato⁹⁶, wheat⁹⁷, tomato^{80,98}, zucchini⁹⁹ and banana¹⁰⁰. Several studies have attempted to identify stable reference genes in strawberry (*Fragaria* spp.). Clancy *et. al.* validated the use

of *FaENPI* as a reference gene in a number of diploid and octoploid tissues¹⁰¹. More recently, Amil-Ruiz *et al.* carried out an analysis of eleven candidate reference genes for studying strawberry gene expression in response to pathogen attack¹⁰² and Galli *et al.* focused on identifying quality reference genes for quantifying the transcriptional responses of strawberry under drought and salt stress¹⁰³. However, no such evaluation of reference genes for use in studying elevated temperature stress in strawberry has been done.

Production of the dessert strawberry *F. ×ananassa*, which is widely recognized for its aromatic qualities, intense sweet flavors, and nutritional value, is negatively impacted by abiotic stresses. Elevated temperature stress, which is a leading factor in limiting plant productivity, is especially problematic for the growth and development of reproductive organs and the subsequent production of fruit¹⁰⁴. Under elevated temperatures fertilization does not occur and fruit are not formed or do not develop normally¹⁰⁵.

As a model plant for the Rosaceae family¹⁰⁶, the diploid woodland strawberry *F. vesca* is a valuable species for studying how elevated temperatures affect reproductive organ development. An ancestor of *F. vesca* is widely considered to be a progenitor of *F. ×ananassa*⁵, making it an attractive system for genetic and functional genomic studies in strawberry. Compared to *F. ×ananassa*, its short seed to seed cycle¹⁰⁷ and smaller sequenced genome⁶⁹, permit forward and reverse genetic studies to be easily conducted.

The aims of this study were to evaluate the expression pattern of ten candidate reference genes, in different organs (young leaves, petals, receptacles, anthers, and

roots) in strawberry under control and elevated temperatures, using geNorm⁸², the geNorm add-on qBase⁸⁴, and NormFinder⁸³ and to validate the suitability of the selected genes as reference genes for heat stress response gene expression studies in strawberry.

2.2: Materials and Methods

2.2.1: Plant Material

F. vesca inbred line 5AF7 (PI 641092) plants were grown under a 14 hour daylength in controlled environment chambers at the USDA facilities located in Beltsville, MD. Seeds were planted in a mixture of ProMix (Premier Horticulture Inc., PA, USA), Farfard 3B (Conrad Fafard Inc. MA, USA), and coarse vermiculite (The Schundler Co., NJ, USA) (2:1:1) supplemented as needed with dolomitic lime. The growth chambers were maintained at 20°C during the night, with an increase to 25°C over two hours following the onset of light. Temperature was maintained at 25°C until the lights were turned off, when they were ramped down to 20°C over a one hour time period. Lighting was supplied by a mixture of incandescent bulbs and cool white fluorescent bulbs to give 250 $\mu\text{mol}\cdot\text{m}^{-2}\cdot\text{s}^{-1}$ of photosynthetically active radiation. Plants were maintained in 10.2cm pots and periodically trimmed by removing older leaves. Plants were watered daily with a dilute solution of Miracle Grow Tomato Plant Food according to the manufacturer's specifications.

2.2.2: Plant Growth at Elevated Temperature

When plants showed their first inflorescence, one half of them were transferred to a different growth chamber in which the temperature was maintained at 32°C during the day and 25°C at night with ramping as described above. Visible inflorescences were removed from all plants and crowns were trimmed to the youngest fully opened leaf¹⁰⁸.

2.2.3: Tissue Sampling

Leaf samples consisted of young, still folded leaves. Open flowers that developed on new inflorescences were harvested and immediately dissected to give petal, and stamen (anther with filament) samples.

Receptacles with pistils attached were harvested as one sample by cutting across the receptacle above the anther whorl but below the bottom-most pistils. Root samples consisted of the youngest tissue and active growing region (up to 3cm from the root tip). All tissues were harvested between 4:00-6:00 PM and samples were immediately frozen in liquid nitrogen until RNA extraction.

2.2.4: RNA Isolation

Frozen plant tissues were powdered with stainless steel beads in a Qiagen Tissue Lyser (Qiagen, Valencia, CA, USA) before extracting RNA. RNA extractions were carried out using the Qiagen RNeasy kit with slight modification to the manufacturer's instructions in that only 50mg or less of tissue was extracted per sample. Samples were treated with RNase-free DNase (Qiagen) on column. RNA

quality was determined using the Experion lab-on-chip (Bio-Rad Laboratories, Hercules, CA, USA). Samples were additionally checked for DNA contamination by PCR using Qiagen HotStar Taq master mix with intron spanning primers (Supplemental Table 1). The amplification reaction included 35 cycles of 5mins at 95°C, 30 s at 94°C, 1 min at 60°C and 1 min at 72°C. RNA was stored at -80°C until use.

2.2.5: Reverse Transcription and Quality Assessment

cDNA was obtained by reverse transcription of 1 µg of RNA using Superscript® III (Life Technologies, Renton, WA, USA) reverse transcriptase primed with oligo dT in a total volume of 20 µl. Each reaction was carried out in triplicate. The reaction mixture was incubated for 50 mins at 50°C. Inactivation of the Superscript® III reverse transcriptase was carried out by heating the reaction mixture for 5mins at 85°C, followed by treatment with 1 µl of RNaseH and incubation for 20mins at 37°C. The quality of the cDNA was assessed by performing a 3':5' ratio qPCR assay using a phosphatidylinositol 4-kinase sequence (Fve gene model # 12872)¹⁰⁹⁻¹¹⁰. Two primer pairs (PK_F5, 5'-TCATCGGGTGACTCCATTTTG-3'; PK_R5, 5'CAGCAATGGAATCCGACTCA-3'; PK_F3, 5'-GGGTATTGTTTGCCCGAGAA-3'; PK_R3, 5'-TGAGGAAAAAGGTTGTTGAGCTT-3') were designed to amplify two cDNA segments, one from the 5' region (85bp) and one from the 3' region (81bp) of the phosphatidylinositol 4-kinase gene. The amplified sequences are located 1,653bp and 396bp, respectively, from the 3' end of the coding sequence. The ratio of amplification from the 3' reaction to that of the 5' reaction products was calculated

using the comparative quantification method¹¹¹. Ratios for all samples were within the range of 1.03- 3.50 (1.61 ± 0.16 ; mean \pm SEM) and below the 4.43 threshold proposed by Die et al¹¹⁰. Therefore, the cDNAs were determined to be suitable for qPCR analysis.

2.2.6: Candidate Reference Genes and Primer Design

Candidates for reference genes were selected from those suggested by Czechowski et al⁹⁵ and others commonly used for qPCR expression analysis (see Obrero et al. ⁹⁹).

F. vesca homologs were identified by performing a BLAST search of the *F. vesca* genome v1.0 hybrid gene transcripts at the Genome Database for Rosaceae (www.rosaceae.org)¹¹². Gene specific primers were designed using Primer Express 3.0 (Applied Biosystems). Primers were selected that resulted in PCR products between 75-196 bp, with an optimal melting temperature (T_m) of 60°C, and at least a 40% GC content. MFOLD¹¹³ was used to evaluate the formation of stable secondary structures at the sites of primer binding, using the default settings (50 mM Na⁺, 3.0 mM Mg²⁺), and an annealing temperature of 60°C (Figure S1).

2.2.7: Measurement of mRNA levels by qPCR

Relative transcript abundance was analyzed by qPCR in a 20 μ l reaction volume using 1 μ l of cDNA (diluted 1:5), 10 μ l iQTMSYBRGreen I Mix (Bio-Rad) and 250nM gene-specific primers. Reactions were performed on the iQ5 iCycler (Bio-Rad). The cycling conditions were as follows: an initial deactivation step at 95°C for 1min and 30 s followed by 40 cycles at 60°C for 1 min. The absence of multiple amplicon species was confirmed by analysis of the dissociation curve (Figure 2.1). The melting curve program consisted of temperatures between 60°C and 95°C. The

PCR efficiency (E) was estimated using LinReg with data obtained from the exponential phase of each individual amplification plot¹¹⁴⁻¹¹⁵.

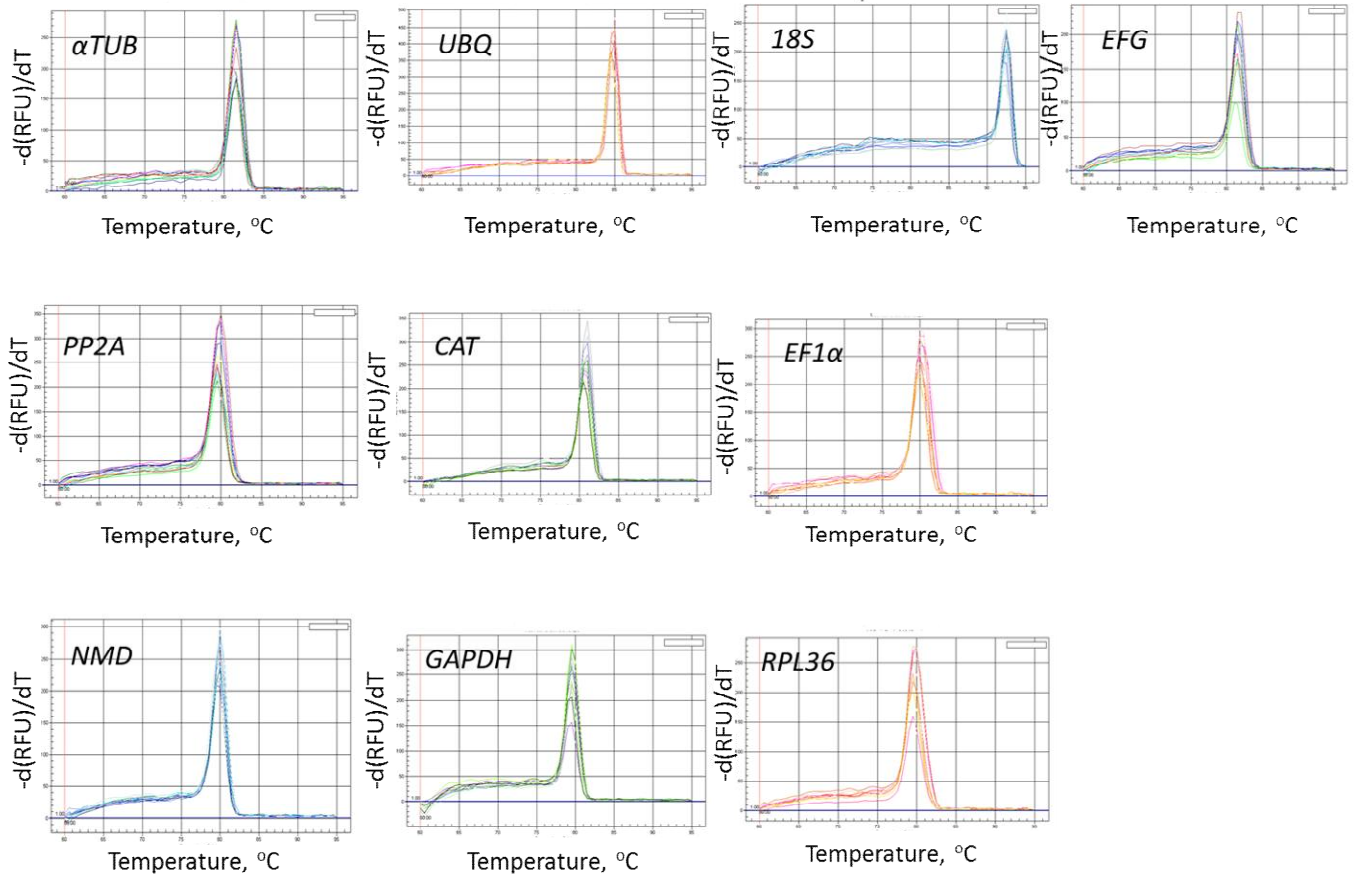


Figure 2.1. Dissociation curves of candidate reference genes showing single peaks.

Table 2.1. General description, *F. vesca* gene number, and biological functions for reference genes evaluated.

Gene Symbol	Gene Name	Function	Strawberry Gene Hybrid Model No. ^a	Arabidopsis Homolog Locus ^b	Amino Acid Identities (%)
αTUB	Alpha tubulin	Cytoskeletal protein	Non-annotated gene ^d	AT1G50010	94
UBQ	Ubiquitin	Protein degradation	09659	AT4G05320	89
18S	18S Ribosomal RNA	Nuclear rRNA transcript ITS1	AF163515 ^c	AT3G41979	96
RPL36	Ribosomal protein L36	Large subunit protein	13245	AT3G53740	85
CAT	Catalase	Decomposition of hydrogen peroxide	10917	AT4G35090	88
PP2A	Protein phosphatase 2A Subunit A	Serine/threonine protein kinase	03773	AT3G25800	90
EF1α	Elongation factor-1 alpha	Translation elongation factor	23217	AT5G60390	96
EFG	Elongation factor G	Translocation of tRNA and mRNA	32259	AT1G62750	84
NMD	NAD-dependent malic dehydrogenase	Mitochondrial cellular respiration	03093	AT2G13560	74
GAPDH	Glyceraldehyde 3-phosphate dehydrogenase	Oxidoreductase in glycolysis and gluconeogenesis	26415	AT3G04120	60

^a *F. vesca* hybrid gene model numbers v1.0. Except for 18S, names are based on similarity to the Arabidopsis homolog

^b The closest Arabidopsis homolog identified using TAIR BLAST(<http://www.arabidopsis.org/Blast/>).

^c Non-annotated gene internal in the opposite sense to the annotated gene 05604, an LRR receptor-like serine-threonine protein kinase. See Figure S1.

^d Genebank accession number.

2.2.8: Data Analysis

Two software applications, geNorm + qBase, and NormFinder were used to evaluate the gene expression stability of the ten candidate reference genes under elevated temperature stress. Average C_q values, acquired from two biological and two technical replicates, were imported into an Excel worksheet and transformed into relative quantities (RQs) using the PCR efficiency of each primer pair and using the sample with the lowest C_q value as the calibrator^{82, 111}. RQ values were then exported into geNorm+ qBase, and NormFinder for analysis.

The geNorm program calculates the expression stability using a pairwise model⁸². This program selects the two most stable genes or a combination of multiple stable genes from a list of candidate reference genes for normalization. The ranking of the genes is based on the stability value (M), where the more stably expressed genes are indicated by smaller M values.

The qBase program, which is an add-on feature of geNorm, calculates the coefficient of variation (CV) of the normalized relative expression levels⁸⁴. This is accomplished by dividing the SEM (of the average normalized RQ) by the average normalized RQ. Genes that exhibit greater variability in expression are indicated by higher CV values.

The NormFinder algorithm relies on an intra and intergroup expression variation model for determining the expression stability of the candidate genes⁸³. Like the geNorm program, stably expressed reference genes are indicated by smaller average expression stability values.

RefFinder⁸⁵ is a web-based comprehensive tool that uses algorithms from four major programs (geNorm, NormFinder, Bestkeeper, and the comparative ΔC_t method) to compare the expression stability of candidate genes. Raw Cq values for each reference are input into the program for direct analysis by the four programs resulting in a recommended comprehensive ranking.

2.2.9: Validation with FveSTI

STI, a stress inducible co-chaperone also known as HOP (HSP70 – HSP90 organizing protein), has been implicated in the eukaryotic response to heat stress ¹¹⁶. An *F. vesca* homolog of a gene encoding STI (Fve gene model # 32258) was chosen as a target gene to validate the different normalization factors (NFs). NFs are based on the geometric average of different reference gene combinations. Primer pairs (forward_5' -GACTGTGACAAGGCTGTTGAAAGG-3' reverse_5' -GGTTGCGATGTTCTGTGAGAGC -3) for FveSTI were verified as described for the reference genes.

2.3: Results

2.3.1: Candidate Reference Genes

To determine the most suitable reference gene for studies of gene expression in strawberry plants growing in moderately elevated temperatures, ten candidate reference genes or sequences commonly used for qPCR were evaluated using cDNAs from control and experimental plants. The candidate genes include a member of the ubiquitin (*UBQ*) gene family, an α -tubulin (*αTUB*) gene, cytoplasmic glyceraldehyde-3-phosphate dehydrogenase (*GAPDH*), elongation factor-1 α (*EF1 α*), and the

interspacer 1 (ITS1) region of the ribosomal RNA transcript (*18S*). Other candidates, chosen from among those evaluated for zucchini⁹⁹, included ribosomal large subunit protein 36a (*RPL36*), elongation factor-G (*EFG*), mitochondrial NAD-dependent malic dehydrogenase (*NMD*), protein phosphatase 2A Subunit A (*PP2A*), and a catalase (*CAT*) gene. The full gene name and general function, gene symbol, *F. vesca* hybrid gene model number, and homologous Arabidopsis gene can be found in Table 1. Primer sequences and reaction characteristics are reported in Table 2. Although all amplifications exhibited PCR efficiency above 100%, ranging from 102.05% for *CAT* to 108.79% for the *PP2A* primer set (Table 2.2), all are within the acceptable range⁷³. PCR efficiencies of the primer pairs reported in Table 2.2 represent the average \pm the standard error of the mean (SEM). Melting curve analyses of the PCR products indicated that a single product was amplified with each primer pair (Figure 2.1).

Table 2.2. Candidate reference genes, primer sequences, amplicon size and T_m , and reaction characteristics

Primer Name	Forward and Reverse Primer Sequence [5' --> 3']	Amplicon Size (bp)	Product T_m ($^{\circ}C$) ^a	qPCR Efficiency ^a	R^{2b}
αTUB	F:CCTACCTACACCAACCTCAACCG R:CACATCCACATTCAAGGCACCATC	185	81.46 \pm 0.04	105.72 \pm 0.03	0.9907
UBQ	F:GACCATTACCCTGGAGGTTGAGAG R:CCCACCACGAAGCCTGAGC	196	84.79 \pm 0.07	106.05 \pm 0.02	0.9990
18S	F:GAAGGATCATTGTCGAAACCTG R:AAGTTCCTTGGCGCAATTC	193	92.42 \pm 0.06	105.59 \pm 0.03	0.9993
RPL36	F:CTGATCGCAAAGGAAAAACCA R:ATACGGTGCAAACCCAGCAA	80	79.73 \pm 0.05	105.51 \pm 0.03	0.9992
CAT	F:TCTGCCCTGCCCTTATTGTC R:CCAAGACGGTGCCTCTGAGT	100	80.71 \pm 0.07	102.05 \pm 0.03	0.9996
PP2A	F:AAACTGCTCCGGTGGTTGT R:CAGCACCTTTGCCACATTGA	75	79.71 \pm 0.07	108.79 \pm 0.03	0.9993
EF1α	F:GCCCCTCCGACTACCACTTC R:CCAGTCTCAACACGTCCAACA	78	80.08 \pm 0.06	106.07 \pm 0.02	0.9993
EFG	F:CACAATTGAGAGGGCTGCAA R:CCCACAAATGGATCGCTCAT	78	81.60 \pm 0.05	104.69 \pm 0.02	0.9995
NMD	F:ACCTGCCATCTTTGCGATGT R:TCCCCACAACAGAGAATGC	78	79.79 \pm 0.07	104.97 \pm 0.03	0.9995
GAPDH	F:GTGGAAGCACCACATGAACT R:GGATCCCTGCCCTCAAAAAC	90	79.50 \pm 0.01	102.13 \pm 0.04	0.9992

^a Average values \pm SEM

^b qPCR efficiencies ($E = \text{slope } 10^{[1/\text{slope}] - 1}$) and correlation coefficients (R^2) were determined using LinReg

2.3.2: Expression Profiles of Reference Genes

The expression profiles of the 10 candidate reference genes were assessed by qPCR. Two separate RNA extractions from pooled tissues were done and separate reverse transcription reactions performed for each control and heat treated tissue to give a total of 20 cDNA samples. Raw quantification cycles (C_q) for all the candidate genes were obtained using the BioRad iQ5 2.1 software. The average C_q values for the reference genes varied from 18.04 for *UBQ* to 31.11 for *GAPDH* in all tested samples (Figure 2.2). The transcript levels of *GAPDH* were about 8599-fold more abundant

than those of *UBQ*, indicating that the tested genes show a wide range of expression levels.

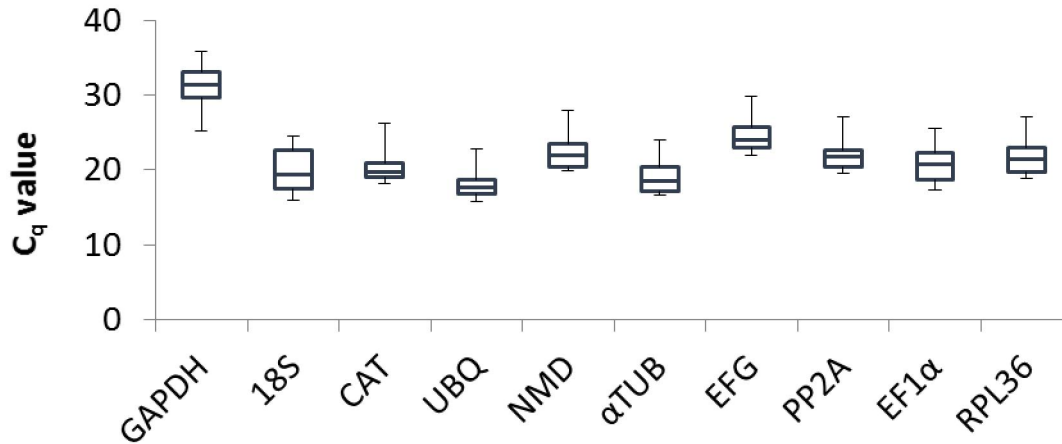


Figure 2.2. qPCR C_q values for the candidate reference genes in all samples. Boxes represent the first and third quartile, while the vertical error bars are indicative of the maximum and minimum C_q values. The central horizontal lines dividing the two boxes represent the median C_q value.

2.3.3: Gene Expression Stability Analysis

For expression stability analysis, C_q values were transformed into RQ values using the PCR efficiency of each primer pair and the sample with the lowest C_q value as the calibrator^{82, 111}. The RQ values were then treated as an input matrix and analyzed using geNorm +qBase, and NormFinder. RefFinder, a web-based comprehensive tool was used to verify results obtained from geNorm+qBase and NormFinder.

geNorm and qBase Analysis

The geNorm program determines the *M* value, a measure of the gene expression stability based on the average-pairwise variation of a particular gene compared with that of all other control genes⁸². More stably expressed reference

genes are indicated by lower M values. qBase, an add on feature to geNorm, was then used to calculate the average CV values for the candidate genes. For heterogeneous panels of cDNAs, stably expressed genes suitable for normalization should maintain average M and CV values that do not exceed 1 and 0.5, respectively⁸⁴. *PP2A* and *NMD* were determined to be the most stably expressed reference genes (Figure 2.3). *GAPDH*, which had the highest calculated M value (2.06) was identified as the most variably expressed gene.

NormFinder Analysis

The NormFinder analysis estimates the expression stability using an intra and intergroup variation algorithm⁸³. Results from both are then combined into a single stability value for each reference gene. Genes that are more stably expressed are indicated by lower stability values. When NormFinder was applied to our data, *PP2A* was identified as the most stably expressed reference gene, followed by *NMD*. *GAPDH* was ranked as the least stably expressed gene (Figure 2.4).

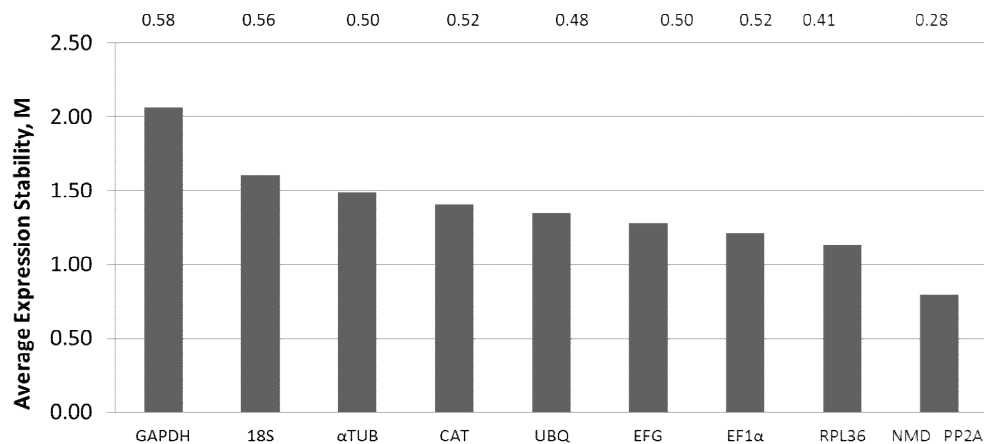


Figure 2.3. Average expression stability (M) of the candidate reference genes evaluated using geNorm. Horizontal numbers across the top represent CV values calculated using qBase.

The two programs used are based on different algorithms, nevertheless, they gave similar results. For geNorm + qBase, and NormFinder, *NMD* and *PP2A* were among the top two most stably expressed reference genes, while *GAPDH* was shown to be the least stably expressed genes. Only slight differences in the ranking of the more variably expressed genes were observed among the results of the three programs. *EFG* was ranked fifth most stable with geNorm + qBase and sixth most stable by NormFinder. Other minor differences among the programs include the ranking of *RPL36* and *CAT*. *RPL36* was ranked third most stable by geNorm and qBase, but fifth by NormFinder. *CAT* was ranked ninth most stable by NormFinder, but more stable (seventh) by geNorm and qBase. The biggest discrepancy among the results from these three programs was the ranking of *UBQ*. *UBQ* was ranked third most stable by NormFinder, but less stable (sixth) by geNorm and qBase.

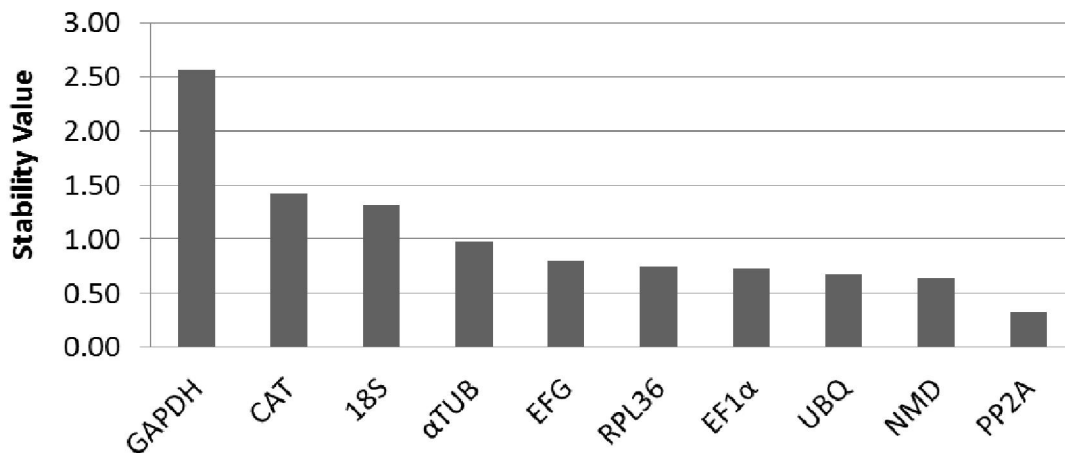


Figure 2.4. NormFinder stability values for candidate genes tested. Reference genes are plotted from least stably expressed (left) to most stably expressed (right).

RefFinder Analysis

RefFinder⁸⁵ was then applied to verify results obtained from geNorm +qBase, and NormFinder. Results from the RefFinder analysis (Table 2.3) were consistent overall with results from independent analyses using geNorm + qBase, and NormFinder. The top two most stably expressed genes, as well as the least stably expressed reference gene, were ranked exactly the same, although there were some differences in the ranking of the other genes.

Table 2.3. Consensus ranking of the reference genes determined using geNorm and NormFinder within RefFinder, and geNorm+qBase and NormFinder as stand alone programs. Rankings are from 1-10, where 1 represents the most stability expressed gene and 10 represent the least stably expressed gene. Numbers shown in parentheses represent rankings from stand alone programs.

Gene Name	Order (Δ Ct Method)	Order (geNorm)	Order (NormFinder)	Ranking Order (Bestkeeper)	Comprehensive Ranking
PP2A	1	1 (1)	1 (1)	2	1
NMD	2	1 (1)	2 (2)	8	2
UBQ	3	5 (5)	3 (3)	1	3
RPL36	4	2 (2)	4 (4)	3	4
EF1 α	5	3 (3)	5 (5)	6	5
EFG	6	4 (4)	6 (6)	5	6
CAT	7	6 (6)	7 (7)	4	7
α TUB	8	7 (7)	8 (8)	7	8
18S	9	8 (8)	9 (9)	10	9
GAPDH	10	9 (9)	10 (10)	9	10

2.3.4: Reference Gene Validation

Currently, scientific articles are still published with results described as being quantitative with only a single reference gene being used for normalization, even

though the under usage of control genes can lead to relatively large errors across samples¹¹⁷, and such practices do not follow the MIQE guidelines⁷³. To demonstrate the impact of inappropriate reference gene selection on conclusions drawn from qPCR experiments, and to validate the suitability of the selected candidate reference genes for normalization, we quantified the abundance of mRNA for stress inducible protein (FveSTI), a known co-chaperone of HSP70/HSP90, in floral tissues (receptacles and anthers) from control plants and plants growing under moderate heat stress conditions. Three NFs were calculated and assessed based on the geometric average of different reference gene combinations: the two most stably expressed reference genes, *PP2A* and *NMD*, identified by geNorm+qBase, and NormFinder (NF₁); the two least stably expressed genes, (*GAPDH* and *18S*), determined by these programs (NF₂); and a single reference gene, *EF1α*, identified in as suitable for hormone and pathogen stressed *F. ×ananassa* samples (NF₃)¹⁰².

Expression analysis using *PP2A* and *NMD* showed that the relative abundance of FveSTI message in receptacles increased in response to elevated temperature. FveSTI transcripts, which were less abundantly expressed in anthers compared to receptacles, showed no apparent difference in heat treated anthers (Figure 2.5A). Expression profile of FveSTI using the two least stable reference genes (*GAPDH* and *18S*) resulted in an overestimation of FveSTI transcript abundance in both control and experimental receptacle and anther tissues (Figure 2.5A) and the samples appeared to have a high degree of variability. When the data was normalized using *EF1α* as a reference gene, the abundance of FveSTI transcripts was calculated to be at higher levels than with NF₁, but not as high as with NF₂ (Figure 2.5A). Figure 2.5B shows

the average CV values calculated for the three NFs. NF₁ exhibited the least amount of variability (CV 21%) while NF₂ showed the greatest (CV 48%) (Figure 2.5B).

Normalization of *FveSTI* expression with NF₃ across control and heat treated samples resulted in an average CV of 26%.

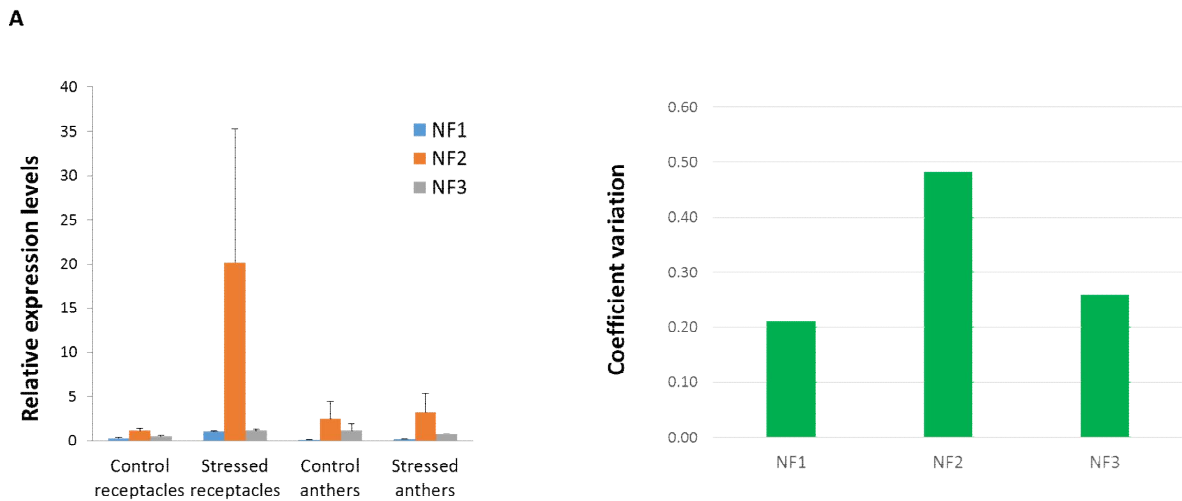


Figure 2.5. A: Expression profile of *FveSTI* in receptacle and anther tissues under control and heat stressed conditions, normalized with three different normalization factors (NF) dependent on the reference gene chosen. NF₁: *PP2A* and *NMD*, NF₂: *GAPDH* and *18S*, NF₃: *EF1α*. Control conditions: (25/20° C). Heat stress conditions: (32/25° C). Error bars indicate standard error of the mean (SEM) from two biological replicates. **B:** Variation in the expression levels of *FveSTI* in receptacle and anther samples are expressed as the average coefficient of variation across the four samples

2.4: Discussion

Accuracy and reproducibility of qPCR gene expression studies are greatly dependent on the reference genes chosen for normalization. To obtain reliable results, it is important to choose reference genes that remain unaffected by experimental conditions used for each experiment. Using reference genes that have not been validated can lead to inaccurate normalization factor calculations and

misleading differences in expression levels for targeted genes. Traditional reference genes such as *GAPDH*, *18S rRNA*, and *Actin*, have been proven to be unstable in many experimental conditions^{76, 95} and, no single reference gene is guaranteed to be stably expressed under all circumstances. Therefore, all potential reference genes must be validated under experimental conditions of interest before using them for normalization. A growing number of publications on selecting reference genes for abiotic stress studies with crop plants have considered the importance of this process for accurate qPCR analysis but such validation studies remain limited for plants in the Rosaceae family. We seek to expand the resources available for gene expression studies in the Rosaceae by examining abiotic stress responses in the diploid strawberry, *F. vesca*. For this study, we used two software applications to evaluate the expression stability of 10 candidate reference genes in 20 total cDNA samples from different organs and tissues of strawberry that were subjected to elevated temperatures.

Prior to performing the qPCR analysis, careful attention was given to preparative steps, which were followed in accordance with the MIQE guidelines. It is known that RNA tissue handling must be carefully controlled to preserve the purity and integrity of the RNA. However, such practices are often overlooked and neglected, resulting in low quality RNA that can strongly compromise the results of downstream applications, which are laborious, time-consuming, and expensive¹¹⁸. To circumvent the acquisition of meaningless gene expression data, careful RNA analysis was conducted using microcapillary electrophoresis with the Experion gene on chip before carrying out gene expression studies. The absence of genomic

contamination, which can lead to an overestimation in the amount of RNA present, was also verified using intron spanning PCR primers. Variations in RNA integrity have also been shown to result in up to 7-fold differences in expression levels¹¹⁸. The expression gene on a chip analysis provides an indirect analysis of the RNA integrity. To obtain a more direct measurement of the mRNA integrity and the quality of cDNA being utilized, a 3' to 5' ratio assay was also performed¹¹⁸.

Once RNA quality parameters were confirmed, expression patterns of the ten candidate reference genes were evaluated using geNorm + qBase, and NormFinder. Our data showed slight differences between geNorm + qBase and NormFinder in the ranking of positions three through nine. Overall, the two programs were consistent in the identification of the top two most stably expressed reference genes (*PP2A* and *NMD*) and the least stably expressed reference gene (*GAPDH*). RefFinder, ranks genes according to the standard ΔC_t method, geNorm, geNorm + qBase, and an additional program, BestKeeper. Based on the results, RefFinder assigns a weight to each gene. It then give an overall ranking by calculating the geometric mean of the weights. The results from RefFinder were consistent with the results from the stand alone programs (geNorm + qBase and NormFinder).

These findings are comparable with the identification of *PP2A* as being among the most stably expressed genes in heat shocked and control *Arabidopsis*⁹⁵, virus infected *Nicotiana*¹¹⁹, and zucchini⁹⁹. *GAPDH* has been found to be the most variably expressed reference gene in strawberry¹⁰³, peas¹²⁰, peach¹²¹ and tomato^{80,98} studies. The minor differences seen in the rankings arise because geNorm assigns stability values based on the assumption that none of the reference genes are co-

regulated⁸² whereas NormFinder, an intra and intergroup variation based algorithm, is more sensitive to the presence of co-regulated reference genes⁸³. Other studies have also reported minor variations in rankings between the two programs^{100,122-123}.

PP2A and *NMD* were the only two genes that had acceptable expression stability values ($M < 1$ and $CV < 0.5$) using geNorm+ qBase. Despite being identified as the third most stably expressed gene, *RPL36* had an M value of 1.13. Inclusion of a third reference gene for normalization would introduce more variability and reduce the accuracy of the gene expression results. Therefore, it was determined that the combination of two genes, *PP2A* and *NMD* provides the most robust normalization factor.

To determine how suboptimal reference genes can influence the conclusions drawn from gene expression analysis, the relative expression levels of *FveSTI* were normalized against three different NFs. The results suggest that *FveSTI* is not regulated by heat stress during reproductive development when normalized against the two most variably expressed genes. *FveSTI* expression normalized with *EF1 α* alone suggests that there are higher levels of *FveSTI* transcripts present in control anthers than in heat stressed anthers although the expression profile of *FveSTI* using the two most stably expressed genes in these same tissues showed that there was no significant differences in *FveSTI* transcript levels.

In summary, analysis of ten candidate reference genes for qPCR analysis of gene expression in tissues from strawberry plants growing at moderately elevated temperatures using geNorm +qBase, and NormFinder identified *PP2A* and *NMD* as the two most suitable genes for normalization. *GAPDH*, a commonly used reference

gene, showed relatively low expression stability across samples and is not recommended for elevated temperature stress studies in strawberry. This work benefits future genes expression studies on elevated temperature stress in strawberry and is applicable to other crops within the Rosaceae family.

2.5: Acknowledgements

The authors would like to thank Dr. José Die (USDA/ARS, Beltsville) for his invaluable advice on performing the experiments and on data analysis, and Samuel S. Jones (USDA/ARS, Beltsville) for his assistance with RNA extraction.

2.6: Supplemental Information

Table S1. Primers used for RT-PCR

Primer Name	Forward and Reverse Primer Sequence [5' --> 3']
GAPDH	F: GAGCATGGCTTCGGCTATAC R: TAGTCATGGTGCCCTTGATG
Tubulin	F: TCTTCAGTGAGACTGGTGCTGGAAAGC R: AAAGCATGAAGTGGATCCTGGGGTATG

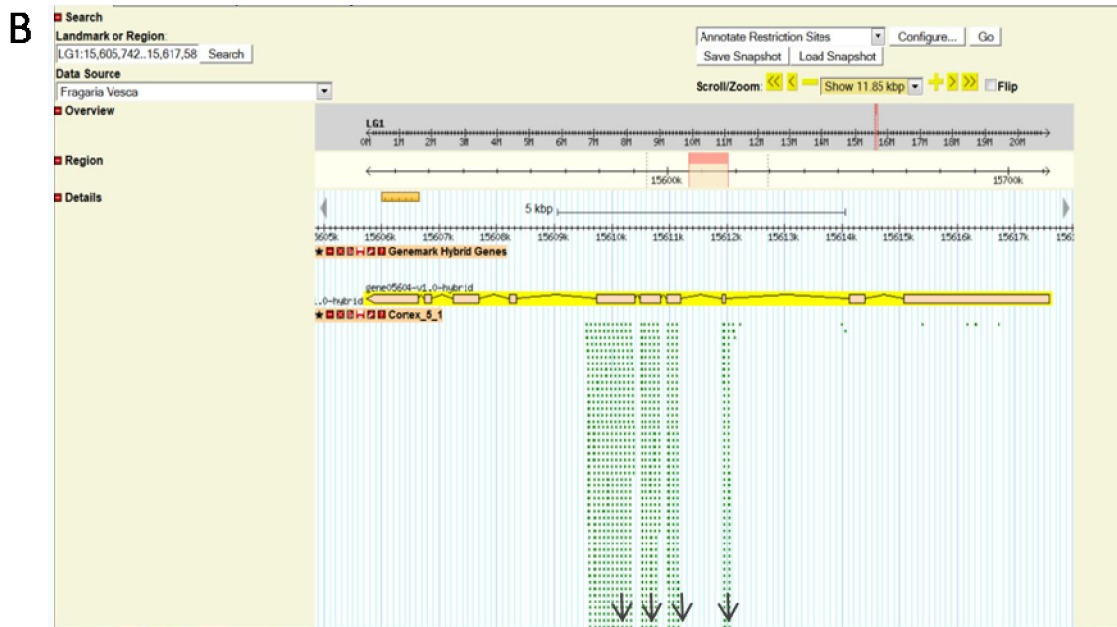
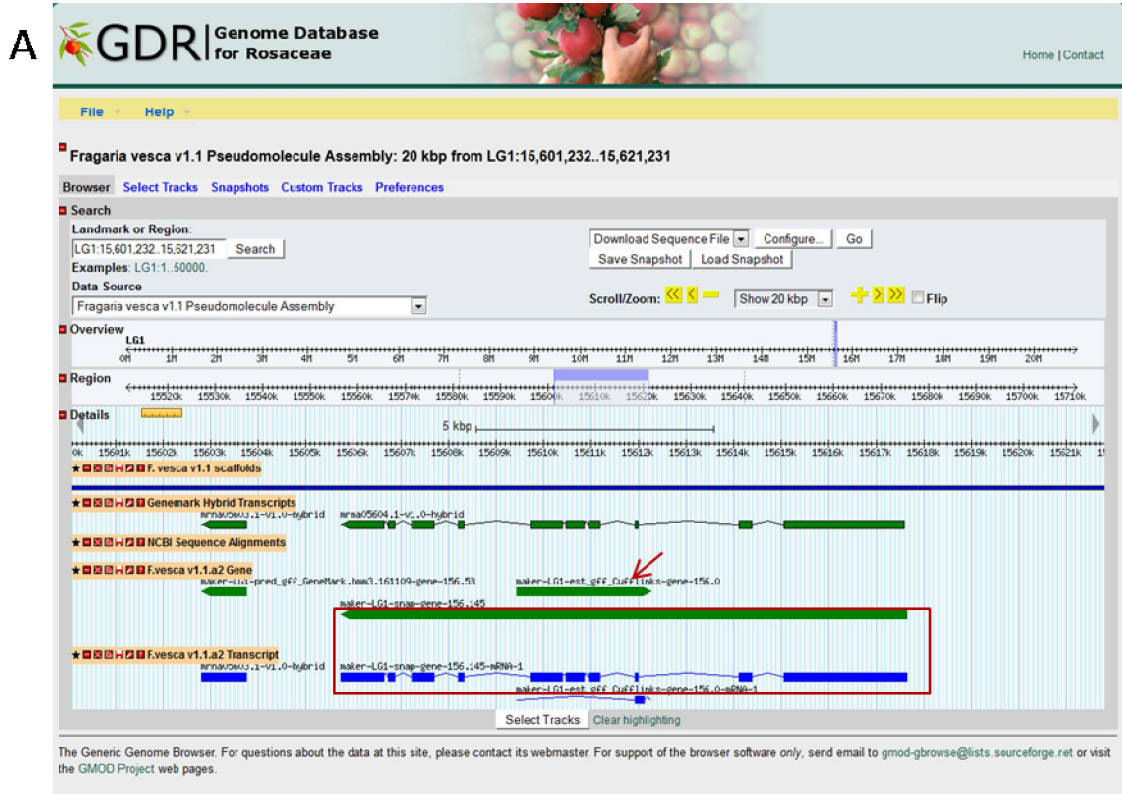


Figure S1. The α -tubulin reference gene is a non-annotated internal sequence of the LRR receptor-like serine/threonine protein kinase gene number 05604. **A:** Screen shot from the GDR genome browser of gene 05604 (red box) and the internal α -tubulin predicted gene (red arrow). **B:** Screen shot from the SGR Genome Browser showing transcript reads (green dashes) from the developing strawberry fruit cortex

mapped to the predicted α -tubulin exons of the LRR gene. Arrows indicate a substantial number of additional reads not included in the screen shot.

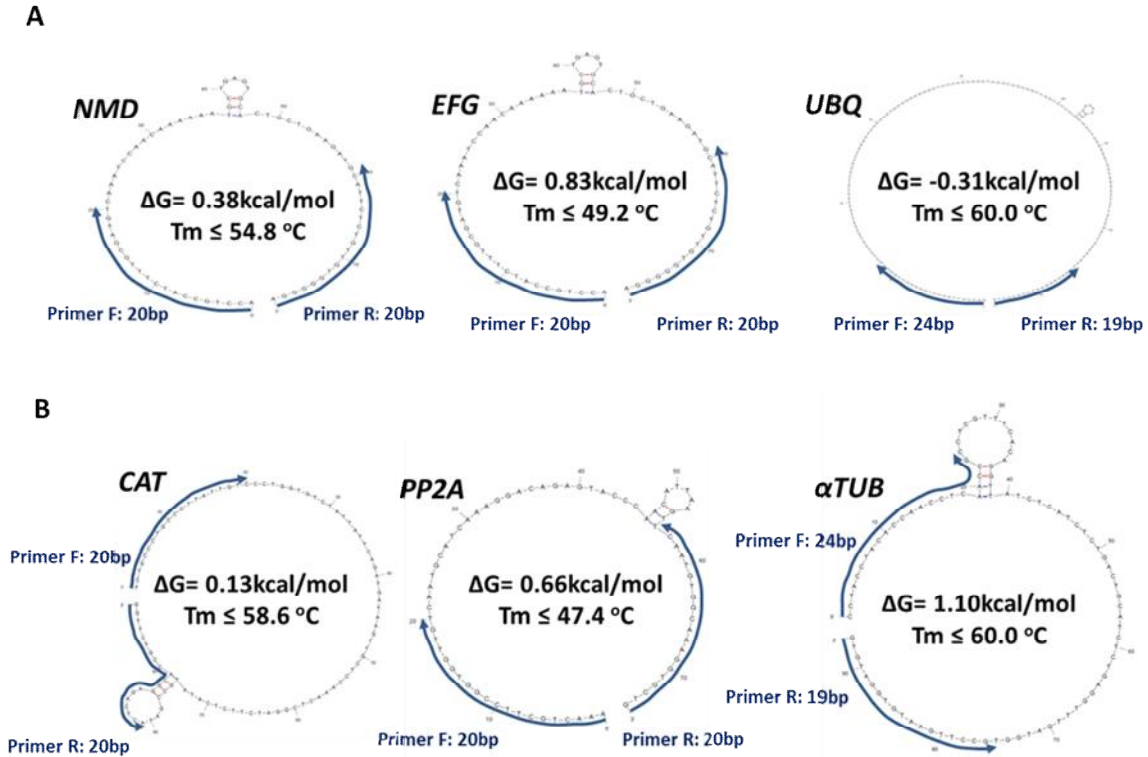


Figure S2. Secondary structures of six representative primer sets illustrating thermodynamic stability (ΔG in kcal/mole) of amplicons. Primers are indicated by blue arrows. **A:** No secondary structures are present where primer anneals and efficient annealing is not hampered by formation of stable secondary structures **B:** The secondary structures at the primer annealing sites have a positive ΔG value and $T_m < 60^{\circ}C$ and does not influence the amplification efficiency.

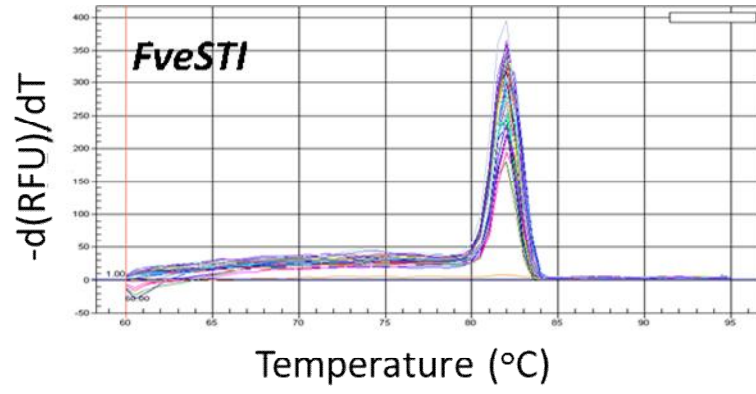


Figure S3. Dissociation curve of targeted gene, *FveSTI* showing a single peak

Chapter 3: Metabolic and Gene Expression Analysis of Strawberry Carotenogenesis in Response to Elevated Temperature

Abstract

Carotenoids are a group of lipid-soluble pigments with many functions in plants. Heat stress, resulting from a rise in temperature beyond a critical threshold for a period of time sufficient to cause irreversible damage, remains a major deterrent for normal plant growth and development and can be especially problematic for reproductive development. Insight into the mechanisms that regulate carotenoid biosynthesis in response to moderately elevated temperature stress is fundamental for developing more heat tolerant crops through breeding strategies. Twelve carotenoid biosynthesis genes in the *Fragaria vesca* genome were identified and characterized in order to examine the effect of moderately elevated temperatures on strawberry anther metabolism during development. qPCR analysis of expression of these genes and targeted metabolic profiling using high resolution LC-MS in leaves, petals, receptacles, anthers, and roots under control and moderately elevated temperature stress showed that gene expression and metabolite accumulation are tissue specific and differentially responsive to elevated temperature stress.

Metabolic analysis identified seven carotenoid compounds. The expression levels of *PDS* were positively correlated with α -, β -, or γ -carotene or lycopene and lutein in heat stressed leaves. *PDS* was also positively correlated with the accumulation of α -cryptoxanthin and lutein in heat stressed anthers.

Keywords: Heat stress, strawberry, *F. vesca*, carotenoids, gene expression

3.1: Introduction

Carotenoids are a class of more than 600 natural lipid-soluble pigments with multiple functions²⁴. As structural components of plants, carotenoids serve as accessory light harvesting complexes and they are responsible for protecting the photosynthetic apparatus against oxidative damage caused by reactive oxygen species (ROS)¹²⁴. Their highly conjugated backbone, which allows them to absorb visible light at various wavelengths, contributes to the yellow, orange, and red colors in a number of flowers, fruits, and vegetables¹²⁵. From a nutrition perspective, carotenoids are recognized as sources of antioxidants, precursors for vitamin A production, and immune modulators for animals and humans, which are incapable of biosynthesizing them *de novo*. Studies show a strong correlation between frequent consumption of fruits and vegetables rich in lutein, zeaxanthin, β -carotene, and lycopene, and a reduced risk for heart disease, visual impairment, and certain forms of cancer¹²⁶⁻¹²⁷.

Carotenoids classified as carotenes (carbon and hydrogen containing carotenoids) or xanthophylls (oxygen-containing carotenoids) are synthesized by all organisms in the plant kingdom, as well as by some bacteria and fungi. In plants, carotenoids are synthesized via the plastidial methyl-erythritol phosphate (MEP) pathway⁵⁶. The first committed step in carotenoid biosynthesis begins with the condensation of two molecules of geranylgeranyl pyrophosphate (GGPP) to give phytoene, catalyzed by the enzyme phytoene synthase (PSY)(Figure 3.1)²²⁻⁵⁹. Dehydrogenation of phytoene, catalyzed by phytoene desaturase (PDS), ζ -carotene desaturase (ZDS), 15-*cis*- ζ -carotene isomerase (ZISO), and prolycopene isomerase (CRTISO) leads to the

formation of all-*trans* lycopene^{128,129}. Lycopene, as the branch carotene in the pathway, can be converted into either α -carotene by formation of non-identical β - and ϵ -end groups, or β -carotene by formation of two β -ionone rings. Lycopene- β -cyclase (LCYB), in concert with lycopene- ϵ -cyclase (LCYE), catalyzes the formation of α -carotene. Two rounds of cyclization of lycopene by LCYB results in the production of β -carotene²²⁻⁵⁹. Subsequent hydroxylations of α -carotene by an ϵ -carotene hydroxylase (EOHASE) known as LUT1 and the β -carotene hydroxylase (BOHASE) called LUT5 produce lutein. In the other branch of the pathway, two dioxygenases with BOHASE activity catalyze the formation of zeaxanthin through the β -cryptoxanthin intermediate (Figure 3.1)²²⁻⁵⁹.

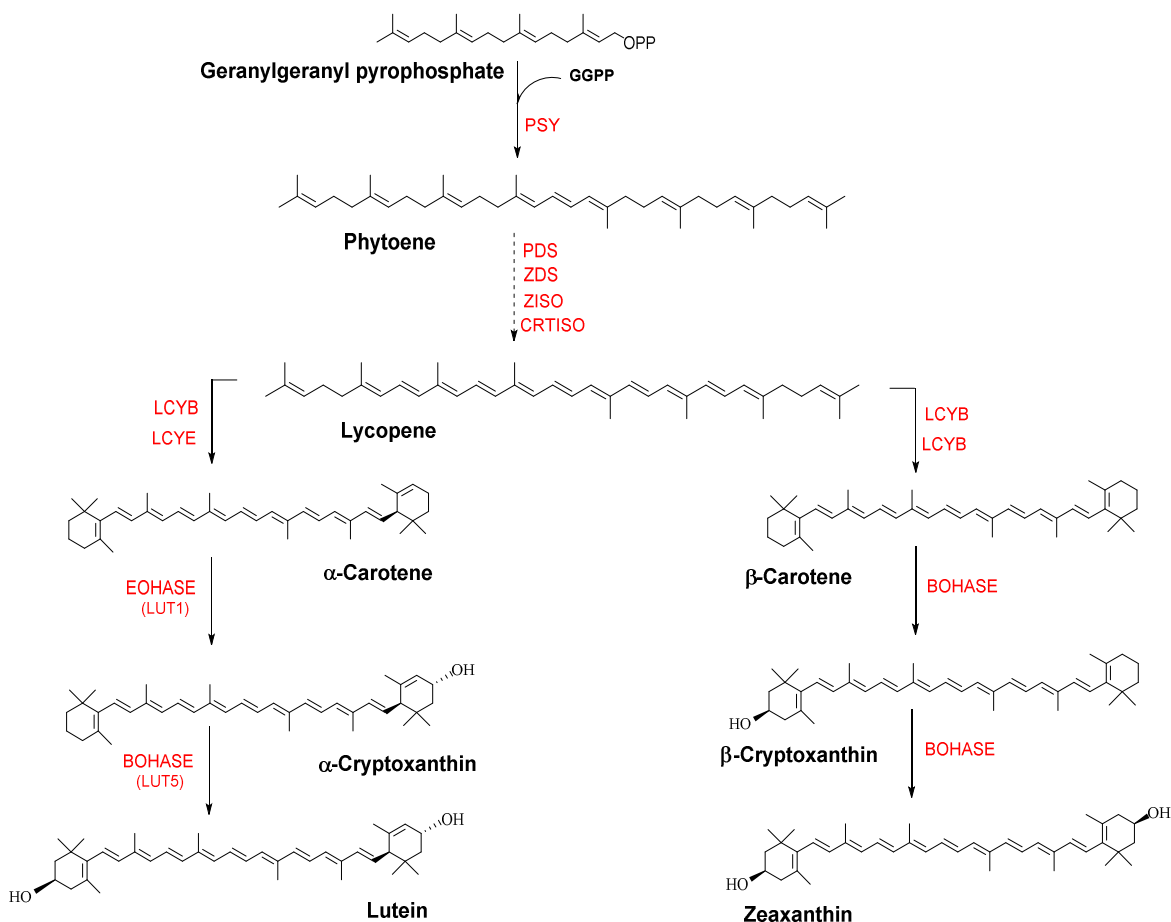


Figure 3.1. The carotenoid biosynthetic pathway in higher plants. Names of compounds are bold and abbreviated names of enzymes are in red. PSY, phytoene synthase; PDS, phytoene desaturase; ZDS, ζ -carotene desaturase; 15-*cis*- ζ -carotene isomerase, ZISO; CRTISO, carotenoid isomerase; LCYB, lycopene- β -cyclase; LCYE, lycopene- ϵ -cyclase; BOHASE, β -carotene hydroxylase; EOHASE, ϵ -carotene hydroxylase.

Research on the physiological roles of carotenoids during plant reproduction has focused on metabolism associated with petal and fruit color, fruit and vegetable nutritional content, flower aroma, or the production of the phytohormones abscisic acid (ABA) and strigalactones^{130,33}. No studies to date have addressed whether carotenoids have roles in mitigating damage in reproductive organs in response to temperature or other abiotic stresses. Threats of climate change due to anthropogenic

emissions of CO₂ and other greenhouse gases make elevated temperature a major concern for agricultural systems⁹³. Heat stress results from an increase in temperature beyond a critical threshold for a period of time sufficient to cause irreversible damage¹³¹, and it disrupts homeostasis as well as limits all phases of plant development⁶¹. One of the major consequences of environmental stress is the production of ROS. It is well known that ROS such as, singlet oxygen (¹O₂), superoxide (O₂⁻), hydrogen peroxide (H₂O₂), and hydroxyl radical (HO·) cause cellular damage by oxidizing protein, unsaturated fatty acids, nucleic acids, and carbohydrates¹³².

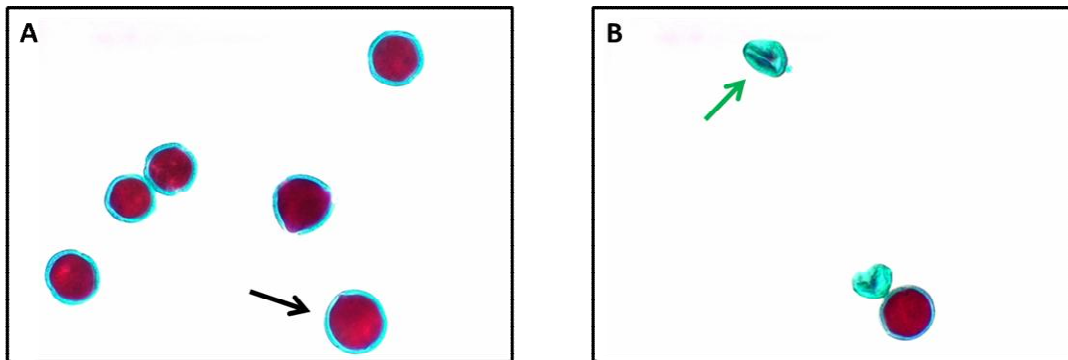


Figure 3.2. Modified Alexander's staining of *F. vesca* 5AF7 pollen from plants growing at **A:** 25°C day/20°C night. **B:** 32°C day/25°C night. Viable pollen stains magenta with a blue perimeter (black arrows) while aborted pollen appears light blue and transparent (green arrow).

The dessert strawberry (*F. ×ananassa*) which is grown throughout the world, is a hybrid of two octoploid species, *F. chiloensis* and *F. virginiana*, and is cultivated for its fruit⁵. Strawberry production depends on the successful development of the reproductive structures and on fertilization, processes that are highly susceptible to

abiotic stresses such as elevated temperature stress¹³³. Alexander's staining of pollen from the diploid strawberry *F. vesca*, Fig. 3.2, shows that moderately elevated temperatures affects pollen production and viability. This results in low rates of fertilization, and fruit are subsequently not formed or develop abnormally¹³³. The diploid woodland strawberry, *F. vesca* has been embraced as the model system for genomic research in strawberries¹⁰⁶. Morphological studies conducted in *F. vesca* show that, like the octoploid dessert strawberry, the flowers of *F. vesca* have orange-yellow anthers, yellow carpels, and yellow pollen¹³⁴ and (Figure 3.3), however the types and role(s) of the responsible pigments are not known.

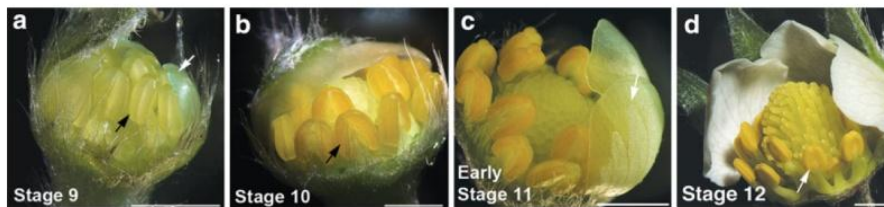


Figure 3.3. Image adopted from Hollender et al.¹³⁴, showing the accumulation of a yellow pigment in anthers during development

Twelve genes involved in carotenoid biosynthesis were identified in the *F. vesca* genome, and their expression profiles in anthers during development during and after meiosis were examined. In light of the negative impact of elevated temperature on pollen production and viability, we examined the effects of elevated temperature stress on expression of these eleven carotenoid biosynthesis genes in floral tissues and leaves in the diploid strawberry, *F. vesca*. In parallel, the effect of heat stress injury on carotenoid accumulation in these tissues was examined. Insight into the functions of known ROS scavengers such as carotenoids in the reproductive structures could

provide the groundwork for breeding or genetically engineering more heat tolerant strawberries and other fruit crops.

3.2: Materials and Methods

3.2.1: Plant Material and Stress Treatment

Plants of *F. vesca* inbred line, 5AF7 (PI 641092) were grown under a 14 hour daylength in controlled environment chambers at the USDA facilities located in Beltsville, MD. The growth chambers were maintained at 20°C during the night, with an increase to 25°C over two hours following the onset of light. Temperature was maintained at 25°C until the lights are turned off, then ramped down to 20°C over one hour. Plants were maintained in 10.2cm pots and watered daily with a dilute solution of Miracle Grow™ Tomato Plant Food according to the manufacturer's specifications. For elevated temperature treatment, seedlings were grown at 25/20°C until plants showed their first open flower. Visible inflorescences were removed from all plants, and crowns were trimmed to the youngest fully opened leaf¹⁰⁸. Five trimmed plants were maintained at 25°C/20°C and five plants were placed at 32°C /25°C for at least three weeks.

3.2.2: Modified Alexander's Staining for Pollen Viability

Pollen viability was analyzed using a modified Alexander's stain¹³⁵. Flower buds or anthers from control (25/20°C) and heat treated (32/25°C) plants were harvested and fixed in Carnoy's solution (ethanol/chloroform/acetic acid, 6:3:1 v/v/v) at room temperature for a minimum of two hours. Buds were manually dissected and anthers were placed on a microscope slide into a drop of Alexander's stain¹³⁵.

Anthers were macerated with a syringe needle prior to being flattened with a coverslip. The slides were gently heated for about 30s over an alcohol flame prior to observation with a Zeiss Axio Scope A1 microscope equipped with an AxioCam camera (Carl Zeiss Microscopy, LLC, USA). The percentage of viable pollen is expressed as the ratio of viable pollen grains to the total grain number. A total of 500 pollen grains were counted from control plants and heat treated plants. Percent viabilities are reported as an average from three replicates of 500 grains each.

3.2.3: RNA Extraction and cDNA Synthesis

Plant tissues, harvested by manual dissection from open flowers between 4:00-6:00 pm, were quick frozen in liquid nitrogen and stored at -80°C. Each sample consisted of tissues pooled from multiple flowers and plants, and some samples consisted of harvests from multiple days. Frozen tissues were powdered with a stainless steel bead in a Qiagen Tissue Lyser (Qiagen, Valencia, CA, USA) before extracting RNA. All RNAs were either immediately stored at -80°C or 1µg of RNA was reverse transcribed using Superscript[®] III (Invitrogen, USA) in a reaction primed with oligo dT as described in the manufacturer's instructions. The absence of genomic DNA was verified by conventional PCR using intron spanning primers for either *FveGAPDH* or *FveTubulin* (Table S1) in a 15 µl reaction using HotStar Plus Master Mix (Qiagen). PCR cycling conditions were as follows: 95°C for 5 mins, 94°C for 30s, 60°C for 30s, 72°C for 1 min for 35 cycles, and a final elongation step at 72°C for 10 mins.

Gene specific primers were designed using Primer Express 3.0 (Applied Biosystems, Foster City, CA, USA). Primers pairs were designed to amplify products

of 75-90 bp, with an optimal melting temperature (T_m) of 60°C, and a GC content of at least 40%. MFOLD (version 3.0)¹¹³, with default settings (50mM Na⁺, 3 mM Mg²⁺), and an annealing temperature of 60°C, was used to verify that the primers selected gave products with minimal secondary structures (Figure S1). Primer pairs for carotenoid biosynthesis genes analyzed in this study are listed in Table 3.1. PCR efficiencies and correlation coefficients (R^2) for each pair were determined using LinReg¹¹⁴.

Table 3.1 Primer sequences for genes involved in carotenoid biosynthesis in strawberry

Primer Name	Forward and Reverse Primer Sequence [5' --> 3']	Amplicon size (bp)	Product Tm (°C)	PCR efficiency ^a	R ²
PSY	F: GGGCCAAATAAAGCGAGCTA R: GCCCACACTGGCCATCTACT	90	81.97	2.00 ± 0.02	0.9952
PDS	F: CGAGACCCGAGCTTGACAAT R: TGGGCGAGGAGAGGATCTAA	80	80.45	2.07 ± 0.02	0.9942
ZDS	F: TCAAGGCAATTGAAGCAAGCT R: GTGCTAGGTCGGCAAAGCA	85	80.58	2.03 ± 0.03	0.9975
LCYB	F: CTGTGAGCAGAAGTGTGGAAAGA R: GCAGAATGGACATGCCAAAA	85	79.99	2.05 ± 0.03	0.9920
LCYE	F: CTCTGGCCAGAAAGGAAA R: GCATGCCCTCAATGTCCATT	85	81.41	2.07 ± 0.02	0.9983
BOHASE1	F: CAGAGCGATTGGCCAAGAAG R: GCCATGGAAGTGATACCAAAGC	85	80.92	2.07 ± 0.02	0.9993
BOHASE2	F: CGAAACAATCTACTTGCCAGAAAA R: CATAACCACGCGTCTCTTTG	90	80.43	1.98 ± 0.01	0.9980
BOHASE (LUT5)	F: ACAAGCCTTTCCGCGTCT R: AGATCAAGCCTGACGAGAATGT	79	86.12	2.04 ± 0.05	0.9971
EOHASE (LUT1)	F: TTGACTCGCTGCATAATGGAAT R: GGAGCACGTCAGCAACTTGA	85	80.51	2.02 ± 0.04	0.9937

^aPCR efficiency($E = \text{slope } 10^{[1/\text{slope}] - 1}$) ± standard error of mean (SEM)

3.2.4: Real-Time Quantitative PCR (qPCR) Analysis

The accumulation of transcripts of nine *F. vesca* genes with homology to Arabidopsis carotenoid metabolism genes was analyzed with an iQ5 iCycler (Bio-Rad) using SYBR Green master mix in a final volume of 20 μ l. The conditions of the program for qPCR were as follows: 1 min and 30s at 95°C, 40 cycles at 60°C for 1 min. At the conclusion of the qPCR experiment, a melting curve analysis was performed over the ranges of 60°C and 95°C to confirm that only a single product was amplified (Figure S2). cDNAs from two biological replicate samples were used for quantitative analysis, and two technical replicates were analyzed for each biological replicate. The relative transcript levels of each gene were normalized to reference genes, NAD-dependent malic dehydrogenase (*NMD*) and protein phosphatase 2A (*PP2A*) based on previous results (Chapter 2). Primer sequences for *NMD* and *PP2A* can be found in Table S1.

3.2.5: Carotenoid Extraction

Tissues for carotenoid analyses were harvested into dichloromethane rinsed, pre-weighed 1.5ml microfuge tubes and the fresh weight of each sample was determined prior to rapid freezing in liquid nitrogen and storage at -80°C. All extractions were performed on dry ice under minimal lighting. Two or three stainless steel beads (1.6 mm diameter) were placed into each tube and 8 times the volume of ice cold analytical grade methylene chloride containing 4 μ M of n-hexadecylbenzamide as the internal standard were added to each tube prior to homogenization at maximum speed for 5 mins in a Geno/Grinder™ 2000

(SpexSamplePrep, Metuchen, NJ, USA). Samples were centrifuged at 10,000 x g for 10 mins at 4°C, then placed on dry ice. Using dry-ice cold pipette tips, the supernatants were transferred to 2 ml amber vials from which 50 µl of extract was loaded into autosampler vials for LC-MS.

3.2.6: Analysis of carotenoids by LC-MS

Carotenoids were analyzed using a DionexUltiMate®3000 RSLC UHPLC system coupled to a Q Exactive™ Hybrid Quadrupole-Orbitrap Mass Spectrometer (Thermo Fisher Scientific, San Jose, California). Samples, 0.25 µl, were injected onto an Agilent Zorbax SB-CN1.8 µm (2.1 x 100 mm) column, operated at 23°C. The mobile phase consisted of 0.1% formic acid in water (v/v) as solvent (A) and 0.1% formic acid in acetonitrile (v/v) as solvent (B). The gradient conditions of the mobile phase were 65% B at 0 min, 95% B at 5 min, 95% B at 7 min, and 95% B at 12 min with a flow rate of 0.4 ml/min. Analytes were detected using an electrospray ionization (ESI) interface operated in positive mode. The conditions of the ESI source were as follows: spray voltage, 3.8kV; capillary temperature, 350°C; probe heater temperature, 375°C. Tuning and calibration was performed before sample analysis. For full scan MS analysis, the spectra were recorded from 340-610 m/z. Data acquisition and processing were performed using XCalibur™ (ThermoFisher Scientific). Metabolites were identified by comparing their retention time and mass spectrometric fragmentation pattern with those of reference compounds. Relative quantities of the identified carotenoids were calculated as the ratio between the peak height of each compound and the peak height of the n-hexadecylbenzamide

(m/z=346.3108) standard. Relative quantities are reported as an average from three biological replicates \pm SEM.

3.2.7: Carotenoid Biosynthesis Gene Identification and Sequence Analysis

Genes identified as encoding enzymes in the carotenoid biosynthetic pathway in Arabidopsis were found by searching the publicly available literature, the TAIR website (www.arabidopsis.org) and the National Center for Biotechnology Information (NCBI) protein and nucleotide databases. Arabidopsis nucleotide and protein sequences were then used to search the strawberry genome using the Basic Alignment Search Tool (BLAST)¹³⁶ at Genome Database for Rosaceae (GDR: www.rosaceae.org)¹³⁷. The gene structures of the identified GeneMark hybrid¹³⁸ strawberry gene models were visualized using the Strawberry Genome browser at GDR. Protein and nucleotide sequences were aligned and compared using CLUSTAL W¹³⁹. The NCBI Conserved Domain Database was used to search protein sequences for conserved domains and motifs¹⁴⁰. Molecular weights of deduced proteins were calculated using the compute pI/Mwtool at the ExpASy: SIB Bioinformatics Research Portal¹⁴¹ and the presence of a signal peptide was predicted using ChloroP¹⁴². Information regarding gene structure was obtained by comparing the cDNA sequence of each gene obtained at Strawberry Genomic Resources¹¹² (SGR: <http://bioinformatics.towson.edu/strawberry/Default.aspx>) with the corresponding genomic sequence.

3.3: Results

3.3.1: Pollen Viability

Both pollen viability and the production of mature pollen grains are affected by elevated temperature. The percentage of viable pollen was determined as the ratio of the number of viable grains to the total grain number counted. Viable pollen grains stained with Alexander's stain appear magenta-red with a blue perimeter; while aborted pollen grains appear pale blue or translucent (Figure 3.2). Almost 100% of the pollen in control plants stained as viable whereas one quarter of the pollen from plants exposed to elevated temperatures stained as aborted (Table 3.2). In addition, the number of grains per anther was substantially lower in the plants exposed to higher temperatures. Three anthers from control plants were sufficient to count 500 pollen grains, while eleven anthers from heat treated plants were required to count the same number of grains.

Table 3.2 Percentage of viable pollen in control plants and plants growing at elevated temperature

Sample	Conditions	Non-aborted pollen (%)
Control	25°C day/20°C night	96.9 ± 0.3
Heat treated	32°C day /25°C night	76.0 ± 2

Values are the mean ±standard deviation from three replicates of 500 grains

3.3.2: Identification of Carotenoid Biosynthesis Genes in Strawberry

To identify carotenoid biosynthesis gene homologs in strawberry, nucleotide and protein sequences acquired from the Arabidopsis genome were used to query the

strawberry genome using BLAST¹³⁶ at GDR¹³⁷. In all, twelve genes were identified. Gene nomenclature follows that in *Arabidopsis*⁵⁹ (Table 3.3). Full and abbreviated gene names, gene model number, gene length, protein length, protein size and chloroplast transit peptide cleavage sites are listed in Table 3.3. Two *F. vesca* genes with homology to one of the *Arabidopsis* carotenoid isomerases¹⁴³ were identified.

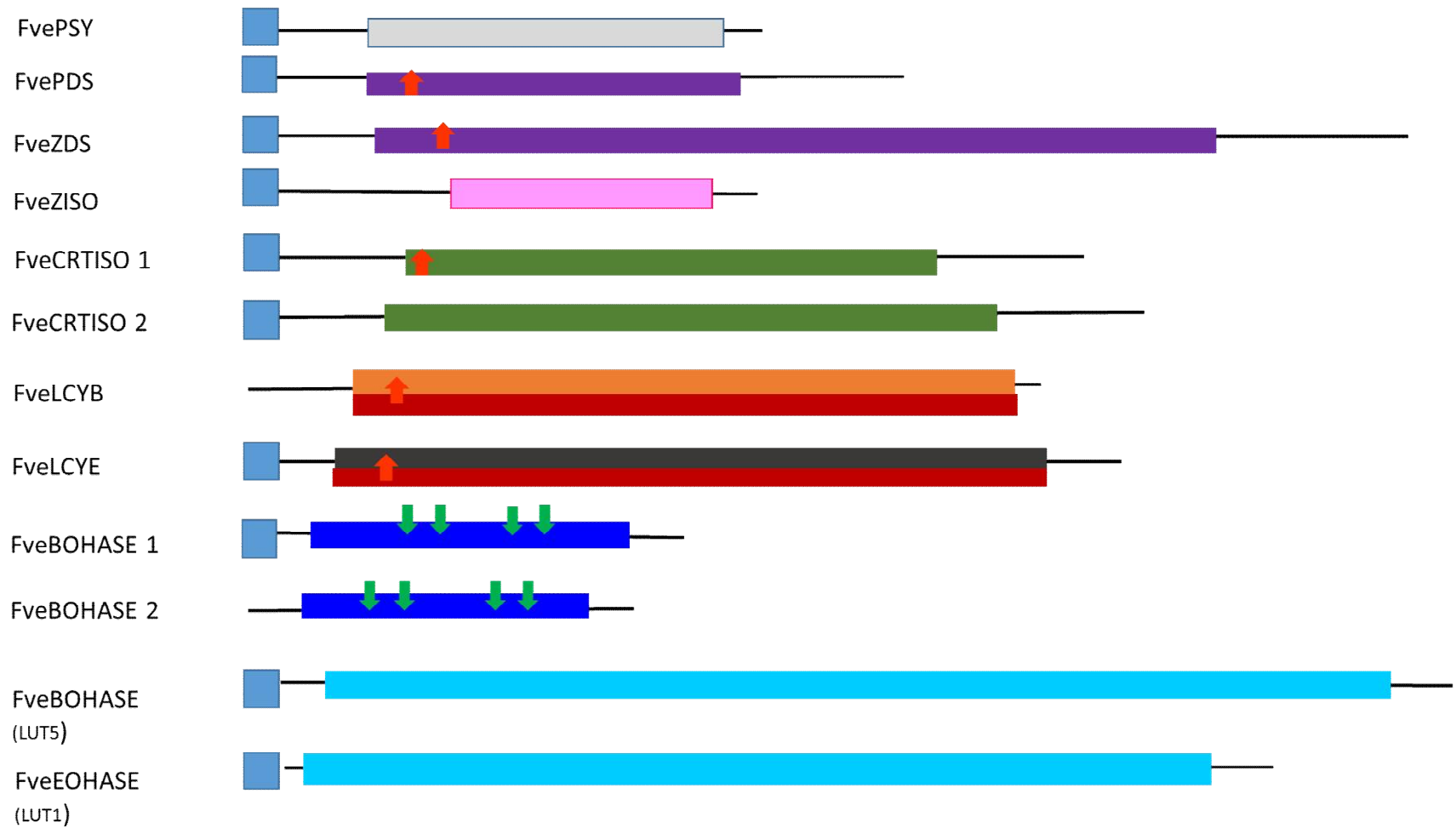
Six of the eleven genes identified are on chromosome 6 (Table S2). Two genes (*LCYE* and *BOHASE1*) are located on chromosome 7, and the desaturases (*PDS* and *ZDS*) are located on chromosomes 4 and 1, respectively. Comparison of the full length cDNA sequences with the corresponding genomic DNA sequence revealed that *LCYB* is the only one of the eleven genes with no introns (Table 3.3). Intron numbers for the remaining ten genes ranged from 4 to 17. Analysis of the cDNA sequences showed that *BOHASE* (LUT 5) has the longest ORF; 2,223 nucleotides encoding 740 amino acids with a calculated molecular mass of 83.43 kDa. *BOHASE* 2, with the shortest ORF; 879 nucleotides encoding 292 amino acids, has a calculated molecular mass of 32.79 kDa (Table 3.3). Conserved domains and motifs are represented for the different *F. vesca* carotenoid biosynthesis enzymes in Figure 3.4. A chloroplast transit peptide sequence could be identified for all except *LCYB* and *BOHASE* 2. The *trans*-isoprenyl pyrophosphate synthase domain, which is responsible for catalyzing the formation of phytoene, is present as expected in *PSY*. The Rossmann fold domain, found in a number of dehydrogenases involved in redox reactions in glycolysis, the Krebs cycle, and photosynthesis, is comprised of a series of alternating β -sheets and α -helices that bind dinucleotides, such as flavinadenine dinucleotides (FAD), nicotinamide adenine dinucleotide (NAD), and nicotinamide

adenine dinucleotide phosphate (NADP)¹⁴⁴. A dinucleotide binding site specific for NAD(P)H is predicted by the presence of a Rossmann fold in both of the desaturases, the cyclases, and one of the isomerases (CRTISO1). PDS and ZDS also have domains associated with flavin containing amino oxidase activity, which catalyzes the oxidation of phytoene to yield ζ -carotene and prolycopene, respectively. LCYB and LCYE have a conserved region identified as the lycopene cyclase motif. BOHASE2 lacks an identifiable signal peptide although it and BOHASE1 each have four transmembrane domains, consistent with being an integral part of membrane systems. Both enzymes also have conserved domains identified as having β -carotene and fatty acid hydroxylase activity.

Table 3.3. *F. vesca*, Hawaii-4 genes encoding enzymes involved in carotenoid biosynthesis

Full Gene Name	Abbreviated Gene Name	Gene No. ^(a)	Gene Structure (kbp) ^(b)	cDNA Structure (bp) ^(c)	No. of Introns ^(d)	Protein Length (aa) ^(e)	Mol Wt (kDa) ^(f)	cTP Length (aa) ^(g)
Phytoene synthase	PSY	28765	2.464	1197	4	398	45.11	55
Phytoene desaturase	PDS	16877	8.019	1521	10	506	55.84	79
ζ-Carotene desaturase	ZDS	16518	5.568	1833	14	610	67.30	73
15-cis ζ-Carotene isomerase	ZISO	22287	2.588	1116	3	391	44.03	92
Carotenoid isomerase 1	CRTISO1	18138	4.812	1743	11	580	63.81	70
Carotenoid isomerase 2	CRTISO2	29208	4.082	1710	8	569	61.55	62
Lycopene-β-cyclase	LCYB	21899	1.494	1494	0	497	55.84	NI
Lycopene-ε-cyclase	LCYE	12683	2.940	1692	10	543	60.42	12
β-Carotene hydroxylase 1	BOHASE1	13195	1.695	936	6	311	34.91	59
β-Carotene hydroxylase 2	BOHASE2	31824	1.582	879	6	292	32.79	NI
β-Carotene hydroxylase	BOHASE (LUT5)	16768	6.872	2223	17	740	83.43	42
ε-Carotene hydroxylase	EOHASE (LUT1)	00959	3.801	1707	8	568	63.42	75

- ^(a)GeneMarkPlus hybrid gene model number
- ^(b) Length of the genomic DNA in kilobase pairs
- ^(c) Length of coding sequence in base pairs
- ^(d) Number of introns within gene
- ^(e)Length of translated protein in amino acids
- ^(f) Calculated molecular weight of polypeptide in kilodaltons using ExPASy
- ^(g)Predicted length of the chloroplast transit peptide sequence using ChloroP1.1. (NI) denotes that a transit peptide sequence was not identified by ChloroP.



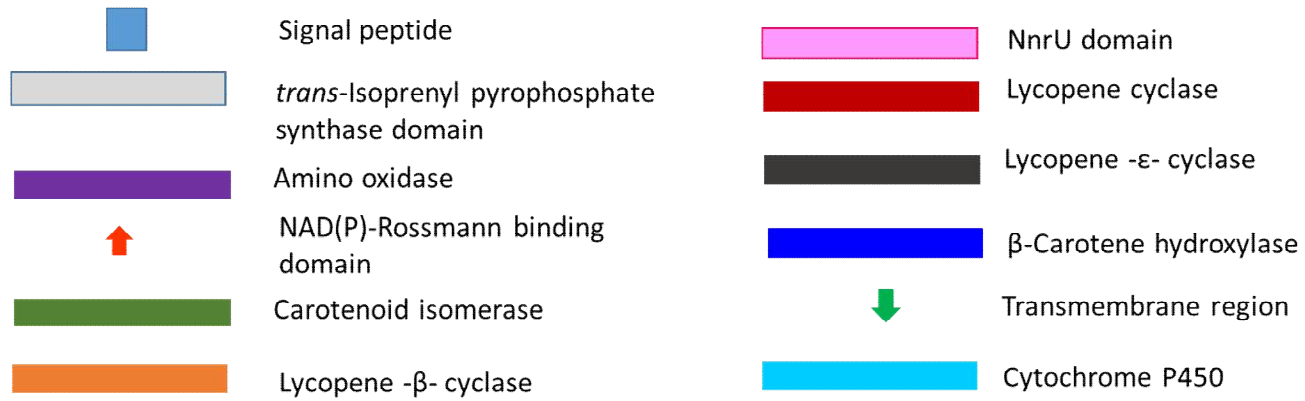


Figure 3.4. Conserved domains in the *F. vesca* carotenoid biosynthesis protein. Protein domains are not drawn to scale

3.3.2: Expression of Carotenoid Biosynthesis Genes During Anther Development

The expression profiles of eleven genes encoding enzymes in the central carotenoid biosynthetic pathway (*PSY*, *PDS*, *ZDS*, *CRTISO1*, *CRTISO2*, *LCYB*, *LCYE*, *BOHASE1*, *BOHASE2*, *BOHASE(LUT 5)*, and *EOHASE (LUT 1)*), were examined with RNA seq data from diploid strawberry anthers at five stages of flower bud development beginning just before meiosis (stages 7-8), progressing through meiosis (stage 9), and through stages 10, 11 and 12, when visual assessment showed the progressive accumulation of yellow/orange pigment(s) (Figure 3.3). The transcriptome data were collected as part of a larger project (Hollander *et al.* 2014)¹³⁴ to obtain transcriptome information from different floral tissues throughout floral development, and are expressed as reads per kilobase of transcript per million mapped reads (RPKM)(Table 3.4).

The accumulation of *PSY* transcripts in anthers increased almost 5 fold between stages 9 and 10, reaching the maximum level in anthers at stage 11, coinciding with the visible change in anther color from translucent and very pale yellow to opaque and dense yellow. Several genes in the pathway followed a similar expression trend except that maximal transcript levels were seen one stage earlier (stage 10). Transcripts of *PDS*, *ZDS*, and *LCYE* increased in abundance between stage 7-8 and stage 9, peaking in accumulation at bud stage 10. *CRTISO1* and *LCYB* appear to follow this general trend as well, except at lower levels of accumulation. However, not all of the genes examined follow this trend. *CRTISO2*, as well as *BOHASE1* and *EOHASE* exhibited low but constant levels of transcript accumulation throughout development. *BOHASE 2* transcripts, required for the production of zeaxanthin, are

hardly detected until the later stages of development, reaching a maximum level at stage 12. Conversely, *BOHASE 1* transcripts were detected maximally in anthers at early stages (7-8). Low levels of transcripts associated with PSY and PDS, but above the 0.5 threshold, were detected in mature pollen (Table 3.4).

Table 3.4. Expression of carotenoid biosynthesis genes in developing anthers of *F. vesca* 5AF7^a

Name	Bud Stage 7-8	Bud Stage 9	Bud Stage 10	Bud Stage 11	Bud Stage 12	Mature Pollen
<i>PSY</i>	40.45	44.75	214.60	293.40	180.75	1.23
<i>PDS</i>	28.85	58.45	150.10	35.55	31.75	5.85
<i>ZDS</i>	22.20	63.90	180.40	43.25	45.15	0.25
<i>ZISO</i>	19.68	22.26	91.13	15.89	5.14	0.00
<i>CRTISO1</i>	7.58	9.51	14.11	6.42	4.28	0.00
<i>CRTISO2</i>	3.38	2.01	1.67	0.33	0.28	0.00
<i>LCYB</i>	13.85	22.90	34.35	16.35	11.10	0.16
<i>LCYE</i>	11.85	158.60	307.00	81.35	58.50	0.10
<i>BOHASE1</i>	40.35	6.85	9.60	12.10	16.30	0.23
<i>BOHASE2</i>	0.43	0.16	0.53	5.10	60.65	0.15
<i>BOHASE/LUT5</i>	18.20	24.85	80.45	38.15	10.85	0.09
<i>EOHASE/LUT1</i>	11.80	14.05	13.30	13.40	7.60	0.07

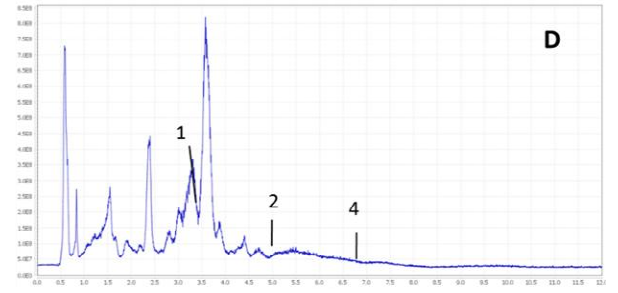
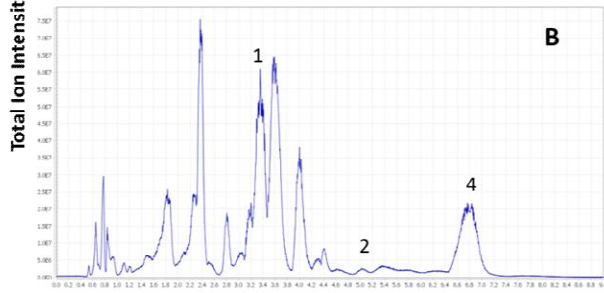
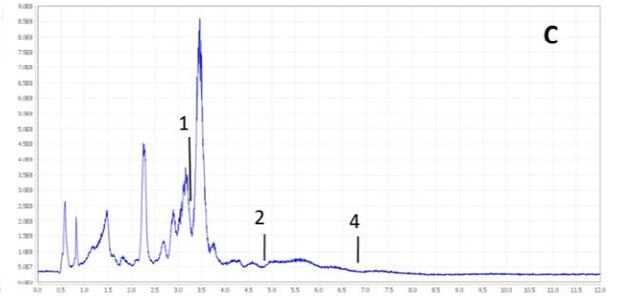
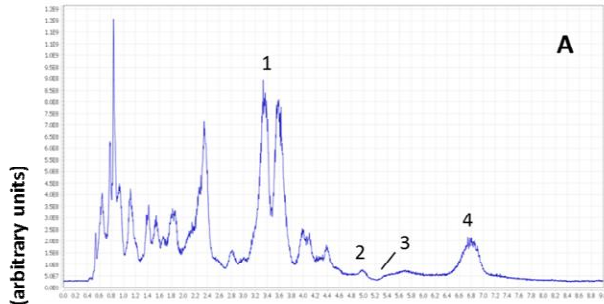
^(a)Data from Hollender et al. 2014¹⁴⁵, obtained from SGR¹¹² expressed as RPKM

3.3.3: Carotenoid Analysis

To define a relationship between carotenoid accumulation and gene expression levels in response to temperature stress, the carotenoid content in the same tissues used to carry out the qPCR studies were compared by liquid chromatography-mass spectrometry (LC-MS). The analysis was capable of identifying seven known carotenoids based on spectra and chromatographic retention (Figure 3.5 and Figure S3). Lutein (1), identified by its retention time and MS fragmentation pattern was

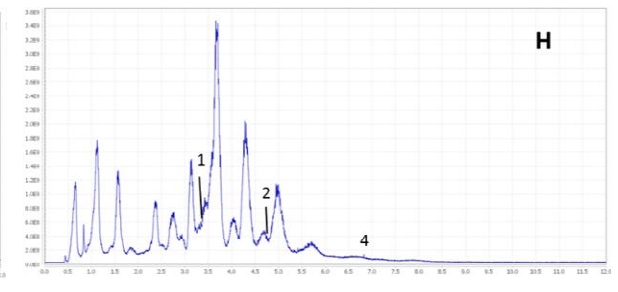
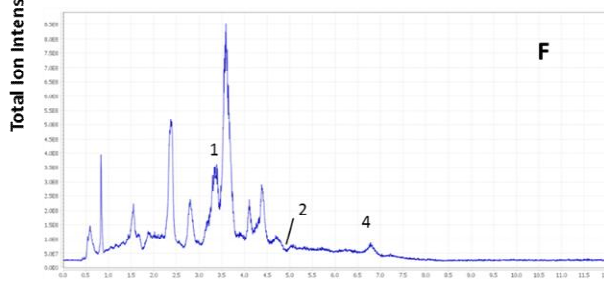
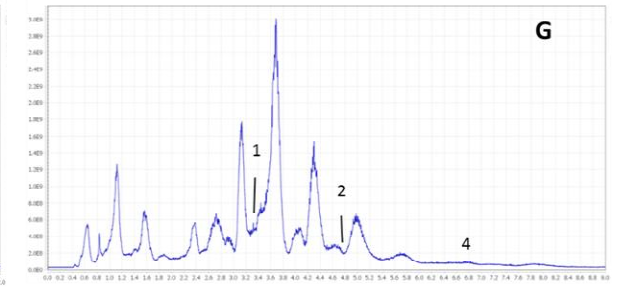
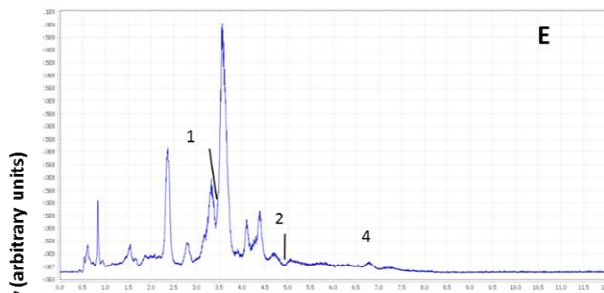
detected in all of the tissues examined. Compound 2 had a quasi-molecular ion at m/z 552.4324 corresponding to α -cryptoxanthin. α -Cryptoxanthin was present in all the tissues except roots, while β -cryptoxanthin (3), eluting at 5.2 min, was detected only in leaves under normal growing conditions. Peak 4 was also detected in all of the tissues examined and produced a quasi-molecular ion at m/z 536.4379 corresponding to α - β -, or γ - carotene or lycopene. The isomers, α - β -, and γ -carotene and lycopene, each with a quasi-molecular ion of 536.4379, could not be fully resolved with the chromatographic method used, and no differential fragmentation characteristics were found for these compounds. For analysis they are therefore grouped together and referred to as peak 4.

Careful comparison with retention times of standard compounds indicates that in leaves, peak 4 is either β -carotene and/or lycopene. However, there are no current reports to suggest that lycopene, which is found in the chromoplasts of fruits (e.g. watermelon, guava, tomato), is present in the chloroplasts of green tissues. Therefore, peak 4 in leaves is most probably β -carotene. To definitively determine the identity of peak 4 in leaves, further analyses need to be conducted. Based on the retention time of the centroid of the experimental peak, petals, receptacles, and roots most likely contain β -and/or γ -carotene. In anthers, this peak is most likely to be predominately γ -carotene. Definitive clarification of which isomer is present in these tissue will require further analyses.



Retention Time (min)

Retention Time (min)



Retention Time (min)

Retention Time (min)

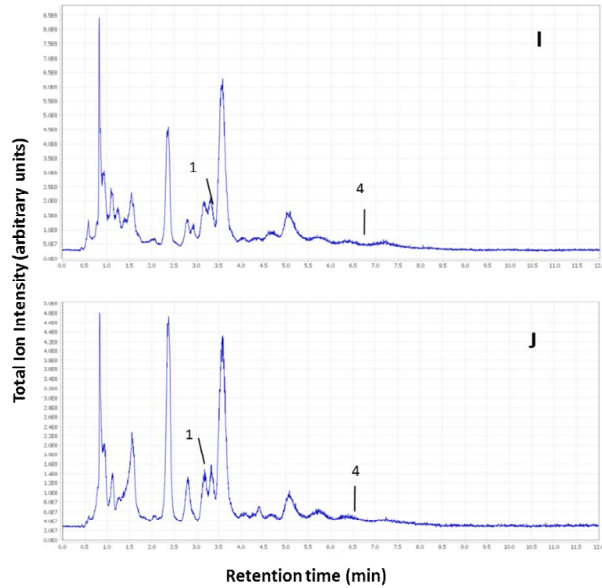


Figure 3.5. LC-ESI-MS chromatograms of *F. vesca* leaves, petals, receptacles, anthers, and roots grown under control (25/20 °C) and heat stressed (32/25 °C) conditions (A) leaves grown at 25/20 °C (B) leaves grown at 32/25 °C, (C) petals grown at 25/20 °C, (D) petals grown at anthers 32/25 °C, (E) receptacles grown at 25/20 °C, (F) receptacles grown at 32/25 °C, (G) anthers grown at 25/20 °C, (H) anthers grown at 32/25 °C. (I) roots grown at 25/20 °C. (J) anther grown at 32/25 °C. Peaks are as follows: 1, lutein; 2, α -cryptoxanthin; 3, β -cryptoxanthin; 4, α - β - or γ -carotene, or lycopene.

Results showed that the relative amounts of peak 4 decreased in heat stressed leaves (Figure 3.6). No significant differences in the relative amounts of the identified carotenoids were observed in heat stressed petals, receptacles, and roots. In heat stressed anthers, however, there was an increase in the accumulation of the xanthophylls α -cryptoxanthin and lutein as compared to controls, but no differences in the accumulation of the carotenes (α -, β -, or γ -carotene or lycopene) were found (Figure 3.6). β -Cryptoxanthin was only detected in leaves and neither α - or β -cryptoxanthin were detected in roots (Figure 3.6).

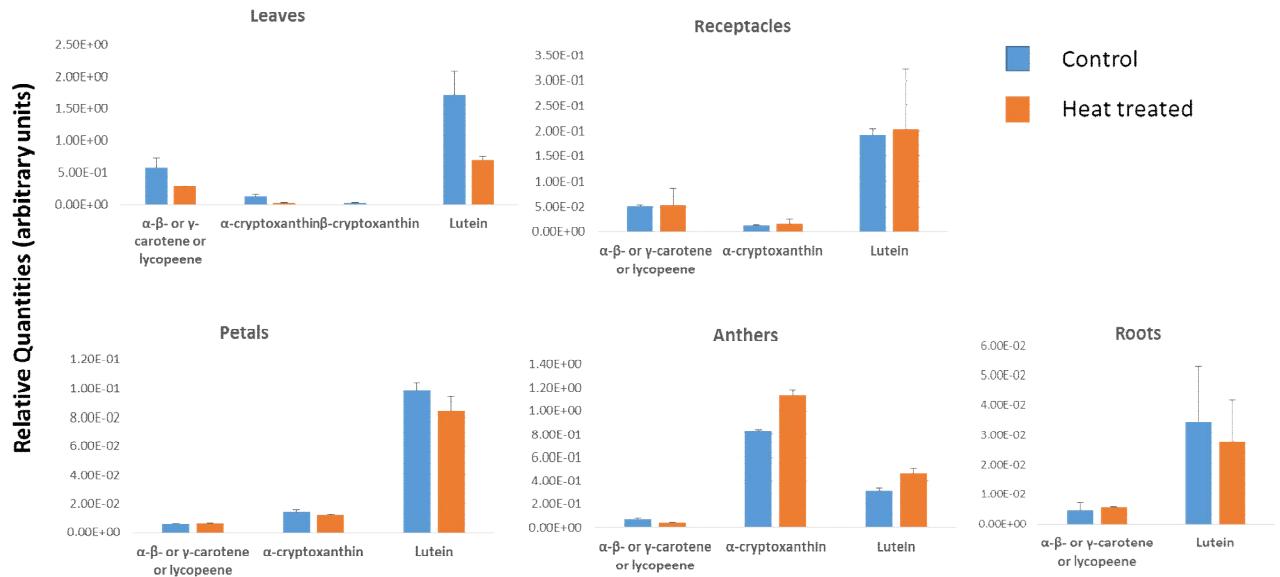


Figure 3.6. Relative accumulation of carotenoids in leaves and floral organs of *F. vesca* grown under control (25/20°C) and moderate heat stress conditions (32/25°C). Relative quantities are normalized to the internal standard, n-hexadecylbenzamide. Error bars represent SEM from three replicates.

3.3.4: Effects of Elevated Temperature on Expression of Carotenoid Biosynthesis Genes

Tissue-specific and heat regulated expression patterns of *PSY*, *PDS*, *ZDS*, *LCYB*, *LCYE*, *BOHASE 1*, *BOHASE 2*, *BOHASE (LUT 5)*, and *EOHASE (LUT 1)* in *F. vesca* during flower development were measured by qPCR. Transcripts of all nine genes were detected in petals, receptacles, and mature anthers. However, transcripts of *PSY* were not found in roots and were barely detectable in leaves (Figure 3.7). Low levels of transcripts of *LCYE* and *BOHASE 2* were also observed in leaves, and in roots.

Levels of *PSY* transcripts declined in heat-treated petals but showed no significant differences in levels in heat stressed leaf, receptacle and anther tissues as

compared to controls (Figure 3.7). Reduced transcript levels in heat treated petals were also observed for *ZDS*, *LCYE*, and *EOHASE (LUT5)*, while no significant differences were observed between heat treated leaf, receptacle, anther, and root samples and controls. Unlike *PSY*, *ZDS*, *LCYE*, and *EOHASE*, *PDS* transcript levels did not appear to be affected by heat stress in petals. However, *PDS* appears to be downregulated in heat stressed leaves, receptacles, and roots, although there is an increase in transcript accumulation in heat stressed anthers as compared to controls. Figure 3.7 shows that *LCYB* transcripts increase in heat stressed receptacles as compared to controls, however heat stress results in fewer transcripts in petals and had no effect in anthers and roots. No significant differences in the expression levels of *BOHASE1*, *BOHASE 2*, and *BOHASE (LUT5)* in response to elevated temperature stress were found in any of the tissues examined (Figure 3.7).

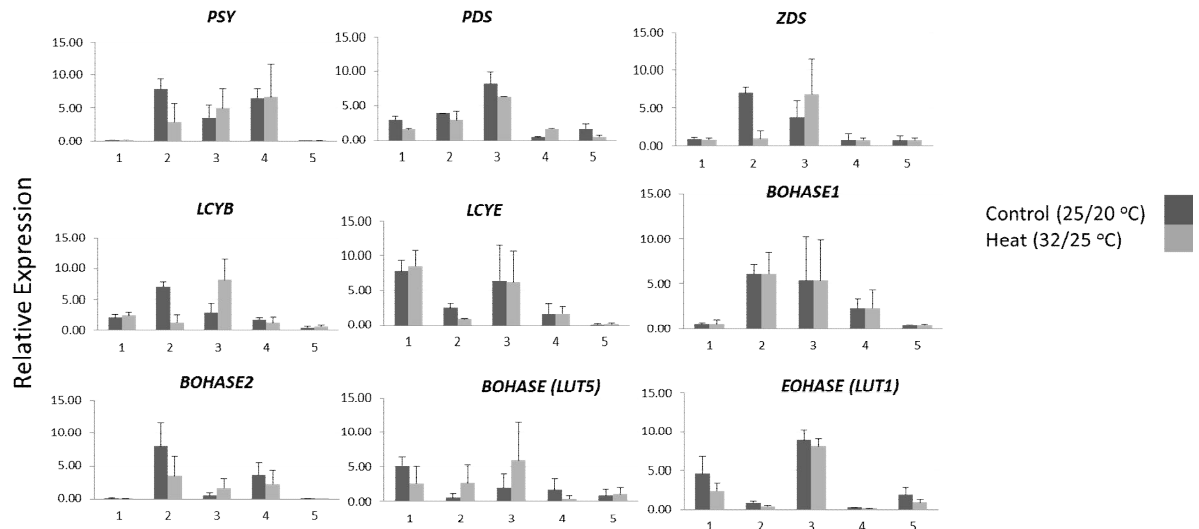


Figure 3.7. Carotenoid biosynthesis gene expression in *F. vesca* in response to moderately elevated temperatures. Relative mRNA levels for individual genes in strawberry (1) leaf, (2) petal, (3) receptacle, (4) anther, and (5) root tissues were

normalized to reference genes, *NMD* and *PP2A*. Error bars indicate SEM from two biological replicates.

3.4: Discussion

Much of the published research on the roles of carotenoids has focused on photosynthesis, coloration of fruits and vegetables, and human health. However, little is known about how temperature stress affects their production and accumulation in plant reproductive organs, which are critical to crop production in many vegetables, grains, and fruits such as strawberry, apple, peach and other members of the Rosaceae family. Little is known about the effects of elevated temperature stress on carotenoid biosynthesis in anthers and carpels, where developmental stages leading to production of the ovule and pollen may be particularly susceptible to disruption of cellular homeostasis and production of ROS. We have begun to address these issues by using genomics and targeted metabolomics in parallel to characterize carotenoid production and accumulation in diploid strawberry flowers and leaves in response to moderate heat stress.

High resolution LC-MS allowed us to analyze the differential accumulation of seven carotenoids in leaf, petals, anthers, receptacles with attached pistils, and roots of control plants and plants growing for several weeks at moderately elevated temperatures. Diploid strawberry anthers weigh less than 1.0 mg each, so the limited amount of anther tissue precluded analysis by routinely used LC-UV/Vis.

Lutein was detected in all of the samples examined, as had been previously described in other crops and flowers such as maize, zucchini, marigolds and Japanese morning glory¹⁴⁶⁻¹⁴⁷. Although zeaxanthin was identified in the leaves and petals of

the Japanese morning glory based on HPLC-UV analyses¹⁴⁷, it was not detected in any of the tissues we examined using a more sensitive technique that detected the zeaxanthin standard. This result, together with the observed expression of the beta-carotene hydroxylases (*BOHASE 1* and *BOHASE 2*) in leaves, petals, receptacles, and anthers, suggests that these tissues might be making zeaxanthin but may not be accumulating it, possibly due to flux through the xanthophyll cycle in leaves. The lack of color in the petals of white chrysanthemums has been attributed to the shunting of carotenoids into the carotenoid cleavage pathway¹⁴⁸. This might also be an explanation for the lack of zeaxanthin in our samples, particularly in the petals, which are white in color. α -Cryptoxanthin was identified in all of the samples except roots, while β -cryptoxanthin, an isomer of α -cryptoxanthin, was only identified in leaves under normal temperature conditions.

LC conditions were selected to maximize retention and resolution compared to the commonly used reverse-phase (RP) methods initially tested and to be compatible with mass spectral analysis. Hydrophilic interaction liquid chromatography (HILIC) proved to be most effective in separating the polar carotenoids. A major limitation of the cyano column we used is that it was unable to fully resolve the carotenes, resulting in the co-elution of the isomers, α -, β -, or γ -carotene or lycopene, designated as peak 4. Unlike the xanthophylls, which were likely retained and resolved through a combination of hydrogen bonding between hydroxyl groups and the cyano stationary phase and electrostatic interactions, the lack of functional groups and high structural similarity among the carotenes made separation difficult by HILIC. It was selected as an alternative strategy to RPLC

because of the increased column retention and solvent compatibility with ESI-MS-based analyses.

Gene expression analyses carried out using qPCR showed that genes involved in biosynthesis genes are differentially expressed during both during vegetative and reproductive development and in response to elevated temperature. Reduced accumulation of both the carotenes (α -, β -, γ -carotene or lycopene) and lutein, together with decreased *PDS* transcript accumulation, in heat stressed leaves, receptacles, and roots suggests that carotenoids are being degraded, perhaps as a function of scavenging ROS in leaves, but they are not being replaced. In contrast, a positive correlation between *PDS* expression and α -cryptoxanthin and lutein accumulation in heat stressed anthers suggest that these carotenoids (possibly functioning as antioxidants) are being replaced. The complex differences in carotenoid accumulation and gene expression profiles of various genes in different tissues in response to elevated temperature suggests that posttranscriptional regulation mechanisms influence carotenoid accumulation, and that translational mechanisms, and enzyme activation by posttranslational modifications need to be considered.

This is the first report addressing carotenoid biosynthesis in response to elevated temperature stress during floral development. In addition to uncovering some of the complexities of this interaction, this study provides a foundation for understanding carotenogenesis in strawberries and other Rosaceae crop plants.

3.5: Acknowledgements

The authors acknowledge Dr. Frederick Khachik for providing the carotenoid standards, Ms. Saima Naseem for pollen images, and Mr. Samuel Jones for assistance with RNA extractions. Carotenoid mass spectrometry analyses were carried out in the laboratory of Dr. Jerry Cohen at the University of Minnesota, with help from Dr. Daniel Abate Pella and Dr. Dana Freund.

3.6: Supplemental Information

Table S1 Primer sequences used in this study

Primer Name	Forward and Reverse Primer Sequence [5' --> 3']
GAPDH	F: GAGCATGGCTTCGGCTATAC R: TAGTCATGGTGCCCTTGATG
Tubulin	F: TCTTCAGTGAGACTGGTGCTGGAAAGC R: AAAGCATGAAGTGGATCCTGGGGTATG
NMD	F: ACCTGCCATCTTTGCGATGT R: TCCCCACAACAGAGAATGC
PP2A	F: AAAGTCTTCCGGTGGTTGT R: CAGCACCTTTGCCACATTGA

Table S2. Chromosome localization of gene encoding enzymes involved in carotenoid metabolism for *F. vesca*, Hawaii-4.

Gene Name	Chromosome No.
Phytoene synthase	6
Phytoene desaturase	4
ζ-Carotene desaturase	1
15-cis-ζ-Carotene isomerase	4
Carotenoid isomerase 1	6
Carotenoid isomerase 2	5
Lycopene-β-cyclase	6
Lycopene-ε-cyclase	7
β-Carotene hydroxylase	7
β-Carotene hydroxylase	6
β-Carotene hydroxylase (LUT 5)	6
ε-Carotene hydroxylase (LUT1)	6

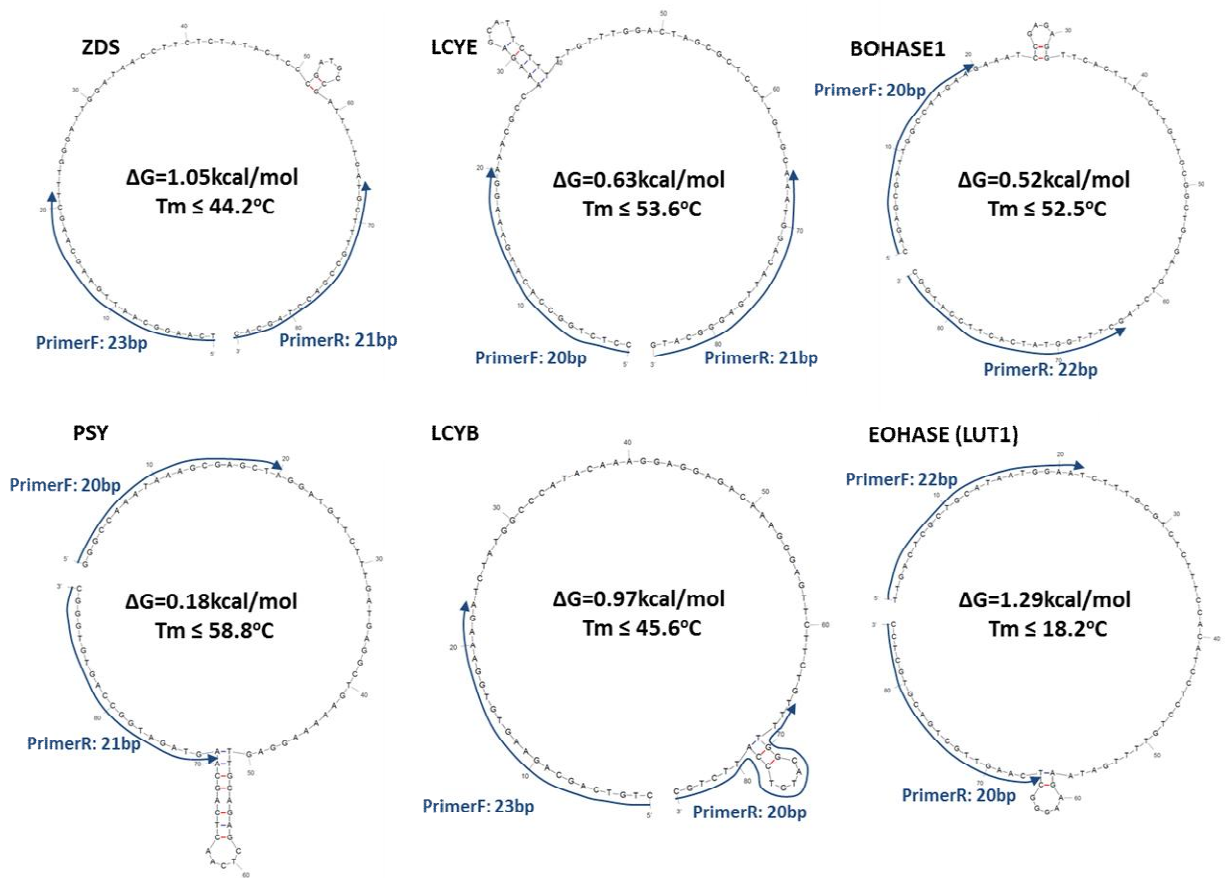


Figure S1. Secondary structures of the amplicons for 6 representative primer sets, illustrating thermodynamic stability (ΔG in kcal/mole) of amplicons. Primers are indicated by blue arrows. **A:** No secondary structures are present where primer anneals and efficient annealing is not hampered by formation of stable secondary structures in the three different examples. **B:** The secondary structures at the primer annealing sites have a positive ΔG value and $T_m < 60^\circ\text{C}$ and hence does not influence the amplification efficiency.

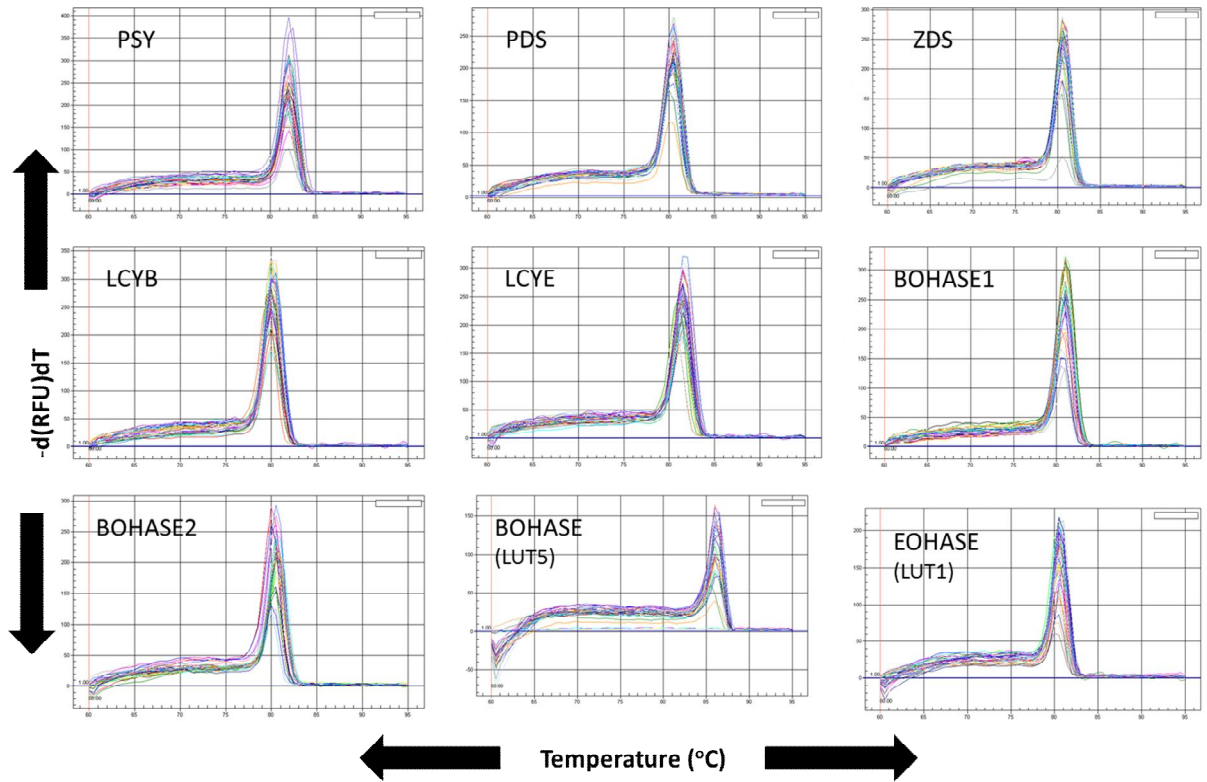


Figure S2. Dissociation curve of nine carotenoid biosynthesis genes, illustrating a single amplicon,

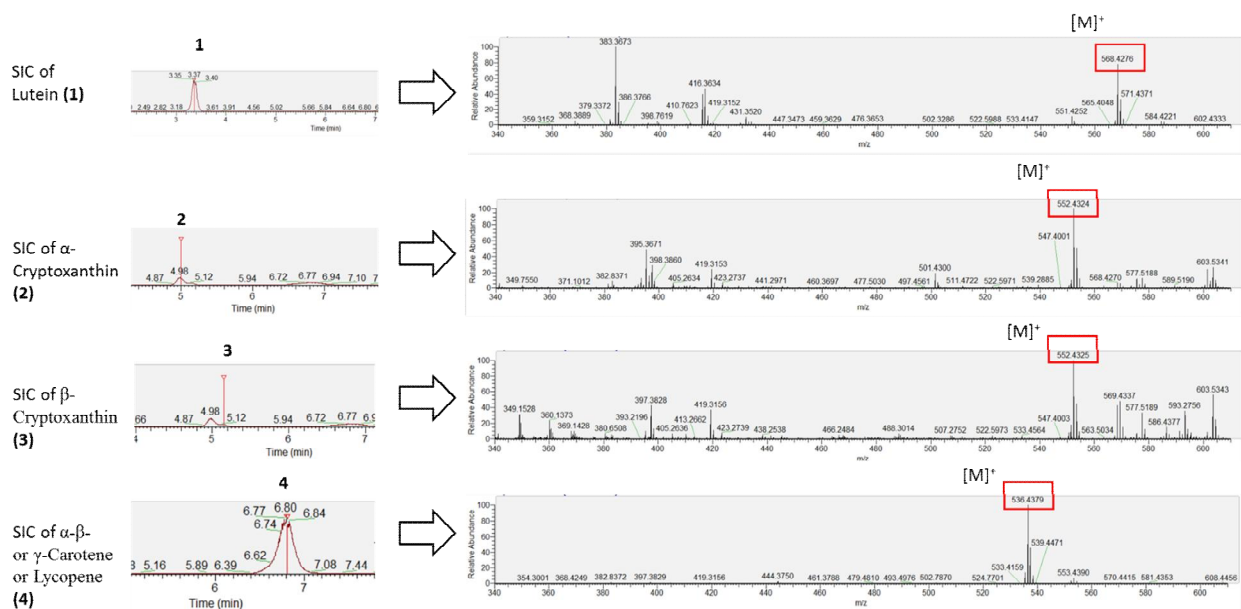


Figure S3. Selected ion chromatograms (SIC) and corresponding mass spectra obtained from the analyzed samples in *F. vesca*.

Chapter 4: Identification and Characterization of Three Phytoene Synthase Genes from the Diploid Strawberry, *Fragaria vesca*

Abstract

Phytoene synthase (PSY), the first enzyme in the biosynthetic pathway for carotenoids, catalyzes the condensation of phytoene from two molecules of geranylgeranyl pyrophosphate. Carotenoids are a diverse family of lipophilic pigments that have important functions in plant physiology and ecology, and human health. PSY is known to be encoded by a small gene family in several different plant species. Here we report the structural and functional characterization of three *PSY* genes in the diploid strawberry, *Fragaria vesca*. Amino acid alignment showed that the catalytic trans-isoprenyl pyrophosphate synthase domain is conserved in all three strawberry enzymes. Phylogenetic analysis indicated three clades within the family. The single Arabidopsis PSY is most homologous to FvePSY2, while FvePSY3 is closely related to one of the peach or loquat PSYs. Genomic analyses revealed that the *PSY* gene family exhibits functional diversity *in plant* tissues, both with respect to location and stage of development, as well as in response to abiotic stress. In leaves and roots, expression of *PSY* family members is not affected by moderately elevated temperature stress, whereas in petals and anthers, PSYs are differentially down regulated. *PSY2* transcripts increased in samples consisting of receptacles with carpels attached from the heat treated plants.

Keywords: *Fragaria vesca*, carotenoids, phytoene synthase, phylogenetic analysis, transcriptional regulation

4.1: Introduction

Carotenoids are a diverse group of more than 600 lipophilic pigments that play essential roles in plant and animal life²⁴. In plants, carotenoids serve as accessory light-harvesting pigments and visual and olfactory attractants for pollinators and seed dispersers^{24, 56}. Carotenoids are also precursors for the production of the hormones abscisic acid (ABA) and strigalactones, which are involved in plant responses to abiotic conditions such as CO₂ levels and drought as well as in plant development^{24, 149}. In animals, carotenoids play roles in sexual reproduction and they help support human health and nutrition by functioning as precursors for vitamin A (retinal, retinol, and retinoic acid)^{24, 150}. Vitamin A, an essential apocarotenoid derived from β -carotene, α -carotene, and β -cryptoxanthin, is required for processes related to vision, immune response, and normal cell growth and development¹⁵⁰. Concerns with vitamin A deficiency and disease, particularly in developing countries, among the elderly, and in communities where malnutrition is most prevalent, has sparked considerable interest to develop transgenic crops with increased levels of pro-vitamin A¹⁵¹.

All carotenoids classified as xanthophylls (the oxygenated carotenoids) or carotenes (the hydrocarbon carotenoids) are derived from the isoprenoid molecules, isopentenyl pyrophosphate (IPP) and dimethylallyl pyrophosphate (DMAPP)¹⁵². *De novo* synthesis, which occurs in the membranes of plastids, including chloroplasts, chromoplasts, and amyloplasts, is mediated by enzymes encoded in the nucleus^{24, 60}.

The first committed step in the pathway is the condensation of two molecules of geranylgeranyl pyrophosphate to the C₄₀ compound phytoene⁵⁹. This step, which is widely considered to be rate-limiting, is catalyzed by phytoene synthase (PSY)^{24, 153}. It is well known that carotenoid flux is controlled by PSY at both transcriptional and *post-transcriptional* levels^{154,155}. For example, studies showed that allelic variations in the wheat PSY resulted in reduced carotenoid levels¹⁵⁶ and in cassava (*Manihot esculenta*), a single nucleotide polymorphism in *MePSY2* resulted in greater production and accumulation of carotenoids in root tissues¹⁵⁷.

In many plants PSY is encoded by a small gene family. While only a single *PSY* gene appears to be present in *Arabidopsis*¹⁵⁸ and daffodil¹⁵⁹, two distinct *PSY* genes have been identified in tobacco, tomato, carrot, cassava and poplar¹⁵⁸. At least three *PSY* genes have been described for zucchini¹⁶⁰, loquat¹⁶¹, banana¹⁶² and several members of the Poaceae family, including maize¹⁶³ and rice¹⁶⁴. Individual members of *PSY* gene families may be differentially expressed suggesting functional diversity. In tomato, *SIPSY1* is predominately expressed in fruits and flowers, where tissues contain chromoplasts, whereas transcripts of *SIPSY2* are found in association with green chloroplast containing tissues such as leaves¹⁶⁵. Two *PSY* genes with different expression profiles during melon fruit development have also been reported¹⁶⁶.

Transcription of *PSY* genes is responsive to environmental cues¹⁵³, as evidenced in rice and maize, where *PSY3*, which is involved in biosynthesis of carotenoids in roots, in response to drought and salt stress, and is positively regulated by ABA, a product of the carotenoid pathway. Despite these findings, there is still a limited number of studies on the roles of temperature in PSY expression and flux

through the carotenoid pathway. Baron et al.¹⁶⁷ showed that ABA biosynthesis increases in response to heat and cold stress in leaves and inflorescence meristems of *Arabidopsis*. Current investigations in blueberry also support upregulation of *ABA*-responsive genes in cold stressed plants (Rowland, personal communication). No studies to date have addressed the impact of elevated temperature stress on the upstream carotenoid biosynthetic pathway which can ultimately regulate ABA levels.

The cultivated strawberry (*Fragaria × ananassa* Duch.), an agronomically important fruit crop in the Rosaceae family, is rich in antioxidants and other phytonutrients known for improvement of human health. Fruit production is best when grown in temperate climates¹⁶⁸, and production of quality berries is negatively impacted by moderately elevated temperatures, which inhibit photosynthesis and affect reproductive development. Fewer fruit are formed and those that are have poor shape as a result of abnormal pollen development¹⁰⁵. As a result, there is a strong demand for attaining heat tolerant strawberries through genetic breeding. The diploid woodland strawberry, *Fragaria vesca*¹⁰⁶, has been embraced as a useful tool for genomic research in *Fragaria* and its short seed to seed cycle⁷⁰ and sequenced genome (240 Mb)⁶⁹ make it more amenable than the octoploid commercial strawberry, *F. ×ananassa*, for laboratory studies of the effects of elevated temperature on reproductive development and carotenoid biosynthesis.

Here, we describe the identification and characterization of the *PSY* gene family in *F. vesca*. Structural evidence is presented that these chloroplast genes encode membrane-bound proteins, each having a conserved trans-isoprenyl pyrophosphate synthase domain, associated with enzymatic activity.

4.2: Materials and Methods

4.2.1: Plant Material and Stress Treatment

Plants of *F. vesca* inbred line, 5AF7 (PI 641092) were grown in controlled environment chambers under a 14 hour daylength, as described in Chapter 3. For heat stress studies, half of the plants kept at 25/20 °C were transferred to a new growth chamber and maintained at 32°C during the day and 25 °C at night. Just before transfer, visible inflorescences were removed from the plants and crowns were trimmed of leaves to the youngest fully opened leaf¹⁰⁸. Tissues were harvested between 4:00-6:00 pm, immediately frozen in liquid nitrogen.

RNA analyzed for alternative splicing analyses was extracted from seedlings growing aseptically on vertical plates containing 0.8% water agar with 0.1% sucrose added. Aseptic, germinated seeds were sown on square plates that were maintained under constant light (120-150 $\mu\text{mol}/\text{m}^2 \text{ s}$) at 25°C. After one week, the seedlings were harvested between 12:00-2:00 pm. Seedlings were rinsed in sterile distilled water and patted dry with paper wipes. They were immediately weighed and frozen in liquid nitrogen. All frozen tissues were stored at -80 °C.

4.2.2: RNA Extraction and cDNA Synthesis

Total RNA from seedlings, leaves, roots, and floral organs were extracted using the RNeasy Plant Mini Kit (Qiagen, Valencia, CA, USA), with slight modification to the manufacturer's instructions. Extractions were carried out using up to 50 mg of tissue per sample instead of 100 mg. Samples were treated with DNase I (Qiagen) prior to elution from the column, and concentration and purity were

determined using a Nanodrop spectrophotometer (Thermo Fisher Scientific, Wilmington, DE, USA). RNA integrity was checked using the Experion lab-on-chip (Bio-Rad Laboratories, Hercules, CA, USA). All samples had RQI values greater than 9.0. cDNA was reverse transcribed from 1 µg of RNA using Superscript[®] III reverse transcriptase (Life Technologies, Renton, WA, USA) primed with oligo dT in a total volume of 20 µl according to the manufacturer's instructions.

The absence of genomic DNA was confirmed by endpoint PCR using primers that spanned introns in *F. vesca* chloroplastic glyceraldehyde and α -tubulin (Supplemental Table 1). PCR reactions, using 2 µl of cDNA (diluted 1:10), 0.4 µM of gene specific primer, and HotStarTaq Plus Master Mix (Qiagen), were performed in a 96 well Eppendorf Mastercycler[®] gradient thermal cycler (Eppendorf, Hamburg, Germany) under the following conditions: 95 °C for 5 mins, 94 °C for 30 s, 60 °C for 30 s, 72 °C for 1 min for 35 cycles, and a final elongation step at 72 °C for 10 mins.

4.2.3: Quantitative Gene Expression Analysis

Gene specific primers for quantitative studies were designed using Primer Express 3.0 (Applied Biosystems, Foster City, CA, USA). Amplicons between 75-90bp, with an optimal melting temperature (T_m) of 60 °C, and a GC content of at least 40% were selected (Table 4.1). qPCR analysis was conducted on an iQ5 iCycler (Bio-Rad) using SYBR Green in a final volume of 20 µl. PCR conditions were as follows: 3 min at 95°C, 30s at 95 °C, and 40 cycles at 60°C for 1 min. At the conclusion of the experiment, a dissociation analysis of the generated amplicons was performed by running a temperature gradient from 60 °C and 95 °C to confirm that only a single

product was amplified (Figure S1). cDNAs prepared from two biological replicates were assessed quantitatively. Two technical replicates were performed for each sample. Quantification of transcript levels was carried out in accordance with the modified ΔCq method as described by Hellemans et al⁸⁴.

4.2.4: Analysis of Alternative Splicing

mRNA structure was analyzed by RT-PCR and visualized by gel comparison of product sizes from cDNA and genomic DNA. Gene specific primers designed to flank the third intron of *FvePSY1* and *FvePSY2*, and the first intron of *FvePSY3* were designed using Primer 3 (<http://bioinfo.ut.ee/primer3-0.4.0/>) (Table 4.1). RT-PCR analysis was carried out in a thermal cycler (Eppendorf) using 2 μ l of cDNA (diluted 1:10) and 0.4 μ M of each primer pair. The cycling parameters were: 35 cycles of 95 °C for 5 mins, 94 °C for 30 s, 57.7 °C for 30 s, and 72 °C for 1 min with a final extension at 72 °C for 10 mins. The PCR amplicons were analyzed by gel electrophoresis on a 1.2 % agarose gel in 1 \times tris-acetate-EDTA buffer. The gel was stained with ethidium bromide and visualized on a UV transilluminator.

4.2.5: Functional Analysis in *Escherichia coli*

To investigate the enzymatic function of the proteins encoded by *F. vesca*, *PSY* genes were analyzed by complementation in *Escherichia coli* (*E. coli*) to produce β -carotene. *PSY* genes (without a transit peptide sequence) were amplified by PCR using Phusion[®] High-Fidelity DNA Polymerase (New England Biolabs, Ipswich, MA, USA) and gene-specific primers (Table 4.1). PCR products were subsequently cloned into the pJET1.2 vector using the pJET1.2/blunt Cloning Vector Kit (Life

Technologies), and constructs were sequenced to ensure that the genes were in the correct reading frame. Each resulting *F. vesca* PSY pJET expression vector was then co-transformed with plasmid, pAC-85b into TOP 10 competent cells (Life Technologies). The plasmid pAC-85b containing *crtE*, *crtI*, and *crtY* carotenoid genes from *Erwinia herbicola*¹⁶⁹, was kindly gifted by Dr. Francis X. Cunningham Jr at the University of Maryland. Transformants were plated on Lauria-Bertani (LB) medium containing agar (15g/L), containing carbenicillin (50 µg/ml) and chloramphenicol (9.69 µg/ml), and incubated at 37 °C overnight, then stored in the dark at room temperature for 4-5 days to accumulate visible orange color. Plasmid, pAtPPSY containing the coding sequence for the Arabidopsis PSY (also a gift from Dr. Francis X. Cunningham Jr.) was used as positive control.

Overnight cultures (5ml) prepared from single colonies were grown in LB medium supplemented with carbenicillin (50 µg/ml) and chloramphenicol (9.69 µg/ml) at 37°C. Cultures (1 ml) were then used to inoculate 50 ml of supplemented LB which was grown at 37°C for 24 h in the dark to maximize carotenoid production. At that time, 5 ml were used to calculate the dry weight of the cultures. A total of 40 ml were used to extract carotenoids. Cultures were prepared in triplicates. To verify the accumulation of β-carotene, the recombinant *E. coli* cells were pelleted by centrifugation (4 °C, 10,000 rpm) and extracted three times with 5ml of HPLC grade acetone (Sigma Aldrich). The combined extracts were concentrated to 5ml under vacuum using a rotary evaporator. The resulting extract were analyzed by UV absorption spectroscopy from 400-800nm. Spectra from experimental samples were

compared to that of commercial β -carotene (Sigma Aldrich) in acetone (see Figure S2).

Table 4.1. Primers used in this study

Primer Name	Forward and Reverse Primer Sequence [5' --> 3']	Application
RTPSY1_F	ACTGATGAACTAGTGGATGGACCTAAT	Gel RT-PCR
RTPSY1_R	TCTCAAGTCTAACCTCATTCTTCTAC	Gel RT-PCR
RTPSY2_F	TTGTCAGATACGGTTACCCTTTTCCT	Gel RT-PCR
RTPSY2_R	TTAGCTGATTTGCAATCCCTAATGCTA	Gel RT-PCR
RTPSY3_F	TTGTCAGATACGGTTACCCTTTTCCT	Gel RT-PCR
RTPSY3_R	TTAGCTGATTTGCAATCCCTAATGCTA	Gel RT-PCR
qPSY1_F	GGGCCAAATAAAGCGAGCTA	qPCR
qPSY1_R	GCCCACACTGGCCATCTACT	qPCR
qPSY2_F	CTTGCACAAGCAGGACTTTCTG	qPCR
qPSY2_R	CTTCATGAAACTCCTCCATTTATCTTG	qPCR
qPSY3_F	ACATGCTTGATGCTGCATTGA	qPCR
qPSY3_R	CGCATACCCTCGATCATCATGTCT	qPCR
cPSY1_F	AGAAGAGAGGGTCTATGAAGTGGTG	Complementation Assay
cPSY1_R	AGTTTATCTTGCCACCAACTGCT	Complementation Assay
cPSY2_F	GAAGAAATAGCAGTGTTCATCGGAACAA	Complementation Assay
cPSY2_R	GATTCAGTGGTCTAAGCTCGAA	Complementation Assay
cPSY3_F	ATACAAGGCATTCCTGTTGCTGAT	Complementation Assay
cPSY3_R	CACGGCTACTGAGAGATCAAA	Complementation Assay

4.2.6: Bioinformatics Analysis

Promoter regions of the *FvePSY1*, *FvePSY2* and *FvePSY3* genes, 1.5-kb sequences upstream from the translation start sites were analyzed for known cis-regulatory elements using the PlantCARE database¹⁷⁰. Protein sequence alignments were carried out using the CLUSTAL W program¹³⁹ and alignments were further formatted using BOXSHADE (http://www.ch.embnet.org/software/BOX_form.html). Conserved protein domains were identified using the NCBI Conserved Domain Database¹⁴⁰. The presence of chloroplast transit peptides was predicted using the ChloroP server version 1.1¹⁴². The protein sequences were further examined for the presence of a transit peptide using other web-based programs such as, SignalP¹⁷¹, Signal-3L¹⁷², and PrediSi¹⁷³. Phylogenetic analysis was conducted using MEGA version 6.0¹⁷⁴. Phylogenetic trees were constructed using the neighbor-joining (NJ) method and bootstrap analysis based on 1,000 replicates.

The transcriptome data were collected as part of a larger project (Hollander *et al.* 2014)¹³⁴ to obtain transcriptome information from different floral tissues throughout floral development, and are expressed as reads per kilobase of transcript per million mapped reads (RPKM). K-means clustering analysis was accomplished using the MultiExperiment Viewer 4.8 (MeV4.8; <http://www.tm4.org/mev/>).

4.3: Results

4.3.1: Sequence and Phylogenetic Analysis

Three members of the *PSY* gene family were identified in *F. vesca*. Gene structure was deduced from the alignment of the full-length cDNA sequences to the *F. vesca* reference genomic sequence. The results (Figure 4.1) show that the gene

structure of *FvePSY2* is most similar to that of the Arabidopsis PSY gene, each having seven exons. *FvePSY1* has five exons, while *FvePSY3* has six. Exons 2, 3 and 4 are essentially the same length in all three strawberry genes, and these are conserved in the Arabidopsis gene as exons 3, 4, and 5.

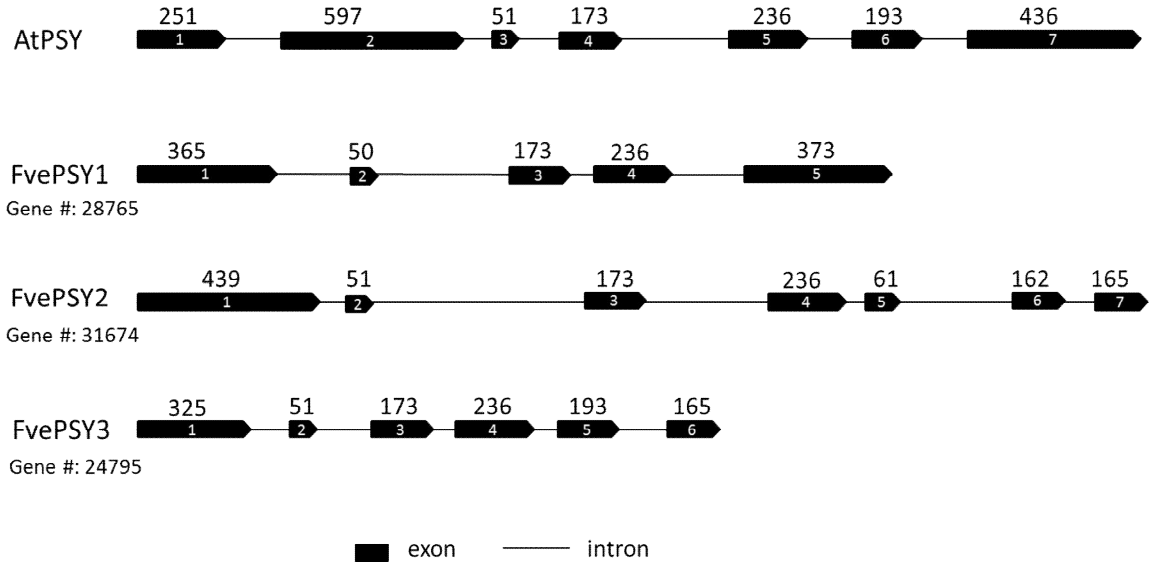


Figure 4.1. Intron-exon structures of *FvePSY* genes relative to *AtPSY*. Lengths are approximately to scale. Numbers above the exons represent the exon size (in bp).

All three PSY genes encode proteins with high amino acid identity and characteristic conserved motifs (Figure 4.2). A signal peptide sequence was predicted for *FvePSY1* and *FvePSY2* but none of the available prediction programs identified a transit peptide for *FvePSY3*. However, as has been described for *OsPSY3*¹⁶⁴, investigation of the sequence upstream of the annotated translation start site for *FvePSY3* revealed that within a 178 nucleotide long sequence there was a 32 amino acid long, non-contiguous sequence, which when attached to the 5' end of the annotated gene sequence resulted in a predicted transit peptide.

A conserved trans-isoprenyl pyrophosphate synthase (*trans*-IPPS) domain was found in all three sequences (boxed in red, Figure 4.2), and several motifs within this domain, including the two active lid regions (blue), a substrate binding pocket, and a catalytic site (DXXXD motif) with two aspartate-rich regions are completely conserved in all three proteins. The *trans*-IPPS domain present in phytoene synthases catalyzes the tail-to-tail condensation of two molecules of geranylgeranyl pyrophosphate to produce phytoene. The DXXXD motif binds substrate and catalyzes the condensation of two molecules of geranylgeranyl pyrophosphate¹⁷⁵ (Figure 4.2).

The phylogenetic relationships among *F. vesca* and other plant PSYs were investigated by constructing a neighbor-joining phylogenetic tree using MEGA 6.0¹⁷⁴ (Figure 4.3). Phylogenetic analysis showed that the PSY genes can be divided into three major clades, designated here as I, II, and III. FvePSY1, along with the single known PSY in the octoploid strawberry (*F. ×ananassa*), are clustered in clade II. FvePSY2, which is most homologous to the Arabidopsis PSY, is in clade I, and FvePSY3, in clade III, appears to be more closely related to homologs from peach, loquat, and cantaloupe.

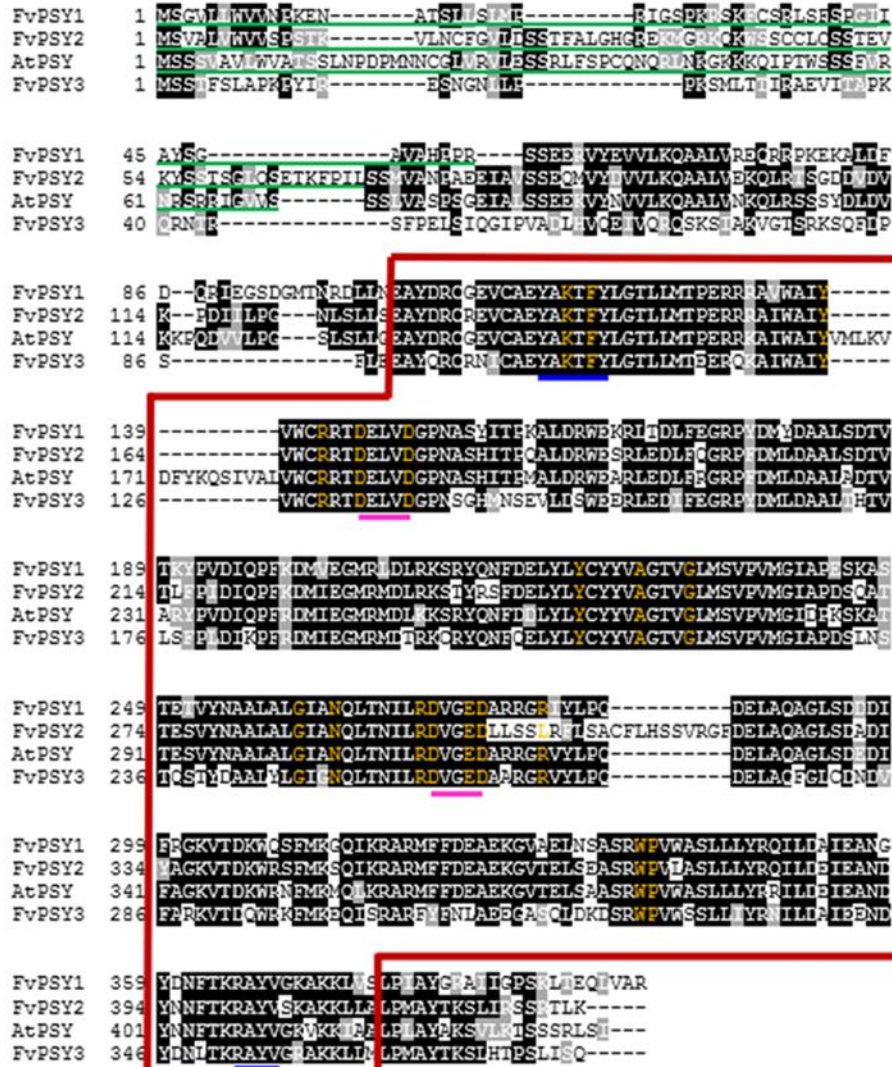


Figure 4.2. Multiple sequence alignment of PSYs from *F. vesca* and Arabidopsis. Conserved amino acids are denoted by a black background with white lettering, similar amino acids are indicated by a grey background with white lettering, and dissimilar amino acids are shown with a white background and black lettering. FvePSY1 and FvePSY2 have their predicted chloroplast transit peptide underlined in green. The conserved trans-isoprenyl pyrophosphate synthase domain is boxed in red. The putative catalytic site (DXXXD motif), which includes the substrate and Mg^{2+} binding sites, and the aspartate rich regions 1 and 2, are underlined in pink. The active lid residues are underlined in blue and the substrate binding pocket residues are highlighted in orange.

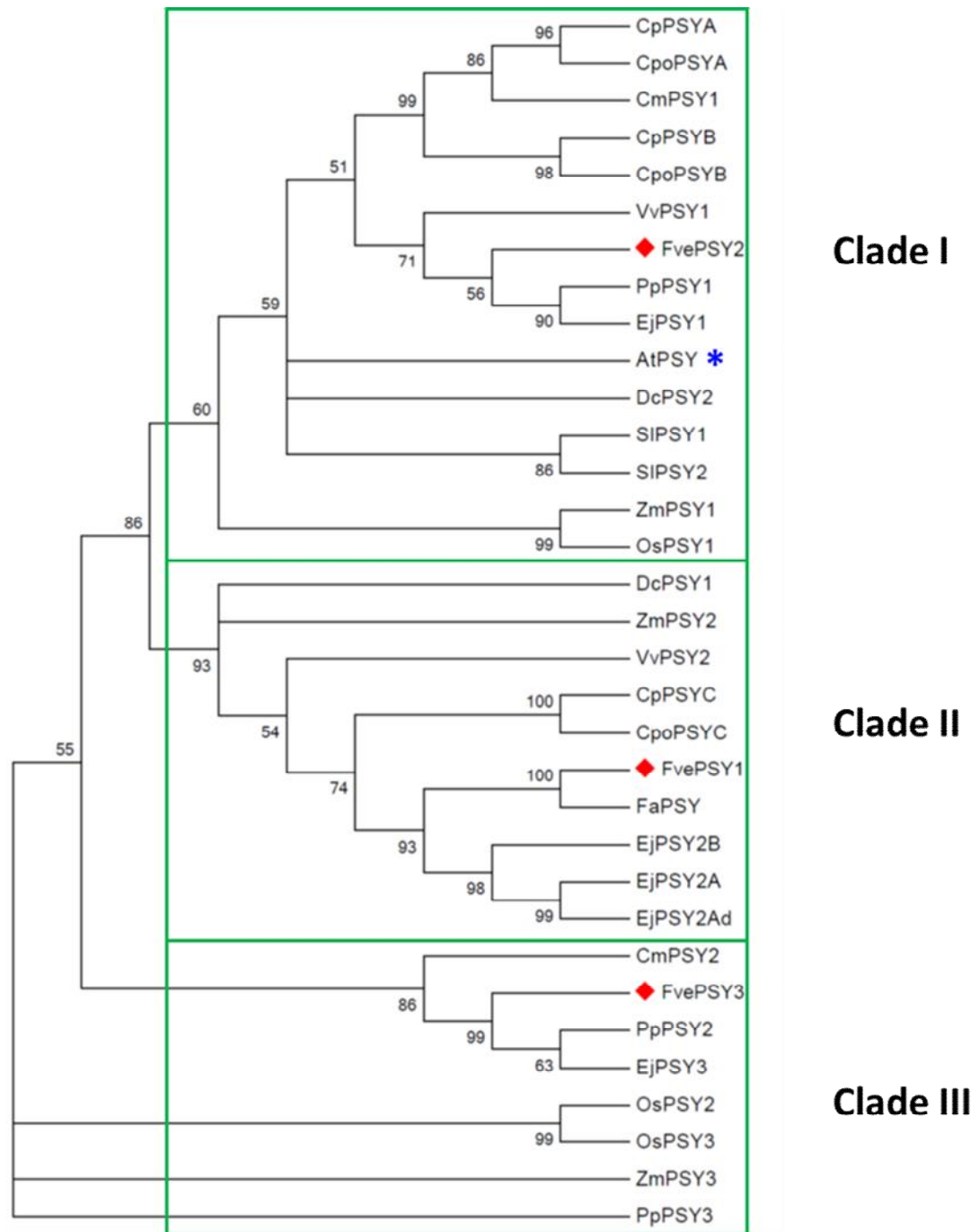


Figure 4.3. A neighbor-joining phylogram of PSY proteins divides the sequences into three clades. At: *Arabidopsis thaliana* (thale cress) (AtPSY: At5g17230); Cm: *Cucumis melo* (cantaloupe) (CmPSY1: XP_008463168; CmPSY2: XP_008449808) Cp: *Cucurbita pepo* subsp. *pepo* (zucchini) (CpPSYA: AFV33362; CpPSYB: AFV33359; CpPSYC: AFV33364); Cpo: *Cucurbita pepo* subsp. *ovifera* (zucchini) CpoPSYA: AFV33361; CpoPSYB: AFV33358; CpoPSYC: AFV33363) Dc: *Daucus*

carota (carrot) (DcPSY1: Q9SSU8; DCPSY2: ABB52068) Ej: *Eriobotrya japonica* (loquat) (EjPSY1:AIT18246; EjPSY2A: AIT18247; EjPSY2B: AIT18249; EjPSY2d: AIT18248; EjPSY3: AIT18250); Fa: *F. × ananassa* (octoploid strawberry) (FaPSY: ACR61392); Fve: *F. vesca* (diploid strawberry, red diamonds) (FvePSY1: XP_004303895; FvePSY2: XP_004289567; FvePSY3: XP004296190); Os: *Oryza sativa* (rice) (OsPSY1: NP_001058647; OsPSY2: NP_001063892; OsPSY3: ACI62767); Pp: *Prunus persica* (peach) (PpPSY1: XP_007215407; PpPSY2: XP_007207410; PpPSY3:XP_007199882); Sl: *Solanum lycopersicum* (tomato) (SIPSY: NP_001234812; SIPSY2: NP_001234671); Vv: *Vitis vinifera* (grape) (VvPSY1: AFP28795; VvPSY2: XP_003633261); Zm: *Zea mays* (corn) (ZmPSY1: ACY70893; ZmPSY2: NP_001108117; ZmPSY3: NP_001108125).

4.3.2 Promoter Analysis

Analysis of a 1.5kb fragment upstream of the translation start site for each gene revealed the presence of known cis-acting regulatory elements (Table 4.2). From this analysis, all three strawberry PSY genes are predicted to be responsive to light and circadian rhythms, however, the differential presence of elements for hormone responses, pathogen response and abiotic stress responses suggest functional diversity within this gene family.

The proximal upstream predicted TATA box in the *PSY1* promoter was located at -230 nt, suggesting the presence of an approximately 200 nt 5' untranslated region (UTR). No CAAT box, a transcriptional initiation enhancer, was predicted close to this TATA box. The promoter region of *PSY2* contained a TATA box and a CAAT box at -146nt and -141nt, respectively. Similarly, a TATA box and a CAAT box were found less than 10 nt apart from one another in the promoter region of *PSY3*. Six light response elements were found in the *PSY1* promoter, as were salicylic acid, auxin, and gibberellin response elements. The presence of a cold stress response element (LTR) and an ARE element reportedly involved in anaerobic induction,

together with a salicylic acid response element suggests that this gene may play a role in abiotic stress responses.

Analysis of the *FvePSY2* promoter revealed multiple light responsive elements, two unique gibberellin responsive elements (P-box and TATC-box), an ABA responsive element (ABRE), an ethylene responsive element (ERE), and a methyl-jasmonate response element (TGACG). Also present in the promoter region of *FvePSY2* are two temperature related response elements (HSE and LTR). HSE, the heat shock responsive element, is located at -862nt while a cold response element is predicted further upstream at -1.234nt, and an abscisic acid response element (ABRE), which is involved in both cold response and drought response, is predicted at about 100nt downstream from the LTR.

The promoter region of *FvePSY3* has three of the light response elements predicted in the *FvePSY1* and *FvePSY2* promoter regions. Unlike *FvePSY1* and *FvePSY2*, it lacks an LTR element, but like the promoter of *FvePSY2*, an HSE and a methyl jasmonate response element are predicted. *FvePSY3* also has a unique fungal elicitor responsive element (Box-W1), and an element associated with seed-specific regulation (RY-element).

Table 4.2. Predicted cis-regulatory elements in the promoter of *PSY1*, *PSY2*, and *PSY3*

Cis- element	Sequence	Position upstream ATG (in nt)			Function
		<u>PSY1</u>	<u>PSY2</u>	<u>PSY3</u>	
TATA-box	TATA; TATAAA; ATATA(A)T; TTTA; TACAAA	230	146	211	Core promoter element
CAAT- box	CAAT; CCAAT; CAATT	128	141	205	cis-acting element in promoter and enhancer regions
GAG-motif	AGAGATG; ACTCTCT	839	373	150	Light responsive element
GT1-motif	GGTTAAT	331	635	343	Light responsive element
I-box	CCCTATC	1110	786	237	Light responsive element
3-AF1 binding site	TAAGAGAGGAA	606	755	NIL	Light responsive element
G box	GTCGTG	1324	1079	NIL	Light responsive element
Box 4	ATTAAT	NIL	410	NIL	Part of module involved in light responsiveness
Sp1	CC(G/A)CCC	44	1375	NIL	Light responsive element
ABRE	CGCACGTGTC	NIL	1133	NIL	ABA responsive element
TGA element	AACGAC	813	1229	NIL	Auxin responsive element
ERE	ATTTCAA	NIL	857	NIL	Ethylene responsive element
P-box	CCTTTTG	NIL	135	NIL	Gibberellin responsive element
TATC-box	TATCCCA	NIL	783	NIL	Gibberellin responsive element
GARE-motif	AAACAGA	563	NIL	973	Gibberellin responsive element
HSE	ACAAAATTTC	NIL	862	1074	Heat stress responsive element
LTR	TTTCGG	1152	1234	NIL	Cold stress responsive element
TCA-element	CAGAAAAGGA	1377	587	NIL	Salicylic acid responsive element
TGACG-motif	TGACG	NIL	1083	418	Methyl-jasmonate responsive element
ARE	TGGTTT	889	1066	NIL	Element involved in anaerobic induction
RY-element	CATGCATG	NIL	NIL	1722	Element involved in seed-specific regulation
Box-W1	TTGACC	NIL	NIL	843	Fungal elicitor responsive element
Circadian	CAANNNNATC	483	685	889	Element involved in circadian control

4.3.3: Expression Profiles of PSY Family Members

Gene expression patterns can provide useful clues to the functions of these genes. The expression patterns of the three *F. vesca* PSY family members in anthers during later stages of flower development revealed that each gene is active a different stage of development (Figure 4.4). The RNA-seq data were obtained as part of a

larger project (Hollender et al 2014)¹⁴⁵ to obtain tissue specific transcriptomes during *F. vesca* flower development. *PSY1* is most highly expressed during stages 10 and 11, which occur after meiosis but during the time when anthers are becoming opaque yellow. *PSY2* is also highly expressed during stage 10, but unlike for *PSY1*, expression does not remain high into stage 11. *PSY3*, shows a very different expression pattern, being highly expressed pre-meiosis (bud stages 7-8) and later at stage 12, just before the flower opens.

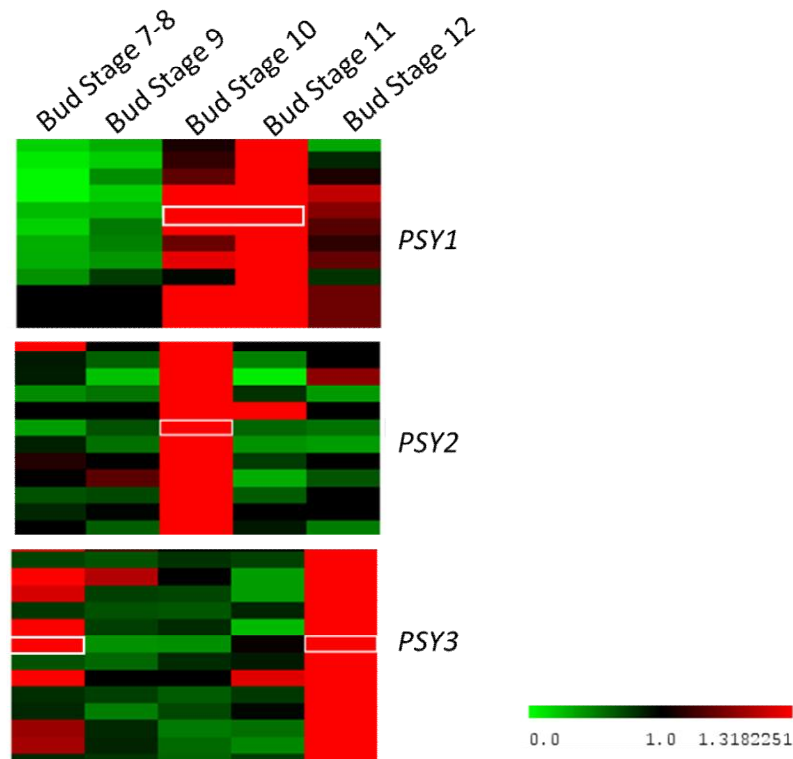


Figure 4.4. Heat map of expression of *F. vesca* *PSY* genes in anthers from pre-meiosis (stages 7-8) to just before flower opening (stage 12) based on transcriptome data from Hollender et al. 2014¹⁴⁵. Relative expression levels are represented as colors ranging from green (0: little or no expression) to red (1.3: highest expression within the five stages of floral development) for each gene. The white box denotes the specific *PSY*s, which are surrounded by rows representing other genes expressed with similar patterns.

To investigate the expression pattern of *FvePSY1*, *FvePSY2*, and *FvePSY3* in response to heat during anthesis (floral bud stage 13), total RNA was extracted from heat stressed floral, leaf, and root tissues and were subjected to quantitative real-time PCR (qPCR) analysis. The results indicated that the *PSY* gene family is not affected by elevated temperature stress in leaves and roots (Figure 4.5). In petals, *PSY1* was downregulated in response to heat stress. No change in expression levels was observed *PSY2* and *PSY3*. In receptacles, *PSY2* transcripts increased in response to heat stress. No change in expression levels was observed for *PSY1* and *PSY3*. While in anthers, *PSY3* appears to be upregulated in response to elevated temperature stress.

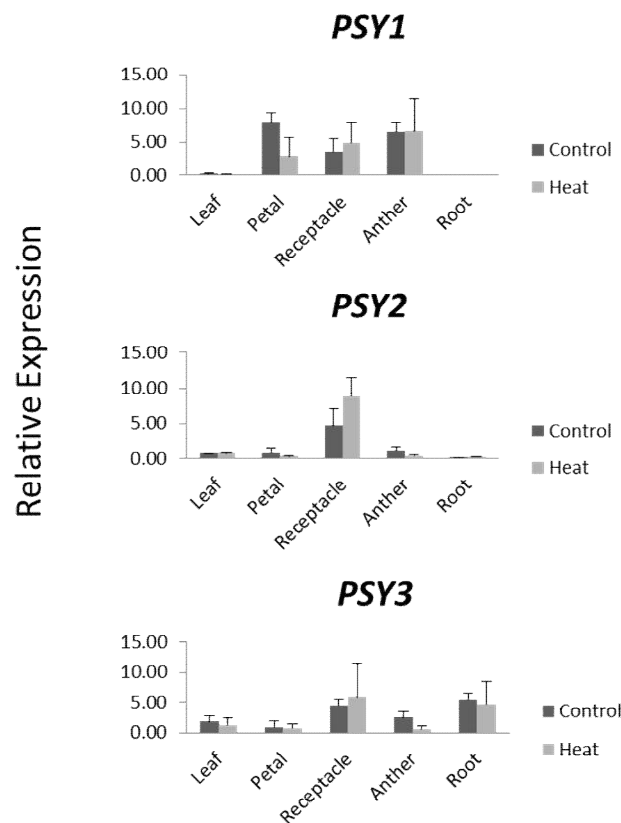


Figure 4.5. Real-time PCR expression profiles of the *F. vesca* *PSY* gene family members in leaves, mature open flower (stage 13) organs, and roots from plants

growing under control temperature conditions (25°C day/20°C night) and moderately elevated temperatures (32°C day/25°C night). Relative mRNA levels were normalized to reference genes, *NMD* and *PP2A*. Error bars indicate SEM from two biological replicates.

4.3.4: Alternative Splicing Analysis

During our initial investigation of the carotenoid biosynthetic pathway, we observed that not all of the transcripts were being processed. Analysis of *FvePSY* gene family transcripts obtained by RT-PCR showed complete intron-3-retention for *PSY1* and *PSY2*, and complete intron-1-retention for *PSY3* in leaves and seedlings (Figure 4.6A). Translation of *PSY1*, *PSY2*, and *PSY3* with their respective introns retained resulted in a protein with a truncated *trans-IPPS* catalytic domain (Figure 4.6B), suggesting that the enzymes lack activity.

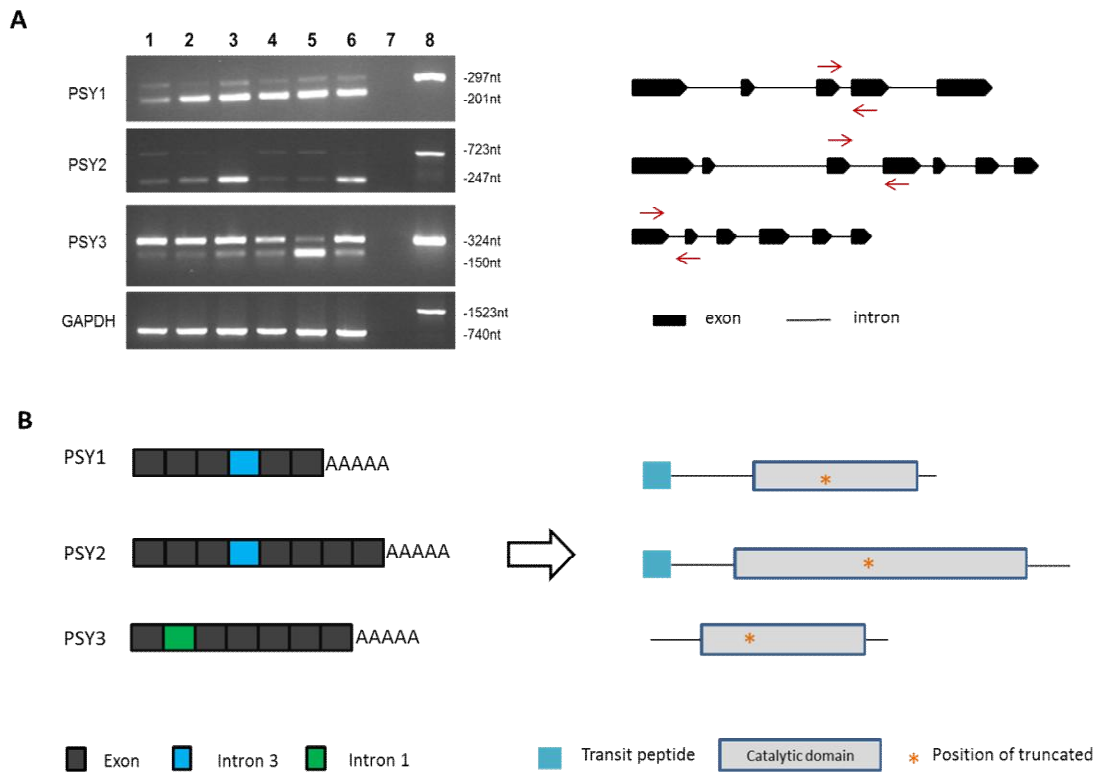


Figure 4.6 A: RT-PCR analysis of *PSY* gene family showing intron retention in mRNA from leaves of *F. vesca* inbred lines, Hawaii-4, 5AF7, and Ruegen (Lanes 1,

2, and 3) and seedlings (Lanes 4, 5, and 6) of the same inbred lines Lane 7) No template Lane 8) 5AF7 genomic DNA. Intron spanning primers for *GAPDH* was used as a control for genomic DNA contamination. **B:** Schematic representation of *FvePSY* transcripts that results in a protein with loss of catalytic domain

4.3.5: PSY Functional Complementation Assay in *Escherichia coli*

To test whether the three genes encode a protein with phytoene synthase activity, the three *F. vesca* PSY coding sequences, without a transit peptide sequence, were amplified by PCR and cloned into an *E. coli* expression vector. These were then transformed into *E. coli* harboring plasmid pAC-85b. If the strawberry gene encoded an active PSY the *E. coli* were capable of producing β -carotene and the colonies would appear orange in color. A plasmid containing the coding sequence of the Arabidopsis PSY (pAtPSY) was used as a positive control. *E. coli* co-transformed with pAC-85b alone was used as a negative control. Acetone extracts of pelleted cells from 40 ml cultures were analyzed by UV absorption spectroscopy. Based on the spectra, only the Arabidopsis gene product exhibited phytoene synthase activity in this system although the *FvePSY2* spectrum indicated absorbance at 452nm, suggesting the presence of a carotenoid (Figure 4.7).

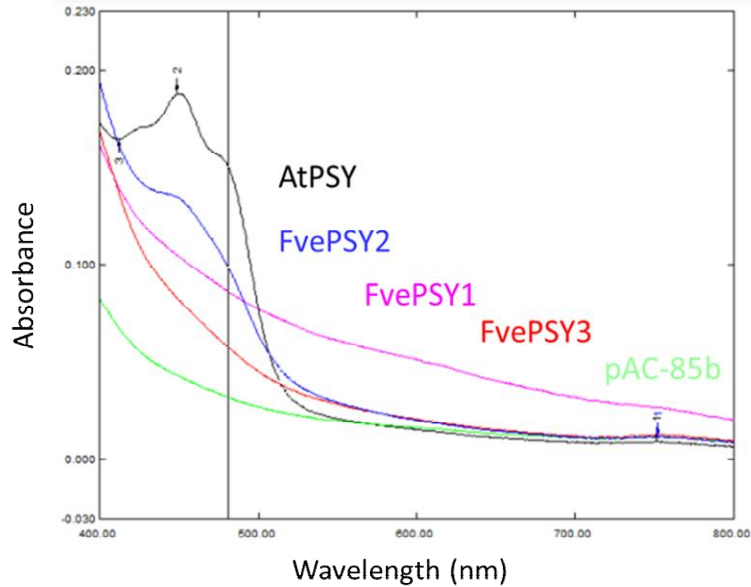


Figure 4.7. Functional complementation assay of *F. vesca* *PSY* genes. Absorbance spectra of acetone extracts from *E. coli* transformed with pAC-85b, pAtPSY, pFvePSY1, pFvePSY2, and pFvePSY3 obtained from 400-800nm. β -Carotene absorption maximum is at 452nm

4.4: Discussion

Carotenoids are an important class of phytochemicals with a broad range of health benefits. Their synthesis, which begins with the production of a colorless compound called phytoene, is regulated by PSY. Because PSY is encoded by small gene families in several crops, one of the objectives of this study was to determine how many *PSY* genes exist in *F. vesca*. We found that PSY is encoded by at least three different nuclear genes in *F. vesca*. Comparison of the three *F. vesca* genes with the *PSY* gene from Arabidopsis revealed genes with similar size exons, although the length of introns was quite variable. Sequence analysis of the 5' flanking region revealed the presence of two potential cis-regulatory elements (LTR and HSE) which are responsive to high and low temperature stress. In addition, I-box, GAG-motif,

and GT1-motif involved in light responsiveness were also identified in the promoter regions of *FvePSY1*, *FvePSY2*, and *FvePSY3*, suggesting that these genes may be regulated by similar environmental factors. Differences observed in the 5' flanking region of the PSY gene family suggests that duplicated genes may have evolved because they also have unique regulatory features.

The alignment showed that this gene family encodes proteins that have high amino acid identity and contain characteristic motifs including a putative active site despite having proteins of varying lengths (Figure 2). The highest level of sequence discrepancy among the *F. vesca* proteins was found at the N terminus where all except PSY3 have a predicted signal peptide until further analyzed, revealing a non-contiguous 32 amino acid long sequence separated from the annotated gene by a stop codon. Re-sequencing of the region upstream of the annotated translation start site for *FvePSY3* will be required to determine whether the genome sequence is an error, which is likely given the highly repetitive nature of the nucleotide sequence in question. The phylogenetic analysis showed that *FvePSY1* and *FvePSY2* share homology between one another, while *FvePSY3* is more similar to PSYs from other species.

RNA-seq gene expression analysis showed that *PSY1*, *PSY2*, and *PSY3* are differentially expressed during anther development. It was determined that the PSY gene family is not affected by elevated temperature stress in leaves and roots. In petals (harvested from stage 13 flower buds), *PSY1* was downregulated in response to heat stress. Elevated temperature stress resulted in an increase in *PSY2* transcripts in receptacles. In anthers, *PSY3* was found to be downregulated in response to heat stress.

However, no distinct expression pattern correlating with response to moderately elevated temperature stress was observed.

Functionality of *PSY1*, *PSY2*, and *PSY3* tested in a color complementation assay showed that only transcripts of *PSY2* may lead to functional proteins in the bacterial system. *FvePSY1* and *FvePSY3* lacked catalytic activity. *PSY3* from loquat also lacked enzymatic activity when transformed in *E. coli*. Alternative splicing events detected in *PSY1*, *PSY2*, and *PSY3* at the transcript level revealed a loss of catalytic domains when translated with their respective introns included (Figure 4.6 B). This cannot explain lack of activity given that reading frames of the cloned PCR products were verified by sequencing prior to being co-transformed with pAC-85b. The low β -carotene accumulation for *FvePSY2* and failure to detect any β -carotene when *E. coli* cells were independently co-transformed with *FvePSY1* and *FvePSY3* reflect the need to investigate the functionality of the three PSYs in *F. vesca* at the protein level.

In conclusion, the comprehensive information obtained in this study improves our knowledge about how the *FvePSY* gene family participate in strawberry plant development and in response to moderately elevated temperature stress.

4.5: Acknowledgements

The authors would like to thank Dr. Francis X. Cunningham Jr for providing the pAC-85b and AtPSY plasmids.

4.6: Supplemental Information

Table S1. Primers used to confirm the absence of genomic DNA contamination and conduct qPCR analysis

Primer Name	Forward and Reverse Primer Sequence [5' --> 3']	Application
GAPDH	F: GAGCATGGCTTCGGCTATAC R: TAGTCATGGTGCCCTTGATG	RT-PCR
α -Tubulin	F: TCTTCAGTGAGACTGGTGCTGGAAAGC R: AAAGCATGAAGTGGATCCTGGGGTATG	RT-PCR
NMD	F: ACCTGCCATCTTTGCGATGT R: TCCCCACAACAGAGAATGC	qPCR
PP2A	F: AAAGTCTTCCGGTGGTTGT R: CAGCACCTTTGCCACATTGA	qPCR

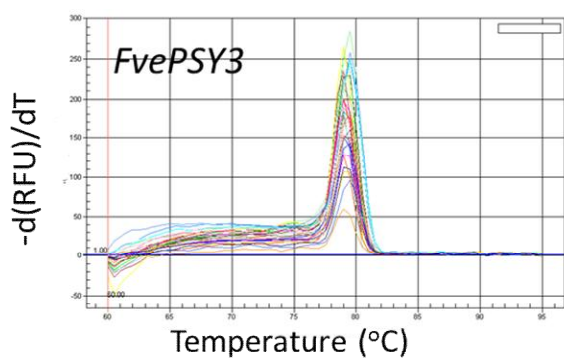
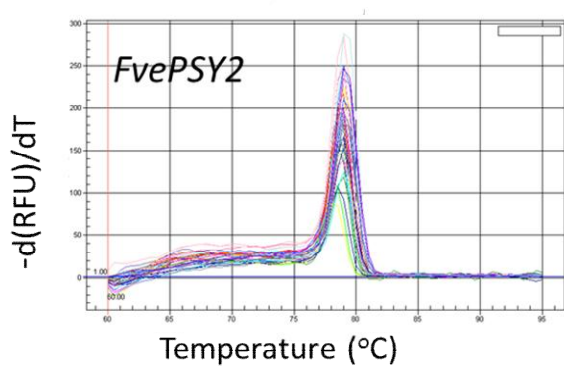
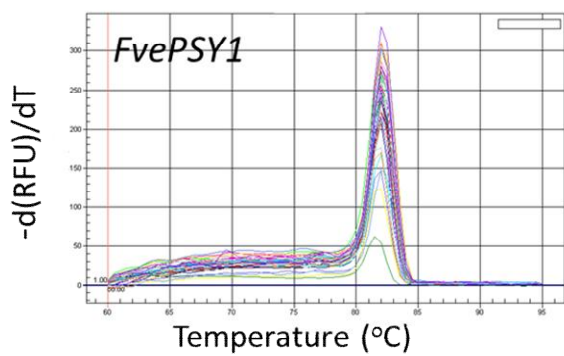


Figure S1. Melt curves of *FvePSY1*, *FvePSY2*, and *FvePSY3*, showing the amplification of a single product.

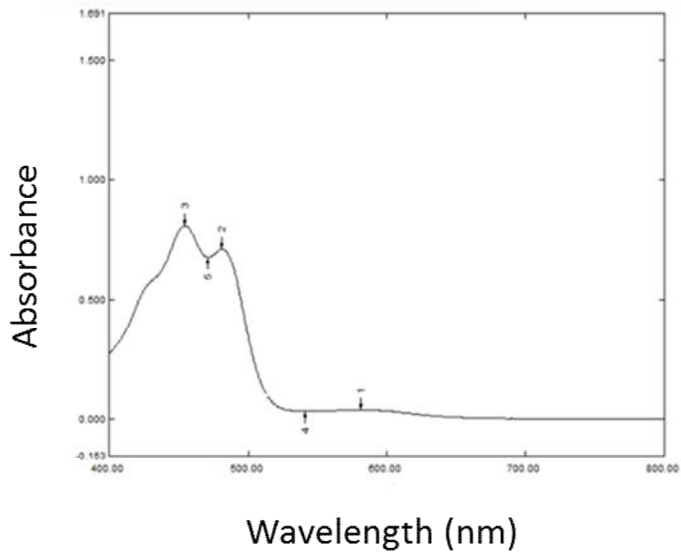


Figure S2. Absorbance spectrum of the β -carotene standard obtained from 400-800 nm.

Chapter 5: General Conclusions and Future Perspectives

The studies presented in this dissertation represent a progression in our understanding of the carotenoid biosynthetic pathway in response to moderately elevated temperature stress in the diploid strawberry, *Fragaria vesca*. This study is important because it provides a molecular basis for developing more thermotolerant strawberries, as well as other crops within the Rosaceae family.

The first study of the dissertation (Chapter 2) focused on identifying stably expressed reference genes that would permit accurate and reliable gene expression studies in strawberry. The variability of candidate reference genes, *GAPDH*, *18S*, *αTUB*, *UBQ*, *CAT*, *NMD*, *PP2A*, *EF1α*, *RPL36*, and *EFG* expression levels in different tissues from plants growing under control and moderately elevated temperatures were assessed. Statistical analyses using geNorm plus qBase and Normfinder software programs showed that *PP2A* and *NMD* were the least variably expressed genes. As a result, they were used as controls for normalization of the heat-stress responsive gene expression data described in Chapters 3 and 4.

In Chapter 3, the carotenoid biosynthetic pathway in the diploid woodland strawberry was examined for pathway specific trends in expression and metabolite accumulation under sub-optimal temperatures. The LC-HRMS method we developed for carotenoid analysis in *F. vesca* allowed us to identify and quantify seven carotenoid metabolites in control and heat stressed leaves, petals, receptacles, anthers, and roots. Unlike LC-UV, our method enabled us to detect and quantify the relative amounts of α - β -, γ -carotene or lycopene, α -cryptoxanthin and lutein in anthers using

only 10.0 mg of tissues. Gene expression analyses carried out using transcriptome data mining and qPCR showed that genes involved in biosynthesis are differentially expressed during both vegetative and reproductive development and in response to elevated temperature. Reduced accumulation of both the carotenes (α -, β -, γ -carotene or lycopene) and lutein in heat stressed leaves, receptacles, and roots correlated with decreased *PDS* transcript accumulation, and suggested that carotenoids were being degraded, perhaps as a function of scavenging ROS or cleavage to apocarotenoids, but they were not being replaced. The positive correlation between enhanced *PDS* expression and α -cryptoxanthin and lutein accumulation in heat stressed anthers supports the hypothesis that carotenoids offer protection from heat stress during plant reproduction, possibly by functioning as antioxidants.

Further review of the strawberry carotenoid biosynthetic pathway genes revealed the existence of several small genes families. PSY, the first enzyme involved in carotenoid biosynthesis, was found to be encoded by three different nuclear genes in *F. vesca* as outlined in Chapter 4. To clarify the roles of *PSY1* (gene: 28765), *PSY2* (gene: 31674), and *PSY3* (gene: 24795) in strawberry, we investigated their structural and functional differences. Comparison of the genomic structure of the three genes showed similar exon size and numbers, although the intron lengths varied. Promoter analysis indicated that the genes most probably exhibit functional diversity in plant tissues, both with respect to location and stage of development, as well as in response to abiotic stress. These findings were supported by RNA-seq gene expression analysis, showing that the three genes were differentially expressed during anther development. However, it was unclear from the qPCR expression studies whether or

not the *PSYs* in *F. vesca* are differentially responsive to heat stress. Overall, the information obtained in this study helped to improve our knowledge about how the *FvePSY* gene family participates in strawberry plant development and in response to moderately elevated temperature stress.

Despite the tremendous progress that has been made in investigating the potential of carotenoids to serve as protective compounds against heat-induced oxidative damage, there are still many areas of research that need to be addressed. The response of carotenoids to moderately elevated temperature stress at the metabolite and transcript level was found to be quite complex. With the exception of leaves and anthers, no trend or correlation between carotenoid accumulation and gene expression levels in response to heat stress could be made, indicating that there are several mechanisms regulating posttranscriptional and posttranslational processes that need to be considered. While the LC-HRMS method developed for the analysis of carotenoids was effective in separating the oxygen containing carotenoids, improvements could be made to provide more sensitivity that would permit full resolution of constitutional isomers that are devoid of any oxygen functional groups.

Several attempts were made to determine the functionality of the *PSYs* in a color complementation assay. While, no definitive conclusions could be drawn from the *E. coli* complementation assay described in Chapter 4, results suggest that *PSY2* encodes a functional protein in the bacterial system. The lack of activity seen with *PSY1* and *PSY3* could mean that *PSY1* and *PSY3* do not encode functional proteins. However, the negative results could also reflect problems with gene expression. Therefore, future work could entail a more detailed examination of the *FvePSY* gene

family at the protein level. Immunoassays that utilize antibodies to detect targeted proteins may offer more conclusive evidence into the functionality of the three PSYs in *F. vesca*.

Using a combination of genomics and metabolomics, this work identified the major pathway genes for carotenoid biosynthesis in *F vesca* and for the first time, carotenoids found in both vegetative and reproductive tissues have been analyzed. Quantitative analysis of expression of the major biosynthetic pathway genes in response to moderately elevated temperatures, combined with assessment of carotenoids in leaves and flower organs, indicated that complex mechanisms for regulation of carotenoid accumulation exist. While a definitive role for carotenoids as protection from heat stress generated ROS in anthers was not supported by these analyses, the data indicate that further investigation into the mechanisms for regulation of carotenoid accumulation is warranted to facilitate breeding or engineering strawberries that remain productive at higher temperatures.

References

1. Slavin, J. L.; Lloyd, B., Health Benefits of Fruits and Vegetables. *Adv Nutr.* **2012**, *3* (4), 506-516.
2. Hung, H.-C.; Joshipura, K. J.; Jiang, R.; Hu, F. B.; Hunter, D.; Smith-Warner, S. A.; Colditz, G. A.; Rosner, B.; Spiegelman, D.; Willett, W. C., Fruit and Vegetable Intake and Risk of Major Chronic Disease. *J Natl Cancer Inst.* **2004**, *96* (21), 1577-1584.
3. Lake, I. R.; Hooper, L.; Abdelhamid, A.; Bentham, G.; Boxall, A. B.; Draper, A.; Fairweather-Tait, S.; Hulme, M.; Hunter, P. R.; Nichols, G.; Waldron, K. W., Climate Change and Food Security: Health Impacts in Developed Countries. *Environ Health Perspect.* **2012**, *120* (11), 1520-6.
4. Wheeler, T.; Von Braun, J., Climate Change Impacts on Global Food Security. *Science.* **2013**, *341* (6145), 508-513.
5. Darrow, G. M., The Strawberry Species. In *The Strawberry: History, Breeding and Physiology*, Holt, Rinehart and Winston: New York, Chicago, San Francisco, 1966; pp 108-129.
6. Giampieri, F.; Tulipani, S.; Alvarez-Suarez, J. M.; Quiles, J. L.; Mezzetti, B.; Battino, M., The Strawberry: Composition, Nutritional Quality, and Impact on Human Health. *Nutrition.* **2012**, *28* (1), 9-19.
7. Li, H.; Li, T.; Gordon, R. J.; Asiedu, S. K.; Hu, K., Strawberry Plant Fruiting Efficiency and its Correlation with Solar Irradiance, Temperature and Reflectance Water Index Variation. *Environ Exper Bot.* **2010**, *68* (2), 165-174.
8. Cramer, G.; Urano, K.; Delrot, S.; Pezzotti, M.; Shinozaki, K., Effects of Abiotic Stress on Plants: A Systems Biology Perspective. *BMC Plant Biol.* **2011**, *11* (1), 163.
9. Mittler, R., Abiotic Stress, The Field Environment and Stress Combination. *Trends Plant Sci.* **2006**, *11* (1), 15-19.

10. Atkinson, N. J.; Urwin, P. E., The Interaction of Plant Biotic and Abiotic Stresses: From Genes to the Field. *J Exp Bot.* **2012**, *63* (10), 3523-3543.
11. Wang, W.; Vinocur, B.; Shoseyov, O.; Altman, A., Roles of Plant Heat-Shock Proteins and Molecular Chaperones in the Abiotic Stress Response *Trends Plant Sci.* **2004**, *9*, 244-252.
12. dos Reis, S. P.; Lima, A. M.; de Souza, C. R. B., Recent Molecular Advances on Downstream Plant Responses to Abiotic Stress. *Int J Mol Sci.* **2012**, *13* (7), 8628-8647.
13. Mittler, R.; Blumwald, E., Genetic Engineering for Modern Agriculture: Challenges and Perspectives. *Annu Rev Plant Biol.* **2010**, *61*, 443-462.
14. Van Regenmortel, M. H. V., Reductionism and Complexity in Molecular Biology. *EMBO Rep.* **2004**, *5*, 1016-1020.
15. Mazzocchi, F., Complexity in Biology. Exceeding the Limits of Reductionism and Determinism using Complexity Theory. *EMBO Rep.* **2008**, *9*, 10-14.
16. Edreva, A.; Velikova, V.; Tsonev, T.; Dagnon, S.; Gürel, A.; Aktaş, L.; Gesheva, E., Stress-Protective Roles of Secondary Metabolites: Diversity of Functions and Mechanisms. *Gen Appl Plant Physiol.* **2008**, *34* (1-2), 67-68.
17. Bennett, R. N.; Wallsgrove, R. M., Secondary Metabolites in Plant Defence Mechanisms. *New Phytol.* **1994**, *127* (4), 617-633.
18. Harborne, J. B., Classes and Functions of Secondary Products from Plants. In *Chemicals from Plants: Perspectives on Plant Secondary Products*, Walton, N. J. B., D.E., Ed. Imperial College Press and World Scientific Publishing Co. Pte Ltd: Covent Garden, London, 1999.
19. Ramakrishna, A.; Ravishankar, G. A., Influence of Abiotic Stress Signals on Secondary Metabolites in Plants. *Plant Signal Behav.* **2011**, *6*, 1720-1731.
20. Gill, S. S.; Tuteja, N., Reactive Oxygen Species and Antioxidant Machinery in Abiotic Stress Tolerance in Crop Plants. *Plant Physiol Biochem.* **2010**, *48*, 909-930.

21. Goodwin, T. W., *The Biochemistry of the Carotenoids*. 2 ed.; Chapman and Hall: London, 1980; Vol. 1.
22. Cazzonelli, C. I.; Nisar, N.; Hussain, D.; Carmody, M. D.; Pogson, B. J., Biosynthesis and Regulation of Carotenoids in Plants—Micronutrients, Vitamins and Health Benefits. In *Plant Developmental Biology - Biotechnological Perspectives*, Davey, M. R. P., Eng Chong, Ed. Springer Verlag Berlin Heidelberg, 2010; Vol. 2, pp 117-137.
23. Vishnevetsky, M.; Ovadis, M.; Zuker, A.; Vainstein, A., Molecular Mechanisms Underlying Carotenogenesis in the Chromoplast: Multilevel Regulation of Carotenoid-Associated Genes. *The Plant Journal* **1999**, *20* (4), 423-431.
24. Cazzonelli, C. I., Carotenoids in Nature: Insights from Plants and Beyond. *Funct Plant Biol.* **2011**, *38*, 833-847.
25. Maoka, T., Carotenoids in Marine Animals. *Marine Drugs* **2011**, *9* (2), 278-293.
26. McGraw, K. J.; Nolan, P. M.; Crino, O. L., Carotenoid Accumulation Strategies for Becoming a Colourful House Finch: Analyses of Plasma and Liver Pigments in Wild Moulting Birds. *Funct Ecol.* **2006**, *20* (4), 678-688.
27. Clotfelter, E. D.; Ardia, D. R.; McGraw, K. J., Red fish, Blue fish: Trade-offs Between Pigmentation and Immunity in Betta Splendens. *Behav Ecol.* **2007**, *18* (6), 1139-1145.
28. Dutta, D.; Chaudhuri, U. R.; Chakraborty, R., Structure, Health Benefits, Antioxidant Property and Processing and Storage of Carotenoids. *Afr. J Biotechnol.* **2004**, *4*, 1510-1520.
29. Britton, G.; Liaaen-Jensen, S.; Pfander, H., *Carotenoids: Handbook*. Birkhauser Verlag, Basel-Boston-Berlin: 2004.
30. Britton, G., Structure and Properties of Carotenoids in Relation to Function. *The FASEB Journal.* **1995**, *9* (15), 1551-8.

31. IUPAC Commission on the Nomenclature of Organic Chemistry (CNO) and IUPAC-IUB Commission on Biochemical Nomenclature (CBN). *Eur. J. Biochem.* **1972**, *25* (3), 397-408.
32. Gruszecki, W. I.; Strzałka, K., Carotenoids as Modulators of Lipid Membrane Physical Properties. *Biochim Biophys Acta.* **2005**, *1740* (2), 108-115.
33. Khoo, H.-E.; Prasad, K. N.; Kong, K.-W.; Jiang, Y.; Ismail, A., Carotenoids and Their Isomers: Color Pigments in Fruits and Vegetables. *Molecules.* **2011**, *16* (2), 1710-1738.
34. Updike, A. A.; Schwartz, S. J., Thermal Processing of Vegetables Increases Cis Isomers of Lutein and Zeaxanthin. *J Agric Food Chem.* **2003**, *51* (21), 6184-6190.
35. Widomska, J.; Subczynski, W. K., Transmembrane Localization of Cis-isomers of Zeaxanthin in the Host Dimyristoylphosphatidylcholine Bilayer Membrane. *Biochim Biophys Acta.* **2008**, *1778* (1), 10-19.
36. Cogdell, R. J., Carotenoids in Photosynthesis. *Pure Appl Chem.* **1985**, *57* (5), 723-728.
37. Muller, P.; Li, X.; Niyogi, K. K., Non-Photochemical Quenching. A Response to Excess Light Energy. *Plant Physiol.* **2001**, *125* (4), 1558-1566.
38. Demmig-Adams, B.; Adams, W. W., III, The Role of Xanthophyll Cycle Carotenoids in the Protection of Photosynthesis. *Trends Plant Sci.* **1996**, *1* (1), 21-26.
39. Stanier, R. Y.; Cohen-Bazire, G., The role of light in the microbial world: some facts and speculations. In *Microbial Ecology*, Spicer, R. E. O. W. a. C. C., Ed. Cambridge University Press: London, 1957; pp 56-89.
40. Apel, K.; Hirt, H., Reactive Oxygen Species: Metabolism, Oxidative Stress, and Signal Transduction. *Annu Rev Plant Biol.* **2004**, *55*, 373-399.
41. Demmig-Adams, B.; Gilmore, A. M.; Adams, W. W., Carotenoids 3: In Vivo Function of Carotenoids in Higher Plants. *The FASEB Journal.* **1996**, *10* (4), 403-12.

42. Winterhalter, P.; Ebeler, S. E., Carotenoid Cleavage Products: An Introduction. In *Carotenoid Cleavage Products*, American Chemical Society: 2013; Vol. 1134, pp 3-9.
43. Vogel, J. T.; Tan, B.-C.; McCarty, D. R.; Klee, H. J., The Carotenoid Cleavage Dioxygenase 1 Enzyme has Broad Substrate Specificity, Cleaving Multiple Carotenoids at Two Different Bond Positions. *J Biol Chem.* **2008**, *283*, 11364–11373.
44. Schwartz, S. H.; Tan, B. C.; Gage, D. A.; Zeevaart, J. A. D.; McCarty, D. R., Specific Oxidative Cleavage of Carotenoids by VP14 of Maize. *Science.* **1997**, *276* (5320), 1872-1874.
45. Kohlen, W.; Charnikhova, T.; Lammers, M.; Pollina, T.; Tóth, P.; Haider, I.; Pozo, M. J.; de Maagd, R. A.; Ruyter-Spira, C.; Bouwmeester, H. J.; López-Ráez, J. A., The Tomato Carotenoid Cleavage Dioxygenase 8 (*SICCD8*) Regulates Rhizosphere Signaling, Plant Architecture and Affects Reproductive Development Through Strigolactone Biosynthesis. *New Phytol.* **2012**, *196* (2), 535-547.
46. Vogel, J. T.; Walter, M. H.; Giavalisco, P.; Lytovchenko, A.; Kohlen, W.; Charnikhova, T.; Simkin, A. J.; Goulet, C.; Strack, D.; Bouwmeester, H. J.; Fernie, A. R.; Klee, H. J., *SICCD7* Controls Strigolactone Biosynthesis, Shoot Branching and Mycorrhiza-Induced Apocarotenoid Formation in Tomato. *The Plant Journal* **2010**, *61* (2), 300-311.
47. Zeb, A.; Mehmood, S., Carotenoids Contents from Various Sources and Their Potential Health Applications. *Pakistan J Nutrit.* **2004**, *3*, 199-204.
48. Mortensen, A., Carotenoids and Other Pigments as Natural Colorants. *Pure Appl Chem.* **2006**, *78*, 1477–1491.
49. Landrum, J. T.; Bone, R. A.; Chen, Y.; Herrero, C.; Llerena, C. M.; Ewa Twarowska, E., Carotenoids in the Human Retina. *Pure Appl Chem.* **1999**, *71*, 2237-2244.
50. Abdel-Aal, E.-S. M.; Akhtar, H.; Zaheer, K.; Ali, R., Dietary Sources of Lutein and Zeaxanthin Carotenoids and their Role in Eye Health. *Nutrients.* **2013**, *5*, 1169-1185.

51. Bernstein, P. S.; Khachik, F.; Carvalho, L. S.; Muir, G. J.; Zhao, D.-Y.; Katz, N. B., Identification and Quantitation of Carotenoids and their Metabolites in the Tissues of the Human Eye. *Exp Eye Res.* **2001**, *72* (3), 215-223.
52. Beatty, S.; Boulton, M.; Henson, D.; Koh, H.; Murray, I., Macular Pigment and Age Related Macular Degeneration. *Br. J Ophthalmol.* **1999**, *83* (7), 867-877.
53. Sommer, A., Vitamin A Deficiency and Clinical Disease: An Historical Overview. *J Nutr.* **2008**, *138* (10), 1835-1839.
54. Rohmer, M., The discovery of a mevalonate-independent pathway for isoprenoid biosynthesis in bacteria, algae, and higher plants. *Nat Prod Rep.* **1999**, *16*, 565-574.
55. Lichtenthaler, H. K., The 1-deoxy-D-xylulose-5-phosphate pathway of isoprenoid biosynthesis in plants. *Annu Rev Plant Biol.* **1999**, *50* (1), 47-65.
56. Hirschberg, J., Carotenoid Biosynthesis in Flowering Plants. *Curr Opin Plant Biol.* **2001**, *4* (3), 210-218.
57. Isaacson, T.; Ronen, G.; Zamir, D.; Hirschberg, J., Cloning of Tangerine from Tomato Reveals a Carotenoid Isomerase Essential for the Production of β -Carotene and Xanthophylls in Plants. *The Plant Cell.* **2002**, *14* (2), 333-342.
58. Cunningham Jr, F. X.; Pogson, B.; Sun, Z.; McDonald, K. A.; DellaPenna, D.; Gantt, E., Functional Analysis of the [beta] and [epsilon] Lycopene Cyclase Enzymes of Arabidopsis Reveals a Mechanism for Control of Cyclic Carotenoid Formation. *The Plant Cell.* **1996**, *8* (9), 1613-1626.
59. DellaPenna, D.; Pogson, B. J., Vitamin Synthesis in Plants: Tocopherols and Carotenoids. *Annu Rev Plant Biol.* **2006**, *57* (1), 711-738.
60. Cunningham, F. X.; Gantt, E., Genes and Enzymes of Carotenoid in Plants *Annu Rev Plant Biol.* **1998**, *49* (1), 557-583.
61. Zinn, K. E.; Tunc-Ozdemir, M.; Harper, J. F., Temperature Stress and Plant Sexual Reproduction: Uncovering the Weakest Link. *J Exp Bot.* **2010**, *61*, 1959-1968.

62. Fait, A.; Hanhineva, K.; Beleggia, R.; Dai, N.; Rogachev, I.; Nikiforova, V. J.; Fernie, A. R.; Aharoni, A., Reconfiguration of the Achene and Receptacle Metabolic Networks During Strawberry Fruit Development. *Plant Physiol.* **2008**, *148*, 730-750.
63. Kaplan, F.; Kopka, J.; Haskwell, D. W.; Zhao, W.; Schiller, C., K.; Gatzke, N., Exploring the Temperature-Stress Metabolome of Arabidopsis *Plant Physiol.* **2004**, *136*, 4159-4168.
64. Thakur, P.; Kumar, S.; Malik, J. A.; Berger, J. D.; Nayyar, H., Cold stress effects on reproductive development in grain crops: An overview *Environ Exp Bot.* **2010**, *67*, 429-443.
65. Sakata, T.; Oshino, T.; Miura, S.; Tomabeche, M.; Tsunaga, Y.; Higashitani, N.; Miyazawa, Y.; Takahashi, H.; Watanabe, M.; Higashitani, A., Auxins reverse plant male sterility caused by high temperatures. *Proc Natl Acad Sci. USA* **2010**, *107*, 8569-8574.
66. Hummer, K. E.; Janicks, J., Rosaceae: Taxonomy, Economic Importance, Genomics. In *Genetics and Genomics of Rosaceae*, Folta, K. M.; Gardiner, S. E., Eds. Springer: New York, NY, 2009; Vol. 6, pp 1-7.
67. Davis, T. M.; Denoyes-Rothan, B.; Lerceteau-Köhler, E., Strawberry. In *Fruits and Nuts*, Kole, C., Ed. Springer Berlin Heidelberg: 2007; Vol. 4, pp 189-205.
68. Akiyama, Y., Yamamoto, Y., Ohmido, N., Oshima, M. and; Fukui, K., Estimation of the Nuclear DNA Content of Strawberries (*Fragaria* spp.) Compared with Arabidopsis Thaliana by Using Dual System Flow Cytometry, . *Cytologia.* **2001**, *66*, 431-436.
69. Shulaev, V.; Sargent, D. J.; Crowhurst, R. N.; Mockler, T. C.; Folkerts, O.; Delcher, A. L.; Jaiswal, P.; Mockaitis, K.; Liston, A.; Mane, S. P.; Burns, P.; Davis, T. M.; Slovin, J. P.; Bassil, N.; Hellens, R. P.; Evans, C.; Harkins, T.; Kodira, C.; Desany, B.; Crasta, O. R.; Jensen, R. V.; Allan, A. C.; Michael, T. P.; Setubal, J. C.; Celton, J.-M.; Rees, D. J. G.; Williams, K. P.; Holt, S. H.; Rojas, J. J. R.; Chatterjee, M.; Liu, B.; Silva, H.; Meisel, L.; Adato, A.; Filichkin, S. A.; Troggio, M.; Viola, R.; Ashman, T.-L.; Wang, H.; Dharmawardhana, P.; Elser, J.; Raja, R.; Priest, H. D.; Bryant, D. W.; Fox, S. E.; Givan, S. A.; Wilhelm, L. J.; Naithani, S.; Christoffels, A.; Salama, D. Y.; Carter, J.; Girona, E. L.; Zdepski, A.; Wang, W.; Kerstetter, R. A.; Schwab, W.; Korban, S. S.; Davik, J.; Monfort, A.; Denoyes-Rothan, B.; Arus, P.; Mittler, R.; Flinn, B.; Aharoni, A.; Bennetzen, J. L.; Salzberg, S. L.; Dickerman, A.

- W.; Velasco, R.; Borodovsky, M.; Veilleux, R. E.; Folta, K. M., The Genome of Woodland Strawberry (*Fragaria vesca*). *Nat Genet.* **2011**, *43* (2), 109-116.
70. Slovin, J.; Schmitt, K.; Folta, K., An Inbred Line of the Diploid Strawberry *Fragaria vesca* f. *Semperflorens* for Genomic and Molecular Genetic Studies in the Rosaceae. *Plant Methods.* **2009**, *5* (1), 15.
71. Bustin, S. A., Quantification of mRNA using Real-Time Reverse Transcription PCR (RT-PCR): Trends and Problems. *J Mol Endocrinol.* **2002**, *29* (1), 23-39.
72. Bustin, S. A.; Benes, V.; Nolan, T.; Pfaffl, M. W., Quantitative Real-time RT-PCR – a perspective. *J Mol Endocrinol.* **2005**, *34* (3), 597-601.
73. Bustin, S. A.; Benes, V.; Garson, J. A.; Hellemans, J.; Huggett, J.; Kubista, M.; Mueller, R.; Nolan, T.; Pfaffl, M. W.; Shipley, G. L.; Vandesompele, J.; Wittwer, C. T., The MIQE Guidelines: Minimum Information for Publication of Quantitative Real-Time PCR Experiments. *Clinical Chem.* **2009**, *55* (4), 611-622.
74. Huggett, J.; Dheda, K.; Bustin, S.; Zumla, A., Real-Time RT-PCR Normalisation: Strategies and Considerations. *Genes Immun.* **2005**, *6* (4), 279 - 284.
75. Dheda, K.; Huggett, J.; Bustin, S.; Johnson, M.; Rook, G.; Zumla, A., Validation of Housekeeping Genes for Normalizing RNA Expression in Real-Time PCR. *BioTechniques.* **2004**, *37*, 112 - 119.
76. Selvey, S.; Thompson, E. W.; Matthaei, K.; Lea, R. A.; Irving, M. G.; Griffiths, L. R., β -Actin—An Unsuitable Internal Control for RT-PCR. *Mol Cell Probes* **2001**, *15* (5), 307-311.
77. Glare, E. M.; Divjak, M.; Bailey, M. J.; Walters, E. H., β -Actin and GAPDH Housekeeping Gene Expression in Asthmatic Airways is Variable and Not Suitable for Normalising mRNA Levels. *Thorax* **2002**, *57* (9), 765-770.
78. Radonić, A.; Thulke, S.; Mackay, I. M.; Landt, O.; Siegert, W.; Nitsche, A., Guideline to Reference Gene Selection for Quantitative RealTime PCR. *Biochem Biophys Res Commun.* **2004**, *313* (4), 856-862.

79. Gutierrez, L.; Mauriat, M.; Guenin, S.; Pelloux, J.; Lefebvre, J.; Louvet, R.; Rusterucci, C.; Moritz, T.; Guerineau, F.; Bellini, C.; Van Wuytswinkel, O., The Lack of A Systematic Validation of Reference Genes: A Serious Pitfall Undervalued in Reverse Transcription-Polymerase Chain Reaction (RT-PCR) Analysis in Plants. *Plant Biotechnol J.* **2008**, (6), 609 - 618.
80. Exposito-Rodriguez, M.; Borges, A.; Borges-Perez, A.; Perez, J., Selection of Internal Control Genes for Quantitative Real-Time RT-PCR Studies During Tomato Development Process. *BMC Plant Biol.* **2008**, 8 (1), 131.
81. Mallona, I.; Lischewski, S.; Weiss, J.; Hause, B.; Egea-Cortines, M., Validation of Reference Genes for Quantitative Real-Time PCR During Leaf and Flower Development in *Petunia hybrida*. *BMC Plant Biol.* **2010**, 10 (1), 4.
82. Vandesompele, J.; De Preter, K.; Pattyn, F.; Poppe, B.; Van Roy, N.; De Paepe, A.; Speleman, F., Accurate Normalization of Real-Time Quantitative RT-PCR Data by Geometric Averaging of Multiple Internal Control Genes. *Genome Biol.* **2002**, 3 (7), research0034.1 - research0034.11.
83. Andersen, C. L.; Jensen, J. L.; Ørntoft, T. F., Normalization of Real-Time Quantitative Reverse Transcription-PCR Data: A Model-Based Variance Estimation Approach to Identify Genes Suited for Normalization, Applied to Bladder and Colon Cancer Data Sets. *Cancer Res.* **2004**, 64 (15), 5245-5250.
84. Hellemans, J.; Mortier, G.; De Paepe, A.; Speleman, F.; Vandesompele, J., qBase Relative Quantification Framework and Software for Management and Automated Analysis of Real-Time Quantitative PCR Data. *Genome Biol.* **2007**, 8 (2), R19.
85. Xie, F.; Xiao, P.; Chen, D.; Xu, L.; Zhang, B., miRDeepFinder: A miRNA Analysis Tool for Deep Sequencing of Plant Small RNAs. *Plant Mol Biol.* **2012**, 80 (1), 75-84.
86. Nygard, A.-B.; Jørgensen, C. B.; Cirera, S.; Fredholm, M., Selection of Reference Genes for Gene Expression Studies in Pig Tissues using SYBR Green qPCR. *BMC Molecular Biol.* **2007**, 8, 67-67.
87. Tatsumi, K.; Ohashi, K.; Taminishi, S.; Okano, T.; Yoshioka, A.; Shima, M., Reference Gene Selection for Real-Time RT-PCR in Regenerating Mouse Livers. *Biochem Biophys Res Commun.* **2008**, 374 (1), 106 - 110.

88. Teste, M.-A.; Duquenne, M.; Francois, J.; Parrou, J.-L., Validation of Reference Genes for Quantitative Expression Analysis by Real-Time RT-PCR in *Saccharomyces cerevisiae*. *BMC Molecular Biol.* **2009**, *10* (1), 99.
89. Gutierrez, L.; Mauriat, M.; Guénin, S.; Pelloux, J.; Lefebvre, J.-F.; Louvet, R.; Rusterucci, C.; Moritz, T.; Guerineau, F.; Bellini, C.; Van Wuytswinkel, O., The Lack of A Systematic Validation of Reference Genes: A Serious Pitfall Undervalued in Reverse Transcription-Polymerase Chain Reaction (RT-PCR) Analysis in Plants. *Plant Biotechnol J.* **2008**, *6* (6), 609-618.
90. Gutierrez, L.; Mauriat, M.; Pelloux, J.; Bellini, C.; Van Wuytswinkel, O., Towards a Systematic Validation of References in Real-Time RT-PCR. *The Plant Cell.* **2008**, *20* (7), 1734-1735.
91. Udvardi, M. K.; Czechowski, T.; Scheible, W.-R., Eleven Golden Rules of Quantitative RT-PCR. *The Plant Cell.* **2008**, *20* (7), 1736-1737.
92. Vickers, C., E. ; Gershenzon, Johnathan; Lerda, Manuel T.; Loreto, Francesco A Unified Mechanism of Action for Volatile Isoprenoids in Plant Abiotic Stress. *Nat Chem Biol.* **2009**, *5* (283-291).
93. Lobell, D. B.; Gourdj, S. M., The Influence of Climate Change on Global Crop Productivity. *Plant Physiol.* **2012**, *160* (4), 1686-1697.
94. Zhang, J.; Klueva, N.; Wang, Z.; Wu, R.; Ho, T.-H.; Nguyen, H., Genetic Engineering for Abiotic Stress Resistance in Crop Plants. *In Vitro Cellular & Developmental Biology - Plant* **2000**, *36* (2), 108-114.
95. Czechowski, T.; Stitt, M.; Altmann, T.; Udvardi, M. K.; Scheible, W. R., Genome-Wide Identification and Testing of Superior Reference Genes for Transcript Normalization in Arabidopsis. *Plant Physiol.* **2005**, *139* (1), 5-17.
96. Nicot, N.; Hausman, J.-F.; Hoffmann, L.; Evers, D., Housekeeping Gene Selection for Real-Time RT-PCR Normalization in Potato During Biotic and Abiotic Stress. *J Exp Bot.* **2005**, *56* (421), 2907-2914.
97. Paolacci, A.; Tanzarella, O.; Porceddu, E.; Ciaffi, M., Identification and Validation of Reference Genes for Quantitative RT-PCR Normalization in Wheat. *BMC Mol Biol.* **2009**, *10* (1), 11.

98. Løvdal, T.; Lillo, C., Reference Gene Selection for Quantitative Real-Time PCR Normalization in Tomato Subjected to Nitrogen, Cold, and Light Stress. *Anal Biochem.* **2009**, *387* (2), 238-242.
99. Obrero, A.; Die, J. V.; Roman, B.; Gonmez, P.; Nadal, S.; Gonzalez-Verdejo, C. I., Selection of Reference Genes for Gene Expression Studies in Zucchini (*Cucurbita pepo*) using qPCR. *J Agric Food Chem.* **2011**, *59* (10), 5402-5411.
100. Chen, L.; Zhong, H. Y.; Kuang, J. F.; Li, J.; Lu, W. J.; Chen, J. Y., Validation of Reference genes for RT-qPCR Studies of Gene Expression in Banana Fruit Under Different Experimental Conditions. *Planta* **2011**, *234* (2), 377-390.
101. Clancy, M.; Rosli, H.; Chamala, S.; Barbazuk, W. B.; Civello, P. M.; Folta, K., Validation of Reference Transcripts in Strawberry (*Fragaria* spp.). *Mol. Genet. Genomics* **2013**, *288* (12), 671-681.
102. Amil-Ruiz, F.; Garrido-Gala, J.; Blanco-Portales, R.; Folta, K. M.; Muñoz-Blanco, J.; Caballero, J. L., Identification and Validation of Reference Genes for Transcript Normalization in Strawberry (*Fragaria* × *ananassa*) Defense Responses. *PLoS ONE.* **2013**, *8* (8), e70603.
103. Galli, V.; Borowski, J. M.; Perin, E. C.; Messias, R. d. S.; Labonde, J.; Pereira, I. d. S.; Silva, S. D. d. A.; Rombaldi, C. V., Validation of Reference Genes for Accurate Normalization of Gene Expression for Real Time-Quantitative PCR in Strawberry Fruits using Different Cultivars and Osmotic Stresses. *Gene* **2015**, *554* (2), 205-214.
104. Kadir, S.; Sidhu, G.; Al-Khatib, K., Strawberry (*Fragaria* × *ananassa* Duch.) Growth and Productivity as Affected by Temperature. *Hort Sci.* **2006**, *41* (6), 1423-1430.
105. Ledesma, N.; Sugiyama, N., Pollen Quality and Performance in Strawberry Plants Exposed to High-temperature Stress. *J Amer. Soc. Hort. Sci.* **2005**, *130* (3), 341-347.
106. Shulaev, V.; Korban, S. S.; Sosinski, B.; Abbott, A. G.; Aldwinckle, H. S.; Folta, K. M.; Iezzoni, A.; Main, D.; Arús, P.; Dandekar, A. M.; Lewers, K.; Brown, S. K.; Davis, T. M.; Gardiner, S. E.; Potter, D.; Veilleux, R. E., Multiple Models for Rosaceae Genomics. *Plant Physiol.* **2008**, *147* (3), 985-1003.

107. Slovin, J. P.; Michael, T. P., Strawberry: Structural and Functional Genomics In *Genetics, Genomics, and Breeding of Berries*, First ed.; Kole, K. M. F. a. C., Ed. Science Publishers: Enfield, 2011; pp 162-193.
108. Chabot, B. F., Environmental Influences on Photosynthesis and Growth in *Fragaria vesca*. *New Phytol.* **1978**, *80*, 87-98.
109. Nolan, T.; Hands, R. E.; Bustin, S. A., Quantification of mRNA using Real-Time RT-PCR. *Nat. Protocols* **2006**, *1* (3), 1559-1582.
110. Die, J. V.; Obrero, Á.; González-Verdejo, C. I.; Román, B., Characterization of the 3':5' Ratio for Reliable Determination of RNA Quality. *Anal Biochem.* **2011**, *419* (2), 336-338.
111. Pfaffl, M. W., A New Mathematical Model for Relative Quantification in Real-Time RT-PCR. *Nucleic Acids Res.* **2001**, *29* (9), e45.
112. Darwish, O.; Slovin, J.; Kang, C.; Hollender, C.; Geretz, A.; Houston, S.; Liu, Z.; Alkharouf, N., SGR: An Online Genomic Resource for the Woodland Strawberry. *BMC Plant Biol.* **2013**, *13* (1), 223.
113. Zuker, M., Mfold Web Server for Nucleic Acid Folding and Hybridization Prediction. *Nucleic Acids Res.* **2003**, *31* (13), 3406-3415.
114. Ramakers, C.; Ruijter, J. M.; Deprez, R. H. L.; Moorman, A. F. M., Assumption-Free Analysis of Quantitative Real-Time Polymerase Chain Reaction Data. *Neurosci Lett.* **2003**, *339*, 62-66.
115. Ruijter, J. M.; Ramakers, C.; Hoogaars, W. M. H.; Karlen, Y.; Bakker, O.; van den Hoff, M. J. B.; Moorman, A. F. M., Amplification Efficiency: Linking Baseline and Bias in the Analysis of Quantitative PCR Data. *Nucleic Acids Res.* **2009**, *37* (6), e45.
116. Nicolet, C. M.; Craig, E. A., Isolation and Characterization of ST11, A Stress-inducible Gene from *Saccharomyces Cerevisiae*. *Mol. Cell. Biol.* **1989**, *9* (9), 3638-3646.
117. Die, J. V.; Rowland, L. J., Superior Cross-Species Reference Genes: A Blueberry Case Study. *PLoS ONE* **2013**, *8* (9), e73354.

118. Die, J. V.; Román, B., RNA Quality Assessment: A View from Plant qPCR Studies. *J Exp Bot.* **2012**, *63*, 6069-6077.
119. Liu, D.; Shi, L.; Han, C.; Yu, J.; Li, D.; Zhang, Y., Validation of Reference Genes for Gene Expression Studies in Virus-Infected *Nicotiana benthamiana* using Quantitative Real-Time PCR. *PLoS ONE.* **2012**, *7* (9), e46451.
120. Die, J. V.; Román, B.; Nadal, S.; González-Verdejo, C., Evaluation of Candidate Reference Genes for Expression Studies in *Pisum sativum* under Different Experimental Conditions. *Planta* **2010**, *232* (1), 145-153.
121. Tong, Z.; Gao, Z.; Wang, F.; Zhou, J.; Zhang, Z., Selection of Reliable Reference Genes for Gene Expression Studies in Peach using Real-Time PCR. *BMC Mol Biol.* **2009**, *10* (1), 71.
122. Lee, J.; Roche, J.; Donaghy, D.; Thrush, A.; Sathish, P., Validation of Reference Genes for Quantitative RT-PCR Studies of Gene Expression in Perennial Ryegrass (*Lolium perenne* L.). *BMC Mol Biol.* **2010**, *11* (1), 8.
123. Zhu, X.; Li, X.; Chen, W.; Chen, J.; Lu, W.; Chen, L.; Fu, D., Evaluation of New Reference Genes in Papaya for Accurate Transcript Normalization under Different Experimental Conditions. *PLoS ONE* **2012**, *7* (8), e44405.
124. Bartley, G. E.; Scolnik, P. A., Plant Carotenoids: Pigments for Photoprotection, Visual Attraction, and Human Health. *Plant Cell.* **1995**, *7*, 1027-1038.
125. Meléndez-Martínez, A. J.; Britton, G.; Vicario, I. M.; Heredia, F. J., Relationship Between The Colour and The Chemical Structure of Carotenoid Pigments. *Food Chem.* **2007**, *101* (3), 1145-1150.
126. Voutilainen, S.; Nurmi, T.; Mursu, J.; Rissanen, T. H., Carotenoids and Cardiovascular Health. *Am J Clin Nutr.* **2006**, *83* (6), 1265-1271.
127. Johnson, E. J., The Role of Carotenoids in Human Health. *Nutr Clin Care.* **2002**, *5*, 56-65.

128. Fantini, E.; Falcone, G.; Frusciante, S.; Giliberto, L.; Giuliano, G., Dissection of Tomato Lycopene Biosynthesis through Virus-Induced Gene Silencing. *Plant Physiol.* **2013**, *163* (2), 986-998.
129. Chen, Y.; Li, F.; Wurtzel, E. T., Isolation and Characterization of the Z-ISO Gene Encoding a Missing Component of Carotenoid Biosynthesis in Plants. *Plant Physiol.* **2010**, *153* (1), 66-79.
130. Zhu, C.; Bai, C.; Sanahuja, G.; Yuan, D.; Farré, G.; Naqvi, S.; Shi, L.; Capell, T.; Christou, P., The Regulation of Carotenoid Pigmentation in Flowers. *Arch Biochem Biophys.* **2010**, *504* (1), 132-141.
131. Wahid, A.; Gelani, S.; Ashraf, M.; Foolad, M. R., Heat Tolerance in Plants: An Overview. *Environ Exp Bot.* **2007**, *61* (3), 199-223.
132. Sharma, P.; Jha, A. B.; Dubey, R. S.; Pessarakli, M., Reactive Oxygen Species, Oxidative Damage, and Antioxidative Defense Mechanism in Plants under Stressful Conditions. *Journal of Botany* **2012**, *2012*, 26.
133. Ledesma, N. A.; Nakata, M.; Sugiyama, N., Effect of High Temperature Stress on the Reproductive Growth of Strawberry cvs. 'Nyoho' and 'Toyonoka'. *Sci Hortic.* **2008**, *116* (2), 186-193.
134. Hollender, C. A. G., A. C.; Slovin, J. P.; Liu, Z., Flower and Early Fruit Development in the Diploid Strawberry, *Fragaria vesca*. *Planta* **2012**, *235*, 1123-1139.
135. Peterson, R.; Slovin, J. P.; Chen, C., A Simplified Method for Differential Staining of Aborted and Non-Aborted Pollen Grains. *Int. J Plant Biol.* **2010**, *1*, 1:e13.
136. Mount, D., *Bioinformatics : Sequence and Genome Analysis - 2nd edition*. Second ed.; Cold Spring Harbor Laboratory Press: Cold Spring Harbor, New York, 2004.
137. Jung, S.; Staton, M.; Lee, T.; Blenda, A.; Svancara, R.; Abbott, A.; Main, D., GDR (Genome Database for Rosaceae): Integrated Web-Database for Rosaceae Genomics and Genetics Data. *Nucleic Acids Res.* **2008**, *36* (Database issue), D1034-D1040.

138. Lomsadze, A.; Ter-Hovhannisyan, V.; Chernoff, Y. O.; Borodovsky, M., Gene Identification in Novel Eukaryotic Genomes by Self-Training Algorithm. *Nucleic Acids Res.* **2005**, *33* (20), 6494-6506.
139. Larkin, M. A.; Blackshields, G.; Brown, N. P.; Chenna, R.; McGettigan, P. A.; McWilliam, H.; Valentin, F.; Wallace, I. M.; Wilm, A.; Lopez, R.; Thompson, J. D.; Gibson, T. J.; Higgins, D. G., Clustal W and Clustal X version 2.0. *Bioinformatics* **2007**, *23* (21), 2947-2948.
140. Marchler-Bauer, A.; Lu, S.; Anderson, J. B.; Chitsaz, F.; Derbyshire, M. K.; DeWeese-Scott, C.; Fong, J. H.; Geer, L. Y.; Geer, R. C.; Gonzales, N. R.; Gwadz, M.; Hurwitz, D. I.; Jackson, J. D.; Ke, Z.; Lanczycki, C. J.; Lu, F.; Marchler, G. H.; Mullokandov, M.; Omelchenko, M. V.; Robertson, C. L.; Song, J. S.; Thanki, N.; Yamashita, R. A.; Zhang, D.; Zhang, N.; Zheng, C.; Bryant, S. H., CDD: A Conserved Domain Database for the Functional Annotation of Proteins. *Nucleic Acids Res.* **2015**, *43* (Database issue), D222-D226.
141. Artimo, P.; Jonnalagedda, M.; Arnold, K.; Baratin, D.; Csardi, G.; de Castro, E.; Duvaud, S.; Flegel, V.; Fortier, A.; Gasteiger, E.; Grosdidier, A.; Hernandez, C.; Ioannidis, V.; Kuznetsov, D.; Liechti, R.; Moretti, S.; Mostaguir, K.; Redaschi, N.; Rossier, G.; Xenarios, I.; Stockinger, H., ExPASy: SIB Bioinformatics Resource Portal. *Nucleic Acids Res.* **2012**, *40* (W1), W597-W603.
142. Emanuelsson, O.; Nielsen, H.; von Heijne, G., ChloroP, A Neural Network-Based Method for Predicting Chloroplast Transit Peptides and their Cleavage Sites. *Protein Sci.* **1999**, *8* (5), 978-984.
143. Ruiz-Sola, M. Á.; Rodríguez-Concepción, M., Carotenoid Biosynthesis in Arabidopsis: A Colorful Pathway. *The Arabidopsis Book* **2012**, *10*, e0158.
144. Bottoms, C. A.; Smith, P. E.; Tanner, J. J., A Structurally Conserved Water Molecule in Rossmann Dinucleotide-Binding Domains. *Protein Sci.* **2002**, *11* (9), 2125-2137.
145. Hollender, C. A.; Kang, C.; Darwish, O.; Geretz, A.; Matthews, B. F.; Slovin, J.; Alkharouf, N.; Liu, Z., Floral Transcriptomes in Woodland Strawberry Uncover Developing Receptacle and Anther Gene Networks. *Plant Physiol.* **2014**.
146. Moehs, C.; Tian, L.; Osteryoung, K.; DellaPenna, D., Analysis of Carotenoid Biosynthetic Gene Expression During Marigold Petal Development. *Plant Mol Biol.* **2001**, *45* (3), 281-293.

147. Yamamizo, C.; Kishimoto, S.; Ohmiya, A., Carotenoid Composition and Carotenogenic Gene Expression During Ipomoea Petal Development. *J Exp Bot.* **2010**, *61* (3), 709-719.
148. Ohmiya, A.; Kishimoto, S.; Aida, R.; Yoshioka, S.; Sumitomo, K., Carotenoid Cleavage Dioxygenase (CmCCD4a) Contributes to White Color Formation in Chrysanthemum Petals. *Plant Physiol.* **2006**, *142* (3), 1193-1201.
149. Auldridge, M. E.; McCarty, D. R.; Klee, H. J., Plant Carotenoid Cleavage Oxygenases and their Apocarotenoid Products. *Curr Opin Plant Biol.* **2006**, *9* (3), 315-321.
150. Eroglu, A.; Harrison, E. H., Carotenoid Metabolism in Mammals, Including Man: Formation, Occurrence, and Function of Apocarotenoids: Thematic Review Series: Fat-Soluble Vitamins: Vitamin A. *J Lipid Res.* **2013**, *54* (7), 1719-1730.
151. Pérez-Massot, E.; Banakar, R.; Gómez-Galera, S.; Zorrilla-López, U.; Sanahuja, G.; Arjó, G.; Miralpeix, B.; Vamvaka, E.; Farré, G.; Rivera, S. M.; Dashevskaya, S.; Berman, J.; Sabalza, M.; Yuan, D.; Bai, C.; Bassie, L.; Twyman, R. M.; Capell, T.; Christou, P.; Zhu, C., The Contribution of Transgenic Plants to Better Health Through Improved Nutrition: Opportunities and Constraints. *Genes & Nutrition* **2013**, *8* (1), 29-41.
152. Vranová, E.; Coman, D.; Gruissem, W., Structure and Dynamics of the Isoprenoid Pathway Network. *Molecular Plant* **2012**, *5* (2), 318-333.
153. Cazzonelli, C. I.; Pogson, B. J., Source to Sink: Regulation of Carotenoid Biosynthesis in Plants. *Trends Plant Sci.* **2010**, *15* (5), 266-74.
154. Zhou, X.; Welsch, R.; Yang, Y.; Álvarez, D.; Riediger, M.; Yuan, H.; Fish, T.; Liu, J.; Thannhauser, T. W.; Li, L., Arabidopsis OR Proteins are the Major Posttranscriptional Regulators of Phytoene Synthase in Controlling Carotenoid Biosynthesis. *PNAS* **2015**, *112* (11), 3558-3563.
155. Rodríguez-Villalón, A.; Gas, E.; Rodríguez-Concepción, M., Colors in the Dark: A Model for the Regulation of Carotenoid Biosynthesis in Etioplasts. *Plant Signal Behav.* **2009**, *4* (10), 965-967.
156. Ravel, C.; Dardevet, M.; Leenhardt, F.; Bordes, J.; Joseph, J.; Perretant, M.; Exbrayat, F.; Poncet, C.; Balfourier, F.; Chanliaud, E.; Charmet, G., Improving the

Yellow Pigment Content of Bread Wheat Flour by Selecting the Three Homoeologous Copies of *Psy1*. *Mol Breed.* **2013**, *31* (1), 87-99.

157. Welsch, R.; Arango, J.; Bär, C.; Salazar, B.; Al-Babili, S.; Beltrán, J.; Chavarriaga, P.; Ceballos, H.; Tohme, J.; Beyer, P., Provitamin A Accumulation in Cassava (*Manihot esculenta*) Roots Driven by a Single Nucleotide Polymorphism in a Phytoene Synthase Gene. *The Plant Cell* **2010**, *22* (10), 3348-3356.

158. Ruiz-Sola, M. Á.; Rodríguez-Concepción, M., Carotenoid Biosynthesis in Arabidopsis: A Colorful Pathway. *The Arabidopsis Book / American Society of Plant Biologists* **2012**, *10*, e0158.

159. Schledz, M. A.-B., Salim; Lintig, Johannes V. ; Rabbani, Said; Kleinig, Hans; Beyer, Peter, Phytoene Synthase from *Narcissus pseudonarcissus*: Functional Expression, Galactolipid Requirement, Topological Distribution in Chromoplasts and Induction during Flowering. *The Plant Journal* **1996**, *10*, 781-792.

160. Obrero, Á.; González-Verdejo, C. I.; Román, B.; Gómez, P.; Die, J. V.; Ampomah-Dwamena, C., Identification, Cloning, and Expression Analysis of Three Phytoene Synthase Genes from *Cucurbita pepo*. *Biol Plant* **2015**, *59* (2), 201-210.

161. Fu, X.; Feng, C.; Wang, C.; Yin, X.; Lu, P.; Grierson, D.; Xu, C.; Chen, K., Involvement of Multiple Phytoene Synthase Genes in Tissue- and Cultivar-Specific Accumulation of Carotenoids in Loquat. *J Exp Bot.* **2014**, *65* (16), 4679-4689.

162. Mlalazi, B.; Welsch, R.; Namanya, P.; Khanna, H.; Geijskes, R. J.; Harrison, M.; Harding, R.; Dale, J.; Bateson, M., Isolation and Functional Characterisation of Banana Phytoene Synthase Genes as Potential Cisgenes. *Planta.* **2012**, *236* (5), 1585-1598.

163. Li, F.; Tsfadia, O.; Wurtzel, E. T., The Phytoene Synthase Gene Family in the Grasses: Subfunctionalization Provides Tissue-Specific Control of Carotenogenesis. *Plant Signal Behav.* **2009**, *4* (3), 208-211.

164. Welsch, R.; Wüst, F.; Bär, C.; Al-Babili, S.; Beyer, P., A Third Phytoene Synthase Is Devoted to Abiotic Stress-Induced Abscisic Acid Formation in Rice and Defines Functional Diversification of Phytoene Synthase Genes. *Plant Physiol.* **2008**, *147* (1), 367-380.

165. Giorio, G.; Stigliani, A. L.; D'Ambrosio, C., Phytoene Synthase Genes in Tomato (*Solanum lycopersicum* L.) – New Data on the Structures, the Deduced Amino Acid Sequences and the Expression Patterns. *FEBS Journal* **2008**, *275* (3), 527-535.
166. Qin, X.; Coku, A.; Inoue, K.; Tian, L., Expression, Subcellular Localization, and Cis-Regulatory Structure of Duplicated Phytoene Synthase Genes in Melon (*Cucumis melo* L.). *Planta* **2011**, *234* (4), 737-748.
167. Baron, K. N.; Schroeder, D. F.; Stasolla, C., Transcriptional Response of Abscisic Acid (ABA) Metabolism and Transport to Cold and Heat Stress Applied at the Reproductive Stage of Development in *Arabidopsis thaliana*. *Plant Sci.* **2012**, *188–189* (0), 48-59.
168. Ledesma, N. A.; Kawabata, S.; Sugiyama, N., Effect of High Temperature on Protein Expression in Strawberry Plants. *Biol Plant* **2004**, *48* (1), 73-79.
169. Cunningham, F. X. J. G., E., A Portfolio of Plasmids for Identification and Analysis of Caotenoid Pathway Enzymes: *Adonis aestivalis*. *Photosynth Res.* **2007**, *92*, 245-259.
170. Lescot, M.; Déhais, P.; Thijs, G.; Marchal, K.; Moreau, Y.; Van de Peer, Y.; Rouzé, P.; Rombauts, S., PlantCARE, a database of plant cis-acting regulatory elements and a portal to tools for in silico analysis of promoter sequences. *Nucleic Acids Research* **2002**, *30* (1), 325-327.
171. Petersen, T. N.; Brunak, S.; von Heijne, G.; Nielsen, H., SignalP 4.0: discriminating signal peptides from transmembrane regions. *Nat Meth.* **2011**, *8* (10), 785-786.
172. Shen, H.-B.; Chou, K.-C., Signal-3L: A 3-layer approach for predicting signal peptides. *Biochemical and Biophysical Research Communications* **2007**, *363* (2), 297-303.
173. Hiller, K.; Grote, A.; Scheer, M.; Münch, R.; Jahn, D., PrediSi: Prediction of Signal Peptides and their Cleavage Positions. *Nucleic Acids Res.* **2004**, *32* (Web Server issue), W375-W379.

174. Tamura, K.; Stecher, G.; Peterson, D.; Filipski, A.; Kumar, S., MEGA6: Molecular Evolutionary Genetics Analysis Version 6.0. *Molecular Biology and Evolution* **2013**, *30* (12), 2725-2729.

175. Liang, P.-H.; Ko, T.-P.; Wang, A. H. J., Structure, Mechanism and Function of Prenyltransferases. *European Journal of Biochem.* **2002**, *269* (14), 3339-3354.